

FACTORS AFFECTING MICROVASCULAR
ENDOTHELIAL TIGHT JUNCTION ASSEMBLY
AND BARRIER FUNCTION IN THE
BLOOD-BRAIN BARRIER

A dissertation submitted for the degree of Ph.D by
Olga C. Colgan, B.Sc

Under the supervision of Professor Paul A. Cahill and Dr.
Philip M. Cummins.

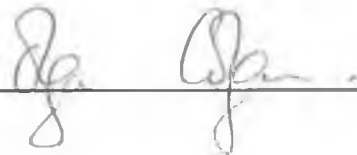
June 2006

Vascular Health Research Centre, Faculty of Science and Health,
Dublin City University, Glasnevin, Dublin 9, Ireland.

Declaration:

I hereby certify that this material, which I now submit for assessment on the programme of study leading to the award of Doctor of Philosophy is entirely my own work and has not been taken from the work of others save and to the extent that such work has been cited and acknowledged within the text of my own work.

Signature: _____

A handwritten signature in black ink, appearing to be 'S. S.', written over a horizontal line.

Student I.D: 98312014

Date: _____

20 September 2006

Acknowledgements

I would like to take this chance to thank Professor Paul Cahill for giving me the opportunity to work and study in the Vascular Health Research Centre and for his intellectual input over the years. I would also like to thank the three senior scientists in the lab, Dr. Yvonne Birney, Dr. Gail Ferguson and Dr. Ronan Murphy, who were not my direct supervisors, but who's advice, recommendations and friendships I have come to rely on. I would especially like to acknowledge all the VHRC postgrads, past and present, for their friendships and willingness to go on tea-breaks at every given opportunity. A very special mention must go to Nora Collins for muddling through with me every step of the way. Most of all, I would like to give my heart-felt thanks to Dr. Philip M. Cummins, I couldn't have done this without you – cheers Philly!

I would like to dedicate this thesis to my parents and family for their financial and emotional support for the last 25 and a half years and for providing a much needed shoulder to cry on when the end wasn't quite in sight. Thanks a million for everything, you're the best!

Abstract

The blood-brain barrier (BBB) is responsible for homeostasis of the brain interstitial fluid (ISF) by separating the central nervous system (CNS) from systemic blood circulation. The BBB exhibits low permeability to hydrophilic solutes and high transendothelial electrical resistance arising from a continuous series of tight junctions (TJ) connecting adjacent microvascular endothelial cells of brain capillaries. The basolateral side of these microvascular endothelial cells are encompassed by astrocyte end feet and bathed in ISF, which is completely devoid of serum. Moreover, the vascular endothelium is continuously exposed to hemodynamic forces, namely shear stress and cyclic circumferential strain, both of which can induce profound changes in endothelial gene expression and cell fate. Disruption of BBB integrity leading to vascular leakage is a central pathophysiologic mechanism of many diseases whilst, the “tightness” of the BBB also proves problematic in drug delivery to the brain. Thus, elucidating the etiology of tight junction formation and the factors effecting BBB permeability may lead to the development of novel strategies to modulate barrier properties and thus have profound clinical impact on several neurological diseases. ***The focus of this PhD project, therefore, was to elucidate the biochemical events affecting tight junction formation and barrier function caused by serum, astrocyte co-culture and biomechanical shear stress.***

In order to assess TJ formation in Bovine Brain Microvascular Cells (BBMvECs), the expression, localization and association of occludin and ZO-1, two pivotal TJ proteins was examined, concomitant with measurement of sucrose permeability across the EC monolayer and TEER to assess EC barrier function. Briefly, this research has shown that the increased association of occludin with ZO-1, in parallel with increased membrane localization of the two proteins, is central to tight junction formation, and correlates directly with increased barrier function.

In-vivo tight junctions forming the BBB prevent serum entering the ISF. This indicates that the effects of serum on tight junction formation and barrier function are highly polar-specific. Our data subsequently indicated that in the absence of basolateral serum, occludin and ZO-1 expression increased, as did their association and the concomitant redistribution of the two proteins to the plasma membrane. These biochemical events were accompanied by an increase in TEER and decrease in sucrose permeability.

Furthermore, our findings indicate that co-culture of BBMvEC with basolaterally applied C6 glioma increases tight junction formation and barrier function and that these changes were enhanced, at least in part, by the removal of serum from the basolateral compartment of the co-culture model.

In the brain microvasculature, shear stress is typically in the region of 4 – 20 dynes/cm². Exposure of BBMvECs to physiological laminar shear stress (pulsatile and non-pulsatile) significantly increases occludin and ZO-1 expression and association, concomitant with translocation of both occludin and ZO-1 to the cell membrane and reduced transendothelial permeability.

In summary, this body of work addresses three of the major factors impacting upon the BBB and assesses their individual impacts on tight junction formation and barrier function. Further studies are required to fully elucidate the exact signaling mechanisms by which these events occur.

Abbreviations

γ GTP	γ -glutamyl-transpeptidase
3-D	3 dimensional
ACW	Actin cortical web
ADP	Adenosine diphosphate
AF-6	ALL fusion partner from chromosome 6
AIDS	Acquired immunodeficiency syndrome
ALP	Alkaline phosphatase
ATP	Adenosine triphosphate
BAEC	Bovine aortic endothelial cells
BBB	Blood-brain barrier
BBMvEC	Bovine brain microvascular endothelial cell
BCA	Bicinchoninic acid
bFGF	Basic fibroblast growth factor
BSA	Bovine serum albumin
C6ACM	C6 glioma astrocyte-conditioned media
Ca	Calcium
cDNA	Complementary DNA
Cl	Chlorine
CLS	Capillary-like structures
CNS	Central nervous system
Cu	Copper
Da	Daltons
DAPI	4',6-diamidino-2-phenylindole
DMEM	Dulbecco's modified eagle's medium
DMSO	Dimethyl sulfoxide
DNA	Deoxy ribonucleic acid
E10.5	Embryonic day 10.5
EC	Endothelial cell
ECM	Extracellular matrix

ECS	Extracapillary space
EDHF	Endothelium-derived hyperpolarization factor
EDTA	Ethylenediaminetetraacetic acid
EG	Endothelial glycocalyx
eNOS	Endothelial NOS
ET-1	Endothelin-1
EtBr	Ethidium bromide
F-actin	Filamentous actin
FCS	Fetal calf serum
FITC	Fluorescein isothiocyanate
GAPDH	Glyceraldehyde phosphate dehydrogenase
GDNF	Glial cell line-derived neurotrophic factor
GDP	Guanosine diphosphate
GFAP	Glial fibrillary acidid protein
GGT	γ -glutamyl transferase
GPCR	G-protein coupled receptor
GTP	Guanosine triphosphate
GTP	Guanosine triphosphate
GUK	guanylate kinase
HBSS	Hank's balanced salt solution
HEPES	4-(2-hydroxyethyl)piperazine-1-ethanesulfonic acid
HMW	High molecular weight
HRP	Horse radish peroxidase
IB	Immunoblot
IFN- γ	Interferon- γ
IL	Interleukin
iNOS	Inducible NOS
IP	Immunoprecipitation
ISF	Interstitial fluid
JAM	Junctional adhesion molecule
JNK	c-jun N-terminal kinase

K ⁺	Postassium
LIF	Leukaemia inhibitory factor
LMW	Low molecular weight
LPA	Lysophosphatidic acid
MAGUK	Membrane-associated guanylate kinase
MAPK	Mitogen-activated protein kinase
MDCK	Madin-Darby canine kidney
MHC	Major histocompatibility complex
mRNA	Messenger RNA
Na	Sodium
NaF	Sodium fluoride
nNOS	Neuronal NOS
NO	Nitric oxide
NOS	Nitric oxide synthase
occ	Occludin
P/S	Penicillin-streptomycin
PBS	Phosphate buffered saline
PCR	Polymerase chain reaction
PDZ	PSD-95/Dlg/ZO-1
P-gp	P-glycoprotein
PKC	Protein kinase C
PML	Progressive multifocal leukoencephalopathy
RGD	Arg-Gly-Asp
RNA	Ribo nucleic acid
RT	Reverse transcription
SDS PAGE	SDS Polyacrylamide gel electrophoresis
SDS	Sodium doecyl sulphate
SEM	Standard error of the mean
SF	Serum free
SH3	Src oncogene homology region 3
SSB	Sample solubilization buffer

SSeCKS	src-suppressed C-kinase substrate
TAE	Tris acetate EDTA
TEE	Trans endothelial exchange
TEER	Transendothelial electrical resistance
TGF- β	Transforming growth factor- β
TJ	Tight junction
TNF- α	Tumor necrosis factor- α
Trp/EDTA	Trypsin/EDTA
TXA ₂	Thromboxane A ₂
UV	Ultraviolet
VEGF	Vascular endothelial growth factor
VEGF-R	VEGF-receptor
ZAK	ZO-1-associated kinase
ZO-1	Zonula occludens-1
ZONAB	ZO-1 nucleic acid binding protein

Units

%	Percent
Ω	Ohms
μCi	Microcurie
μg	Microgram
μL	Microlitre
μm	Micrometer
\AA	Angstroms
bp	Base pair
cm	Centimeter
Da	Daltons
g	Grams
h	Hour
kDa	Kilodaltons
mA	Milliamp
min	Minute
mL	Millilitre
mm	Millimeter
mM	Millimolar
ng	Nanogram
nm	Nanometer
$^{\circ}\text{C}$	Degrees Celsius
RPM	Revolutions per minute
sec	Second
U	Enzyme activity units
V	Volt
v/v	Volume per volume
W	Watt
w/v	Weight per volume

Publications

Peer Reviewed Papers:

- [1] Colgan OC, Collins NT, Ferguson G, Birney YA, Murphy RP Cahill PA, Cummins PM. Regulation of microvascular endothelial tight junction assembly and barrier function by laminar and pulsatile shear stress. *Cardiovascular Research* 2006; (*In Preparation*).
- [2] Collins NT, Colgan OC, Ferguson G, Birney YA, Murphy RP Cahill PA, Cummins PM. Cyclic strain-mediated regulation of vascular endothelial tight junction assembly: putative roles for integrins, G-proteins and Rho-GTPase signaling pathways. *Arteriosclerosis, Thrombosis, & Vascular Biology* 2006; (*In Preparation*)
- [3] Colgan OC/Cummins PM ϕ , Collins NT, Ferguson G, Birney YA, Murphy RP Cahill. Polar Specific Regulation of Vascular Endothelial Occludin and ZO-1: The Influence of Astrocytes and Serum. *AJP-Cell Physiology Feb* 2006; Submitted [**Joint First Author**] ϕ
- [4] Colgan OC/Cummins PM ϕ , Collins NT, Ferguson G, Birney YA, Murphy RP Cahill. The Polar Specific Influence of Serum on Regulation of Vascular Endothelial Occludin and ZO-1. *AJP-Cell Physiology Feb* 2006; Submitted [**Joint First Author**] ϕ
- [5] Collins NT / Cummins PM ϕ , Colgan OC, Ferguson G, Birney YA, Murphy RP, Meade G, Cahill PA. Cyclic strain-mediated regulation of vascular endothelial occludin and ZO-1: Impact on intercellular tight junction assembly and function. *Arteriosclerosis, Thrombosis, & Vascular Biology* 2006;**26**:62-68. [**Joint First Author**] ϕ

Poster Presentations

- [1] Colgan OC, Cummins PM, Collins NT, Birney YA, Ferguson G, Cahill PA. Co-culture of Bovine Brain Microvascular Endothelial Cells (BBMvEC) and C6 Glioma Decreases Endothelial Permeability and Increases Tight Junction Formation *7th Annual Conference on Arteriosclerosis, Thrombosis and Vascular Biology, Denver* (2006)
- [2] Colgan OC, Collins NT, Birney YA, Ferguson G, Cahill PA, Cummins PM. Shear Stress Regulates Microvascular Endothelial Occludin and ZO-1 and Increases Tight Junction Formation. *7th Annual Conference on Arteriosclerosis, Thrombosis and Vascular Biology, Denver*, (2006)
- [3] Collins NT, Cummins PM, Colgan OC, Ferguson-Welsby RP, Murphy, Cahill PA. Cyclic Strain Regulates Occludin and ZO-1 Expression, Phosphorylation and Localisation in Bovine Aortic Endothelial Cells. *American Heart Association Annual Conference, Dallas: Circulation Supplement* (2005)
- [4] Collins NT, Colgan OC, Ferguson G, Murphy RP, Cummins PM, Cahill PA. Cyclic Strain Regulates Occludin and ZO-1 Expression, Phosphorylation and Localisation in Bovine Aortic Endothelial Cells. *American Heart Association Annual Conference, New Orleans: Circulation Supplement* (2004)
- [5] Collins NT, Cummins PM, Colgan OC, Cahill PA. The Effects of Mechanical Forces on Endothelial Cell Permeability in Peripheral Vascular Beds. *15th Annual Meeting of Irish Association of Pharmacologists, Dublin* (2004)

Table of Contents

Declaration	I
Acknowledgements	II
Abstract	III
Abbreviations	IV
Units	VIII
Publications	IX
Chapter 1: Introduction	1
1.0 Introduction	2
1.1 Development of the BBB	3
1.2 Cell Biology of the BBB	4
1.2.1 The Role of Cerebral Pericytes	5
1.2.2 The Role of Cerebral Astrocytes	6
1.2.2.1 C6 Glioma	9
1.3 Tight Junctions	10
1.3.1 Tight Junction Proteins	11
1.3.1.1 Occludin	13
1.3.1.1.1 Occludin Structure and Function	13
1.3.1.1.2 Occludin Regulation	16
1.3.1.1.3 Occludin and Clinical Implications	18
1.3.1.2 Zonula Occludens	18
1.3.1.2.1 ZO-1 Structure and Function	19
1.3.1.2.2 ZO-1 Regulation	22
1.3.1.2.3 ZO-1 and Clinical Implications	22
1.4 Haemodynamics	23
1.4.1 Shear Stress and the BBB	26
1.4.2 Mechanotransduction	27
1.4.2.1 Mechanosensitive Ion Channels	28
1.4.2.2 The Role of G-Proteins in Mechanotransduction	29

1.4.2.3	The Role of Integrins in Mechanotransduction	31
1.4.2.4	The Role of the Endothelial Glycocalyx in Mechanotransduction	32
1.5	Summary	32
1.6	Thesis Overview	33
Chapter 2:	Materials and Methods	34
2.0	Materials and Methods	35
2.1	Materials	35
2.2	Cell Culture Methods	39
2.2.1	Culture of Bovine Brain Microvascular Endothelial Cells (BBMvECs)	39
2.2.2	Culture of C6 Glioma Astroglial Cells	39
2.2.3	Preparation of C6 Glioma Astrocyte-Conditioned Media	40
2.2.4	Trypsinization of BBMvECs and C6 Glioma	40
2.2.5	Cryogenic Preservation and Recovery of Cells	41
2.2.6	Cell Counts	41
2.2.7	Serum and Co-Culture Studies	42
2.2.8	Non-pulsatile Laminar Shear Stress Studies	43
2.2.9	Perfused Transcapillary System	44
2.2.10	Inhibitor Studies	46
2.2.11	Immunocytochemistry	46
2.2.12	Transendothelial Electrical Resistance	47
2.2.13	Permeability Studies	48
2.2.14	¹⁴ C Scintillation Counts	51
2.2.15	Preparation of Whole Cell Lysates	51
2.2.16	Bicinchoninic Acid (BCA) Protein Microassay	51
2.2.17	Preparation of Immunoprecipitates	52

2.3	RNA Preparation Methods	52
2.3.1	RNA Isolation	52
2.3.2	Spectrophotometric Analysis of Nucleic Acids	53
2.3.3	Reverse Transcription (RT) Reaction	54
2.3.4	Real-Time Polymerase Chain Reaction (PCR)	54
2.3.5	Agarose Gel Electrophoresis	55
2.4	Western Blotting	56
2.4.1	Preparation of SDS PAGE Gels	56
2.4.2	SDS PAGE Sample Preparation and Electrophoresis	57
2.4.3	Wet Transfer and Ponceau S Staining	58
2.4.4	Immunodetection	58
2.5	Statistical Analysis	59
Chapter 3: Optimization of cell culture media and characterization of the model		60
3.1	Introduction	61
3.2	Results	62
3.2.1	Media- and serum-dependent proliferation, morphology and viability of BBMvECs	62
3.2.2	Basic Fibroblast Growth Factor (bFGF) is required for maintained BBMvEC proliferation, morphology and viability <i>in vitro</i>	62
3.2.3	Heparin is required for maintained BBMvEC proliferation, morphology and viability <i>in vitro</i>	65
3.2.4	Characterization of BBMvECs grown in in-house media by expression of Von-Willebrand Factor VIII antigen	65
3.2.5	Characterization of C6 Glioma by expression of Glial Fibrillary Acidic Protein (GFAP) antigen and assessment of viability in serum-free media	68
3.3	Discussion	70

Chapter 4:	Examination of the polar-specific effect of serum on endothelial tight junction formation and barrier function	72
4.1	Introduction	73
4.2	Results	74
4.2.1	Apically applied serum-dependent subcellular localization of occludin and ZO-1 in BBMvECs	74
4.2.2	Basolaterally applied serum-dependent expression of occludin in BBMvECs	76
4.2.3	Basolaterally applied serum-dependent expression of ZO-1 in BBMvECs	76
4.2.4	Basolaterally applied serum-dependent association of occludin/ZO-1	79
4.2.5	Basolaterally applied serum-dependent localization of occludin and ZO-1	79
4.2.6	Basolaterally applied serum-dependent transendothelial permeability of BBMvECs to ¹⁴ C sucrose	82
4.2.7	Basolaterally applied serum-dependent transendothelial electrical resistance (TEER) of BBMvECs	82
4.3	Discussion	85
Chapter 5:	Investigation of the role of C6 glioma in regulating BBMvEC occludin and ZO-1 and the effect of co-culture on BBMvEC permeability	89
5.1	Introduction	90
5.2	Results	91
5.2.1	C6 Glioma astrocyte-conditioned media- and serum- dependent subcellular localization of occludin in BBMvECs	91
5.2.2	C6 Glioma astrocyte-conditioned media- and serum- dependent subcellular localization of ZO-1 in BBMvECs	91

5.2.3	Co-culture- and serum-dependent subcellular localization of occludin in BBMvECs	94
5.2.4	Co-culture- and serum-dependent subcellular localization of ZO-1 in BBMvECs	94
5.2.5	Co-culture- and serum-dependent expression of occludin in BBMvECs	97
5.2.6	Co-culture- and serum-dependent expression of ZO-1 in BBMvECs	97
5.2.7	Co-culture- and serum-dependent association of occludin/ZO-1	100
5.2.8	Co-culture- and serum-dependent transendothelial permeability of BBMvECs to ¹⁴ C sucrose	102
5.2.9	Co-culture- and serum-dependent transendothelial electrical resistance (TEER) of BBMvECs	102
5.2.10	Serum-dependent, but not co-culture-dependent, subcellular localization of occludin is attenuated by cycloheximide in BBMvECs	105
5.2.11	Serum-dependent, but not co-culture-dependent, subcellular localization of ZO-1 is attenuated by cycloheximide in BBMvECs	107
5.3	Discussion	109
Chapter 6:	Assessment of the role of laminar shear stress on BBMvEC tight junction formation and barrier function	113
6.1	Introduction	114
6.2	Results	115
6.2.1	Shear stress-dependent increase in occludin expression in BBMvECs	115
6.2.2	Shear stress-dependent increase in ZO-1 expression in BBMvECs	115
6.2.3	Shear stress-dependent association of occludin/ZO-1 in BBMvECs	115
6.2.4	Shear stress-dependent cell realignment and occludin and ZO-1 subcellular localization	119

6.2.5	Shear stress decreases BBMvEC transendothelial permeability to FITC dextran	121
6.2.6	Shear stress-dependent association of occludin/ZO-1 in BBMvECs is partially attenuated by cycloheximide	124
6.2.7	Shear stress-dependent occludin subcellular localization if partially attenuated by cycloheximide	126
6.2.8	Shear stress-dependent ZO-1 subcellular localization if partially attenuated by cycloheximide	126
6.2.9	Shear stress-dependent decrease in BBMvEC transendothelial permeability to FITC dextran is partially attenuated by cycloheximide	129
6.2.10	Pulsatile laminar shear stress-dependent increase in occludin and ZO-1 protein expression in BBMvECs	132
6.2.11	Pulsatile laminar shear stress-dependent association of occludin/ZO-1 in BBMvECs	132
6.2.12	Pulsatile laminar shear stress-dependent transendothelial permeability of BBMvECs to ¹⁴ C-sucrose	132
6.3	Discussion	136
Chapter 7: Final Summary		140
7.1	Final Summary	141
Chapter 8: Bibliography		149

Chapter 1

Introduction

1.0 Introduction

The blood-brain barrier (BBB) is formed by brain microvascular endothelial cells, which line cerebral capillaries, and is characterized by low permeability to hydrophilic molecules, high electrical resistance and low occurrence of pinocytotic vesicles. The existence of the BBB was first noted in the late 19th century by a German microbiologist, Paul Ehrlich, who observed that a coloured dye injected into the blood stream would stain all organs except the brain. Further studies by one of his students, Edwin Goldmann in 1913, revealed that when a dye was injected directly into the spinal fluid it would stain only the brain. These findings lead to the hypothesis that the vasculature in the brain is unique from the peripheral vasculature in that it provided a barrier preventing the passage of solutes from the blood to the brain and vice-versa. The development of the scanning electron microscope in the 1960's revealed that the BBB is an endothelial barrier (Reese and Karnovsky 1967), resulting from the sealing of the paracellular space between adjacent endothelial cells by junctional protein complexes (Robertson 1957; Muir and Peters 1962; Peters 1962; Brightman and Palay 1963; Brightman and Reese 1969). These complexes were later identified as gap junctions, adherens junctions and zonula occludens (tight junctions).

The BBB functions to maintain homeostasis of the brain interstitial fluid (ISF) by preventing blood-borne solutes from entering the brain microenvironment (Abbott *et al.* 2006). It is impermeable to charged particles, proteins, ions, hydrophilic molecules and hormones that could act as neurotransmitters, but has limited permeability to gasses and small molecules with a molecular weight less than 500 Da in proportion to their lipid solubility (Tanobe *et al.* 2003). However, small and large hydrophilic molecules, such as glucose and amino acids, can enter the brain by active transport. For essential nutrients such as these, specific transport proteins are expressed in high concentrations on the apical membrane, thus allowing their entry to the brain. Active transport also occurs in the opposite direction, that is, from the brain to the blood. The efflux transporter, P-glycoprotein (P-gp), which is expressed

in high concentrations in brain endothelial cells, functions in transporting a wide range of lipophilic molecules that have penetrated into brain endothelial cells or through the BBB out of the brain (Schinkel 1999). P-gp has been shown to be a functional part of the blood-brain barrier with knockout mice showing increased sensitivity to circulating drugs and increased toxin accumulation in the brain (Schinkel *et al.* 1994; Schinkel *et al.* 1996).

Disruption of BBB integrity leading to vascular leakage is a central pathophysiologic mechanism of many diseases including, multiple sclerosis (Williams *et al.* 1994), meningitis/encephalitis (Tunkel and Scheld 1993), neurodegenerative diseases such as Parkinson's and Alzheimer's disease (Mattila *et al.* 1994) and progressive multifocal leukoencephalopathy, a form of dementia affecting approximately 10% of all AIDS patients (Poland *et al.* 1995). Vascular leakage is often a negative side effect of a disease, worsening the patients' condition, in cases of head trauma and ischemic stroke for example, or may be the underlying cause of the illness itself. Moreover, the impermeable nature of the BBB is the major rate-limiting step preventing advances in drug development being translated into effective neurotherapeutic agents (for review, see Pardridge 2005a). Thus, elucidating the etiology of tight junction formation and the factors effecting BBB permeability may lead to the development of novel strategies to modulate barrier properties and thus have profound clinical impact on several neurological diseases.

1.1 Development of the BBB

The expression of a BBB phenotype in endothelial cells is defined by low rates of endocytosis, impermeability of the paracellular pathway and high electrical resistance. However, *in vivo*, the time-point at which the BBB develops is quite controversial (Saunders *et al.* 1991). Electrical resistance of capillaries is the best indicator of junction tightness, however there is no direct way to measure it in the brain parenchyma. Instead, electrical resistance has been measured directly in the pial capillaries on the surface of the brain (Butt *et al.* 1990). These vessels have

electrical resistance in the region of 1000 – 2000 $\Omega\cdot\text{cm}^2$, but whether or not they are equivalent to parenchymal capillaries is unclear. In adult rodent brains, barrier function may be assessed by the introduction of dyes into the circulation and monitoring their permeation into the brain, however, in embryonic or neonate animals, the introduction of dyes can disrupt the barrier by increasing either the volume of blood or its oncotic pressure (Rubin and Staddon 1999). However, studies by Qin and Sato have shown that BBB specific markers are detected in the embryonic mouse brain at E10.5, before astrocytes are present (Qin and Sato 1995). Moreover, Saunders *et al.* have demonstrated that in rodent embryos serum proteins are excluded from the brain at relatively early times, but that the ionic barrier responsible for high electrical resistance may not develop until later (Saunders *et al.* 1991). Current data suggests that formation of the BBB *in vivo* is a multi-step process, occurring throughout the late embryonic and early postnatal periods.

1.2 Cell Biology of the BBB

Although the barrier properties of the BBB can be attributed solely to the endothelial cells, it arises as a function of paracrine interactions between the three cellular components of the BBB, namely endothelial cells, astrocytes and pericytes. In the BBB, pericytes are outnumbered 5:1 by endothelial cells (Frank *et al.* 1987) with the pericytes situated basolaterally to endothelial cells and enveloped in “pockets” in the basal lamina (Cancilla *et al.* 1972). These pericytes form cellular projections which penetrate the basal lamina and contact 20 – 30% of the endothelial abluminal membrane (Frank *et al.* 1987). Astrocytes *in vivo* express a stellate morphology with numerous foot processes. These foot processes encircle approximately 99% of the abluminal surface of the capillary basement membrane (Kacem *et al.* 1998) (see Fig. 1.2.1). Adjacent astrocyte foot processes are separated by a ~20 nm gap, which is readily diffusible by dyes (Brightman and Reese 1969), thus indicating they do not contribute to the physical barrier.

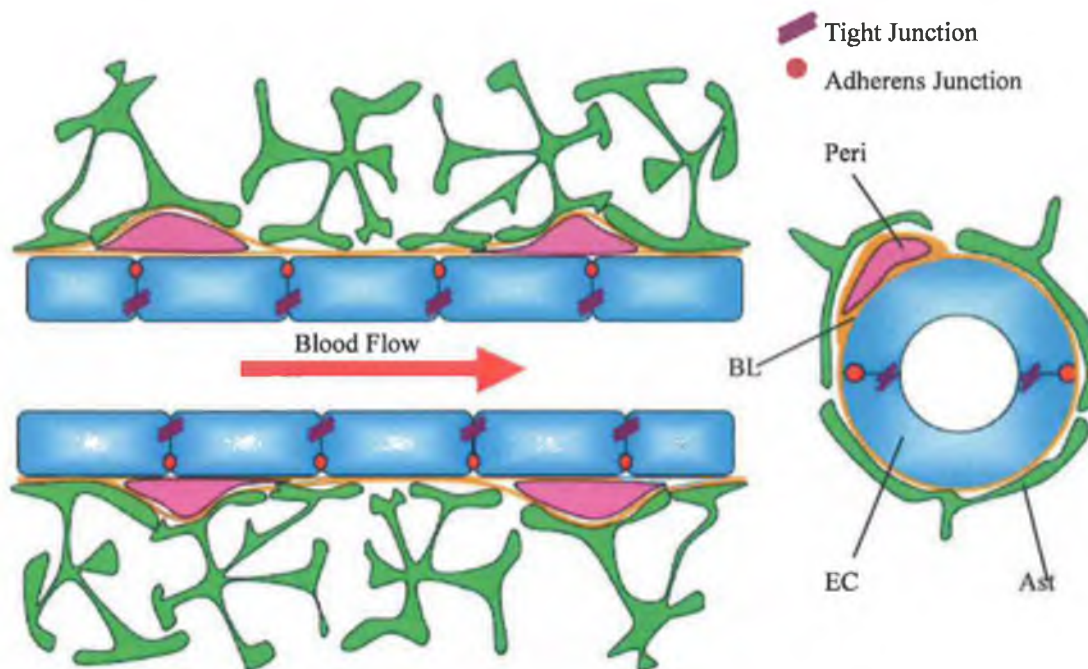


Figure 1.2.1: Schematic diagram of the three-cell model of the blood-brain barrier showing the distribution of endothelial cells (EC), pericytes (Peri), astrocytes (Ast) and basal lamina (BL).

1.2.1 The Role of Cerebral Pericytes

The term pericyte originates from “peri-“ meaning around and “cyto-“ meaning cell was first coined by Zimmermann in 1923 and reflects the pericytes’ location at the abluminal side of microvessels (Zimmermann 1923). Morphologically pericytes have a spherical cell body with a prominent nucleus surrounded by a small amount of cytoplasm, which forms numerous processes (Lafarga and Palacios 1975; Farrell *et al.* 1987). Pericytes are a heterogeneous cell population exhibiting both tissue- and vessel-related morphological and functional characteristics (Hirschi and D’Amore 1996). As depicted above in figure 1.2.1, pericytes are only separated from the endothelial cell by the basal lamina through which they form processes, which contact the endothelial cells directly. In arterioles

and venules, pericytes are rounded with extensive processes. However, in capillaries, such as those of the BBB, they exhibit an elongated cell body with short processes (Nehls and Drenckhahn 1991). BBB associated pericytes carry out a number of physiological processes including regulation of angiogenesis, tight junction formation as well as contributing to the structural stability of capillaries (Balabanov and Dore-Duffy 1998). In addition, under pathological conditions, CNS pericytes engage in pinocytosis (Castejon 1984; Hurter 1984). However, for the purpose of this body of research, only the ability of pericytes to induce BBB characteristics in brain endothelial cells is of interest. Although astrocytes are commonly regarded as the signaling cell responsible for the induction of the BBB, studies where astrocytes are either absent or removed did not prevent formation of tight junctions when pericytes were present (Felts and Smith 1996; Jaeger and Blight 1997). However, more recent studies indicate that CNS pericytes function primarily in BBB angiogenesis and capillary stabilization (Ramsauer *et al.* 2002; Kim *et al.* 2006).

1.2.2 The Role of Cerebral Astrocytes

Of the two principle cell types in the brain, astrocytes and neurons, astrocytes comprise approximately 90% of the human brain mass (Gee and Keller 2005). There are three distinct astrocyte phenotypes found in the brain. Fibrous astrocytes are located primarily in the white matter and express a distinct stellate morphology, whilst protoplasmic astrocytes, found mainly in the grey matter, form highly branched projections, which ensheath neighbouring neurons. Finally, the third class of astrocyte is the Bergmann glia, which are found only in the Purkinje layer of the cerebral cortex. Although astrocytes are electrically non-excitabile cells (Simard *et al.* 2003), they are multifunctional in regulating brain homeostasis and cerebral blood flow (Iadecola 2004). Astrocytes have long been recognized as regulating water homeostasis in the brain (del Zoppo and Hallenbeck 2000) and several recent studies have indicated a role for astrocytes in modulating neuronal signaling via propagative intracellular calcium waves (Haydon 2001; Lin and Bergles 2004a, b).

During neuronal signaling, there is rapid release of extracellular potassium (K^+), which needs to be removed quickly to prevent neuronal damage and erratic neuronal signaling. Astrocytes function in maintaining extracellular K^+ levels through active and passive K^+ uptake and spatial buffering (Ransom and Sontheimer 1995). In addition, astrocytes function as an immunocompetent cell within the brain, regulating the brain immune response. Astrocytes have the capacity to express major histocompatibility complex II (MHC II) antigens, as well as B7 and CD40, the co-stimulatory molecules necessary for antigen presentation and T-cell activation (for review, see Dong and Benveniste 2001). Moreover, astrocytes further modulate the immune and inflammatory response by secretion of cytokines including interleukin-1 (IL-1), tumor necrosis factor- α (TNF- α) and interferon- γ (IFN- γ), which are associated with the inflammatory response, and inhibitors of the inflammatory response such as transforming growth factor- β (TGF- β) and IL-4, -6 and -10 (Aschner 1998). However, the ability of astrocytes to induce barrier formation in brain endothelial cells, thus resulting in the formation of the BBB, is of uppermost interest in relation to this study.

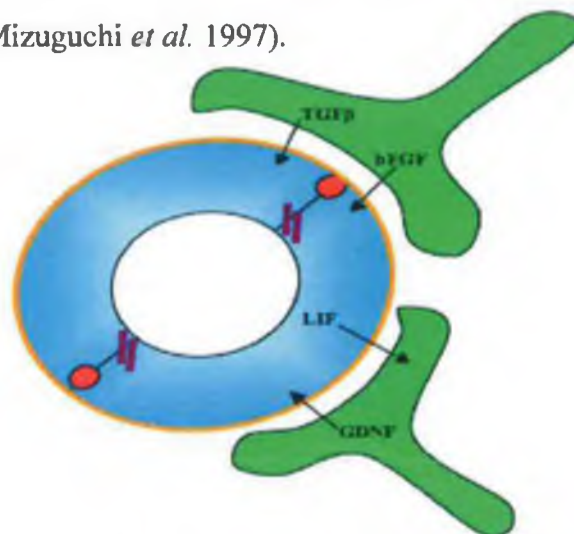
In recent years, numerous studies have demonstrated the ability of astrocytes to induce BBB phenotype in endothelial cells, however the mechanisms by which induction takes place and the agents mediating BBB formation are still largely undefined. Tran *et al.* have demonstrated that in astrocyte-endothelial co-culture models of the blood-brain barrier, levels of activated TGF- β are elevated, which in turn modulated endothelial phenotype (Tran *et al.* 1999). Moreover, studies by Garcia *et al.* again demonstrated that astrocyte-endothelial co-culture increased active TGF- β levels, which correlated with increased γ -glutamyl-transferase (GGT) activity, which is a marker of BBB phenotype in endothelial cells (Garcia *et al.* 2004). However, this study also indicated that contact between the two cell types was required for induction of these properties. In a model of the BBB using bovine brain endothelial cells, it was found that basic fibroblast growth factor (bFGF) reduced L-glucose permeability and increased expression of alkaline phosphatase, in a manner similar to astrocyte conditioned media (Sobue *et al.* 1999). Furthermore,

Ramsauer *et al.* have demonstrated that both astrocytes and pericytes were required for the formation of capillary-like structures (CLS) in 3-D matrigel (Ramsauer *et al.* 2002). Addition of TGF- β to a co-culture of pericytes and endothelial cells led to rearrangement of the endothelial cells into CLS without pericyte recruitment, which were leaky and shorter than the tri-culture CLS. These data indicate that factors other than TGF- β are released by astrocytes and that close association of astrocytes and endothelial cells is required for BBB formation.

Glial cell line-derived neurotrophic factor (GDNF) is a member of the TGF- β family secreted by astrocytes *in vitro* and *in vivo* (Lin *et al.* 1993). Studies by Igarashi *et al.* have demonstrated the ability of GDNF to induce BBB characteristics in porcine brain endothelial cells as assessed by TEER and permeability to mannitol. Furthermore, Lee *et al.* have shown that src-suppressed C-kinase substrate (SSeCKS) released by astrocytes, decreased endothelial permeability via reduction of VEGF expression (Lee *et al.* 2003).

However, signaling between endothelial cells and astrocytes occurs in both directions. For example, recent studies have shown that astrocyte differentiation is induced by endothelium-derived leukaemia inhibitory factor (LIF) (Mi *et al.* 2001) and that astrocyte proliferation is modulated by a soluble factor released by endothelial cells (Estrada *et al.* 1990). Furthermore, up-regulation of endothelial γ -glutamyl-transpeptidase (γ GTP) requires two-way cross talk between astrocytes and endothelial cells in co-culture (Mizuguchi *et al.* 1997).

Figure 1.2.2.1: Schematic diagram showing examples of bidirectional signaling between astrocytes and endothelial cells associated with formation of the BBB



Thus, it would seem that a synergistic relationship exists between astrocytes and endothelial cells; that is, that astrocytes in co-culture with endothelial cells are stimulated to secrete factors leading to tight junction formation in the endothelial cell, and in turn endothelial-derived factors modulate astrocyte growth and differentiation.

1.2.2.1 C6 Glioma

Primary cultures of astrocytes de-differentiate rapidly *in vitro*, and as such are generally used at passage 0 – 2 (Demeuse *et al.* 2002; Zhang and Harder 2002; Jeliaskova-Mecheva and Bobilya 2003; Torok *et al.* 2003; Garcia *et al.* 2004). Rodent pup brains, usually mouse or rat, are most frequently used to isolate astrocytes, but due to the small size of the brain, there is a low cell yield per animal. As such, large numbers of animals must be sacrificed for continuous experimentation, thus leading to batch-to-batch variations between cell populations and raising ethical issues associated with continued animal sacrifice. Furthermore, studies have shown that the primary astrocytes isolated do not arise from pre-existing mature astrocytes, but rather from proliferating glial precursor cells (Juurink *et al.* 1981; Goldman *et al.* 1986). Thus, the resulting mature astrocyte phenotype will be dictated by the culture conditions and growth factors in which the glial precursor cells are cultured, and as such may differ significantly from an astrocyte *in vivo*. For these reasons, immortalized astrocyte cell lines and continuous cultures are frequently used for *in vitro* studies, the most commonly used being the C6 glioma cell line. The C6 glioma cell line was cloned from a rat glial tumor induced by N-nitrosomethylurea (Benda *et al.* 1968). It is an adherent cell line, with a typically fibroblast morphology in culture. C6 glioma in co-culture with endothelial cells have been shown to increase TEER and decrease transendothelial permeability to tracer molecules, two factors indicative of tight junction formation and endothelial barrier function (Abbruscato and Davis 1999; Torok *et al.* 2003). Furthermore, co-culture of endothelial cells with C6 glioma, or C6 glioma-derived

conditioned media, increased expression of BBB-specific markers, including alkaline phosphatase and γ GTP (Beck *et al.* 1984; Beck *et al.* 1986; Rubin *et al.* 1991; Roux *et al.* 1994; Plateel *et al.* 1997). Therefore, the endothelial cell:C6 glioma co-culture is widely accepted as a suitable model of the BBB.

1.3 Tight Junctions

As previously stated, the BBB is responsible for maintenance of brain microenvironment homeostasis by preventing blood-borne solutes from entering into the brain ISF. The paracrine interactions between endothelial cells, astrocytes and to a lesser extent, pericytes are responsible for the induction of the BBB phenotype in endothelial cells. However, it is the tight junctions, which seal the intercellular cleft between adjacent endothelial cells and thus prevent paracellular flux, that are directly responsible for the barrier function in the BBB (Reese and Karnovsky 1967; Brightman and Reese 1969; Nabeshima *et al.* 1975; van Deurs and Koehler 1979; Mollgard and Saunders 1986; Rascher and Wolburg 1997; Kniesel and Wolburg 2000). Freeze fracture studies have shown that structurally tight junctions are formed by continuous bands of parallel intra-membrane strands of proteins, which form a series of individual barriers (Farquhar and Palade 1963; Claude and Goodenough 1973; Schneeberger *et al.* 1978), thus leading to increased electrical resistance and decreased paracellular permeability (Claude 1978). Tight junctions of the BBB are apically (blood-facing) located, with adherens junctions situated at the basal membrane (brain-facing) (see Fig. 1.3.1.1). Furthermore, in tight junctions of the BBB, components of the adherens and tight junctions are interconnected along the intercellular cleft (Schulze and Firth 1993). Experiments by Gumbiner and Simons have revealed that blocking antibodies against E-cadherin, which is essential for adherens junction formation, also prevented tight junction formation, thus indicating that functional adherens junctions are a prerequisite to tight junction formation (Gumbiner and Simons 1986). As tight junctions and adherens junctions are both biochemically and spatially distinct, it would seem that common cytoplasmic or cytoskeletal components are responsible for the interconnection

between the two junctions.

1.3.1 Tight Junction Proteins

Tight junctions are comprised of both integral membrane proteins, which span the intercellular cleft, and peripheral proteins, which function as scaffolding proteins and link the membrane proteins to the cytoskeleton.

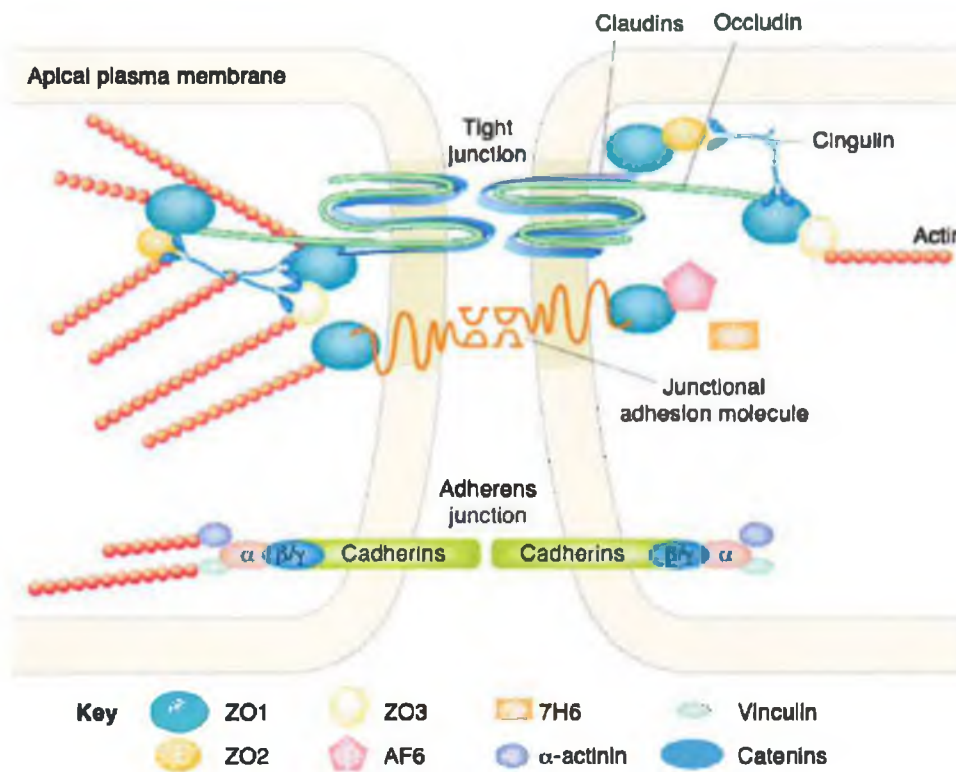


Figure 1.3.1.1: Schematic diagram of the proposed interactions of the major proteins associated with tight junctions and adherens junctions in the BBB. (Originally published in *Trends in Neuroscience* (Huber *et al.* 2001)).

As depicted above, there are three transmembrane proteins in tight junctions, occludin, claudins and junctional adhesion molecules (JAMs). Occludin is a 60-65 kDa protein, and was the first tight junction integral membrane protein to be identified (Furuse *et al.* 1993). Primarily associated with regulation of tight junction function (Hawkins and Davis 2005; Yu *et al.* 2005), the role of occludin in tight

junctions is discussed in detail in section 1.3.1.1. There are approximately 20 identified members of the claudin family of proteins, with molecular masses of approximately 23 kDa and specific distribution patterns depending on tissue localization, which are associated with the differences in tissue permeability (Furuse *et al.* 1999; Rahner *et al.* 2001; Kiuchi-Saishin *et al.* 2002). Claudins have four transmembrane domains, with a short N-terminus, two extracellular loops and a cytoplasmic C-terminal. During tight junction formation, claudins form dimers and bind homotypically to claudin strands on adjacent endothelial cells (Furuse *et al.* 1999). Claudins are anchored to the cytoskeleton via PSD-95/Dlg/ZO-1 (PDZ) binding domains that allow interaction with the zonula occludens (ZO) protein family (Itoh *et al.* 1999; Hamazaki *et al.* 2002). The third family of transmembrane proteins associated with tight junctions are the JAMs. To date, three JAMs have been identified known as JAM-A, JAM-B and JAM-C. JAMs belong to the CTX family of the immunoglobulin superfamily and are associated with formation and maintenance of tight junctions (Martin-Padura *et al.* 1998). Each of the three JAMs have extracellular V-type and C2-type domains, a single transmembrane region and a cytoplasmic C-terminus (Sawada *et al.* 2003). The cytoplasmic tail of all three JAMs can bind to cingulin, occludin, AF-6, and ZO-1 during tight junction formation (Bazzoni *et al.* 2000; Ebnet *et al.* 2000; Hamazaki *et al.* 2002).

The integral membrane proteins of tight junctions are anchored to the cytoskeleton by a complex array of peripheral proteins, which form a cytoplasmic plaque adjacent to the junctional cell membrane. Zonula occludens proteins, namely ZO-1, ZO-2 and ZO-3, belong to the large membrane-associated guanylate kinase-like proteins (MAGUKs), are critical peripheral proteins, and are discussed in detail in section 1.3.1.2. ALL-1 fusion partner from chromosome 6 (AF-6) has a PDZ binding site and interacts with ZO-1 at the N-terminal Ras-binding domain (Yamamoto *et al.* 1997). AF-6 acts as a scaffolding protein regulating cell-cell contacts in tight junction formation. The phosphoprotein, 7H6 antigen (7H6) was first identified by Zhong *et al.* in 1993, and has since been shown to play an essential role in transendothelial permeability to ions and macromolecules (Zhong *et al.* 1993; Zhong

et al. 1994; Satoh *et al.* 1996). Cingulin (140 kDa) was first identified as a peripheral tight junction protein in avian brush-border cells (Citi *et al.* 1988). Further studies have shown that in its purified form, cingulin is a heat-stable dimer, composed of two polypeptides intertwined into a “coiled coil” (Citi *et al.* 1989). Cingulin acts as a scaffolding protein, linking peripheral tight junction proteins to the cytoskeleton, and can bind ZO-1, ZO-2, myosin, JAMs and AF-6 at its N-terminus and myosin and ZO-3 at its C-terminus (Cordenonsi *et al.* 1999).

1.3.1.1 Occludin

In 1993, Furuse *et al.* raised three monoclonal antibodies from chick livers, which were specific for a ~65 kDa protein in rats. Further analysis revealed that this newly identified integral membrane protein is exclusively expressed in endothelial and epithelial tight junctions and was subsequently named occludin. DNA cloning and sequencing revealed that occludin cDNA encoded a 504 amino acid protein of 55.9 kDa. (Furuse *et al.* 1993). Occludin is a highly conserved protein with approximately 90% sequence homology between human, murine and canine forms. However, marsupial and avian occludin retain only 50% homology with the mammalian structure (Ando-Akatsuka *et al.* 1996). Moreover, despite variations in the amino acid sequence, each of the species' occludin homologues contain four transmembrane domains and retain the ability to form a coiled-coil structure within their COOH tail.

1.3.1.1.1 Occludin Structure and Function

Similar to the claudin structure, occludin contains four transmembrane domains, two extracellular loops and cytoplasmic C- and N-terminals (Fig. 1.3.1.1.1.1), however, there is no sequence homology between the two (Furuse *et al.* 1998). The four transmembrane domains divide occludin into five separate domains, referred to as domains A-E (Furuse *et al.* 1994). The cytoplasmic COOH-tail (domain E) of occludin, is rich in charged amino acids, whilst the two

extracellular loops (domains B and D) are rich in glycine and tyrosine residues.

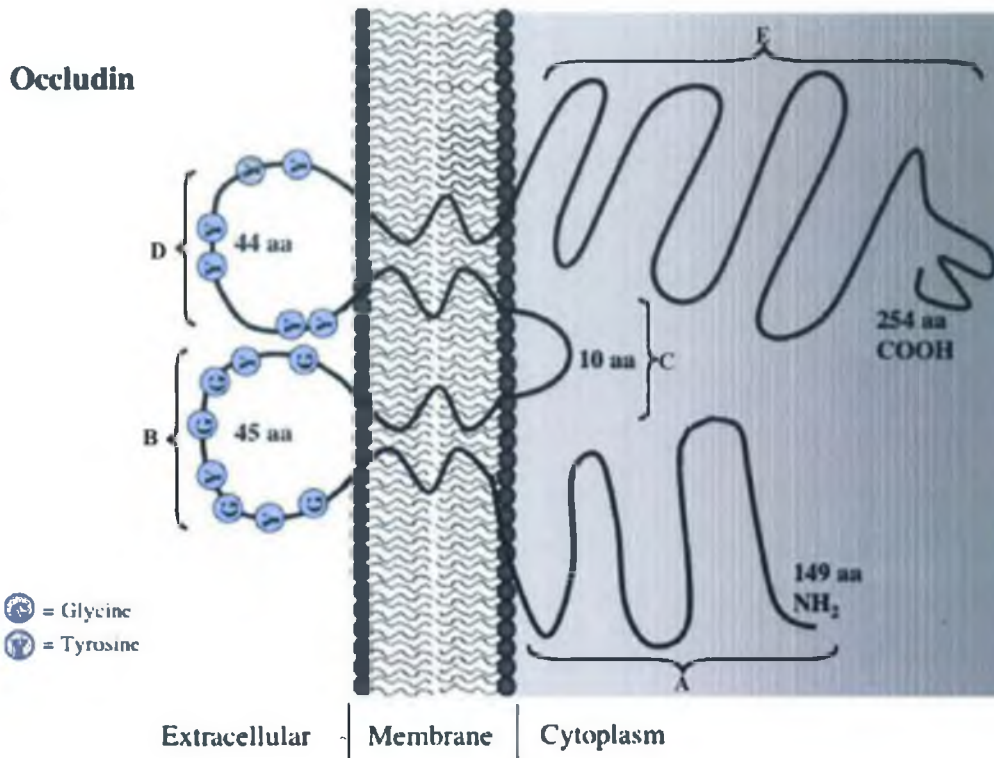


Figure 1.3.1.1.1.1: Schematic representation of occludin structure and domains. Adapted from (Feldman *et al.* 2005).

COOH-terminal fusion protein experiments by Furuse *et al.* indicated that the same sequence within domain E was necessary for both localization of occludin at the tight junction and binding to ZO-1/ZO-2 (Furuse *et al.* 1994). However, conflicting data from Balda *et al.* using COOH-terminally truncated chicken occludin indicated that the cytoplasmic domain of occludin is not essential for incorporation of occludin into the tight junction, but that it may play a regulatory role in dictating tight junction barrier function (Balda *et al.* 1996b). Further studies by McCarthy *et al.* showed that when chick occludin cDNA was transfected into Madin-Darby canine kidney (MDCK) cells, there was an increase in the number of tight junction strands and decreased permeability to mannitol (McCarthy *et al.* 1996). However, continued over expression of occludin led to an increase in paracellular permeability, without loss of transepithelial electrical resistance. McCarthy then hypothesized that

interaction of occludin with ZO-1 was necessary for occludin to function within the tight junction. They postulated that when occludin is grossly over expressed in MDCK cells that the ZO-1 pool of protein becomes saturated and that the free occludin that cannot bind to ZO-1 forms pores within the tight junction, thus increasing paracellular flux (McCarthy *et al.* 1996).

Experiments by Chen *et al.* using *Xenopus* embryos, indicated that during tight junction formation, there is oligomerization of occludin strands (Chen *et al.* 1997) and that this interaction occurs via a coiled-coil structure within the COOH terminus (Ando-Akatsuka *et al.* 1996). Subsequent studies have indicated a role for the COOH terminal in intracellular trafficking of occludin to the tight junction and that trafficking occurs via an intermediate insertion into the basolateral membrane (Matter and Balda 1998). Moreover, Mueller *et al.* have revealed that the coiled-coil domain within the C-terminus of occludin dimerizes and interacts with ZO-1 as a four-helix bundle. This four-helix bundle (406 – 521) interacts with the hinge region (591 – 632) and GuK domain (726 – 754) of ZO-1 (Muller *et al.* 2005).

While it is evident that the C-terminal of occludin is associated with binding to ZO-1 and protein trafficking, the extracellular and transmembrane domains function primarily in cell-cell adhesion and regulation of the tight junction barrier. Studies by Lacaz-Vieira *et al.* have shown that the first extracellular loop of occludin functions in sealing tight junctions by homologous interaction with occludin extracellular loops on adjacent cells (Lacaz-Vieira *et al.* 1999). They demonstrated that the sealing potential of occludin was reduced, as shown by electrical resistance readings, following addition of synthetic peptides homologous to regions of the first extracellular loop of occludin. Moreover, the second extracellular loop of occludin has been shown to modulate tight junction integrity, localization of occludin at the tight junction and overall occludin protein content within the cell (Wong and Gumbiner 1997). Further studies by Medina *et al.* have indicated a role for the second extracellular loop in trafficking occludin from the intermediate stop-off point at the basolateral membrane to the apical tight junction (Medina *et al.* 2000).

However, Balda *et al.* have shown that multiple extracellular and transmembrane domains of occludin regulate the selective paracellular permeability associated with tight junctions (Balda *et al.* 2000).

Although many studies have focused on the functions of the C-terminal, transmembrane and extracellular domains of occludin, little is known about the N-terminus. By using an N-terminally truncated occludin construct, which lacked the N-terminus and extracellular domains, Bamforth *et al.* showed that the truncated occludin associated with ZO-1 and became incorporated into the tight junction, but that barrier function was reduced (Bamforth *et al.* 1999).

The human occludin gene has been mapped to chromosome band 5q.13.1, however northern blot analysis indicates that there are several splice variants of the gene (Saitou *et al.* 1997). Mankertz *et al.* identified four splice variants of occludin, two of which (occludin II and III) do not express the fourth transmembrane domain. Both occludin II and III fail to bind to ZO-1 and show altered cellular distribution, thus indicating a role for the fourth transmembrane domain in regulating occludin trafficking and binding to ZO-1 (Mankertz *et al.* 2002). A larger form of occludin named occludin 1B has been identified as an alternative splice variant, which contained a 193 bp insertion sequence corresponding to a unique 56 amino acid N-terminal sequence (Muresan *et al.* 2000). Occludin 1B shows identical expression and localization patterns as occludin and is highly conserved throughout a range of tissues and species (Muresan *et al.* 2000). Therefore, it is possible that occludin 1B plays a putative role in regulating barrier function via the alternative insertion of occludin or occludin 1B into tight junctions.

1.3.1.1.2 Occludin Regulation

Although it has been shown that occludin can be regulated by cytokines (Jiang *et al.* 1999; Lui *et al.* 2001, 2003), proteases (Wan *et al.* 1999; Wu *et al.* 2000; Wan *et al.* 2001) and small GTPases (Gopalakrishnan *et al.* 1998; Jou *et al.* 1998; Li

and Mrsny 2000), for the most part, it would seem that occludin is primarily regulated via its phosphorylation state. The action of specific kinases and phosphatases allows the rapid phosphorylation and dephosphorylation of occludin on both serine/threonine and tyrosine residues, and appears to be a key mechanism in regulating occludin function.

Several studies have elucidated that occludin is not only expressed as a 65 kDa protein, but that it occurs in many phosphorylation states between 65 – 82 kDa (Sakakibara *et al.* 1997; Wong 1997; Farshori and Kachar 1999). Tai *et al.* demonstrated that in T84 human colon cancer cells, occludin is regulated by protein kinase C (PKC) and that inhibition of PKC using specific inhibitors led to reduced electrical resistance, indicative of loss of barrier function (Tai *et al.* 1996). Furthermore, in MDCK cells, highly phosphorylated forms of occludin on serine/threonine residues are concentrated at the tight junction and correlate with increased electrical resistance (Sakakibara *et al.* 1997). Moreover, in calcium switch experiments, which induce tight junction formation in MDCK cells, treatment with potato acid phosphatase prevented the appearance of high molecular weight (HMW) forms of occludin. Occludin was detected as low molecular weight (LMW) bands ranging from 65 – 68 kDa, thus indicating that the HMW occludin arise from the extensive phosphorylation of LMW occludin (Wong 1997). Furthermore, addition of a synthetic peptide corresponding to an extracellular domain of occludin reduced expression of HMW occludin, without significant change in LMW occludin expression, and lowered MDCK electrical resistance, thus indicating that hyperphosphorylation of occludin occurs on the extracellular loops (Wong 1997). Although phosphorylation of occludin on serine/threonine residues is associated with increased barrier function, tyrosine phosphorylation of occludin is associated with loss of tight junction integrity and increased paracellular permeability (Staddon *et al.* 1995; Gloor *et al.* 1997; Wachtel *et al.* 1999). Studies in our laboratory by Collins *et al.* have shown that the cyclic strain-induced tight junction formation in bovine aortic endothelial cells (BAEC) is associated with decreased occludin tyrosine phosphorylation. Moreover, inhibition of tyrosine dephosphorylation by

dephostatin prevented the cyclic strain-induced occludin localization at the cell membrane, indicating that tyrosine dephosphorylation is necessary for incorporation of occludin into tight junctions (Collins *et al.* 2006).

1.3.1.1.3 Occludin and Clinical Implications

Altered occludin expression, localization and phosphorylation are associated with a variety of maladies and disease states. Diarrhoea caused by bacterial infection is a major cause of infant mortality in the third world. In cases of chronic diarrhoea associated with infection by *Escherichia coli*, *Clostridium perfringens* and *Vibrio cholera*, there is often redistribution of occludin from the cell periphery, proteolytic digestion of occludin and/or dissociation of occludin from peripheral tight junction proteins (Singh *et al.* 2000; Wu *et al.* 2000; McNamara *et al.* 2001). Furthermore, *Chlamydia pneumoniae* infection and *Cryptococcus neoformans*-induced encephalitis are associated with altered occludin localization and expression within brain capillaries (MacIntyre *et al.* 2002; Chen *et al.* 2003). In addition, occludin expression is altered in numerous forms of cancer (Papadopoulos *et al.* 2001; Davies 2002; Billings *et al.* 2004; Tobioka *et al.* 2004b; Tobioka *et al.* 2004a; Tokunaga *et al.* 2004), in the blood-retinal barrier in diabetes (Antonetti *et al.* 1998; Barber and Antonetti 2003), and in some forms of inflammation (Huber *et al.* 2000) and allergies (Robinson *et al.* 2001). Moreover, occludin is a critical component of tight junctions, which give rise to the BBB, which in turn is the major rate-limiting step in neurotherapeutic drug development. Therefore, by elucidating the mechanisms of occludin regulation and function, we may be able to manipulate the “open” and “closed” state of tight junctions and thus have a profound clinical impact on a variety of diseases.

1.3.1.2 Zonula Occludens

The first tight junction protein to be identified was the peripheral membrane associated zonula occludens-1 (ZO-1) (Stevenson *et al.* 1986). There are three

known members of the zonula occludens family, ZO-1 (210 – 225 kDa), ZO-2 (180 kDa) and ZO-3 (130 kDa), all of which are ubiquitously expressed in tight junctions and adherens junctions of endothelial and epithelial cells (Anderson *et al.* 1988; Jesaitis and Goodenough 1994; Haskins *et al.* 1998). Based on their structure, the ZO proteins are members of the membrane-associated guanylate kinase (MAGUK) family and have similar structures and a large degree of sequence homology.

1.3.1.2.1 ZO-1 Structure and Function

The N-terminal half of ZO-1 contains three PDZ domains, an Src oncogene homology region 3 (SH3) and a catalytically inactive guanylate kinase (GUK) homologue. In addition, the C-terminal half contains an acidic region, a variable splice region (α -domain) and a proline-rich terminal region.

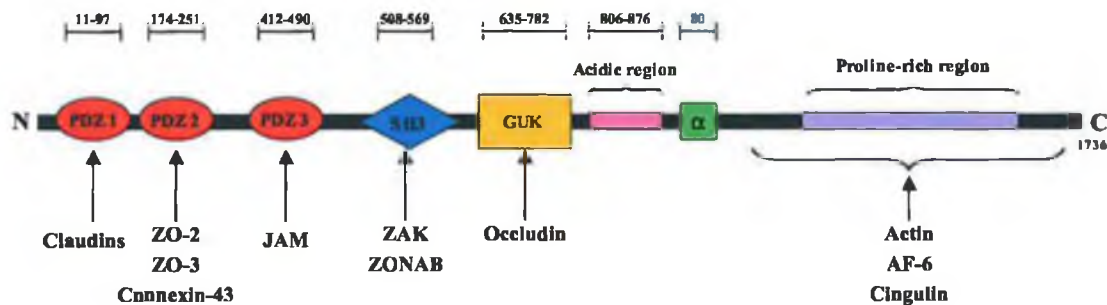


Figure 1.3.1.2.1.1: Diagrammatic representation of the structure of ZO-1 protein indicating binding domains and partners, proline-rich and acidic regions, and variable splice region- α . Numbers of amino acid from published sequences for human ZO-1 (Willott *et al.* 1993).

PDZ binding domains, found in ZO-1, are typically between 80 – 90 amino acids long and undergo folding, which forms a hydrophobic groove into which the COOH terminal of target proteins can bind (Fanning and Anderson 1999). The PDZ-1 domain of ZO-1 binds directly to the carboxy-terminal of claudins 1 – 8 (Itoh *et al.* 1999) and thus anchors the transmembrane proteins to the actin cytoskeleton. However, PDZ binding domains may also bind to other PDZ sites by forming homomeric and hetromeric complexes (Brenman *et al.* 1996). For example, ZO-1

binds to ZO-2 and ZO-3 via dimerization of their PDZ domains (Fanning *et al.* 1998; Haskins *et al.* 1998; Wittchen *et al.* 1999). In addition to binding ZO-2 and -3, PDZ-2 of ZO-1 interacts with the extreme carboxyl terminal of connexin-43 where it serves to recruit signaling proteins into gap junctions (Giepmans and Moolenaar 1998). Furthermore, studies by Bazzoni *et al.* have shown that JAM-1 co-precipitates with ZO-1 and that interaction between the two occurs via the PDZ-3 binding site on ZO-1 and a putative C-terminal binding motif on JAM-1 (Bazzoni *et al.* 2000).

ZO-1 expression in confluent epithelial and endothelial cells is in the form of a continuous submembranous plaque adjacent to tight junction strands. However, in subconfluent monolayers or at the edge of wounded monolayers, ZO-1 localizes to the nucleus (Gottardi *et al.* 1996). Moreover, the SH3 domain of ZO-1 binds to the ZO-1 nucleic acid binding protein (ZONAB), a Y-box transcription factor where it regulates gene expression, including the *erbB-2* proto-oncogene (Balda and Matter 2000). ZO-1 and ZONAB co-localize at both the tight junction and the nucleus, and bind to specific promoter sequences containing an inverted CCAAT box, through which they modulate cell cycle progression and paracellular permeability (Balda and Matter 2000). Furthermore, the SH3 domain of ZO-1 binds ZO-1-associated kinase (ZAK), a serine protein kinase which, phosphorylates serine residues in a region immediately C-terminal to the SH3 domain of ZO-1 (Balda *et al.* 1996a).

As previously stated in section 1.3.1.1.1, binding of occludin with ZO-1 is required for trafficking of occludin to the tight junction (Mankertz *et al.* 2002). The four-helix bundle of occludin binds to ZO-1 at two points; the hinge region (located N-terminally from the GUK domain 591-632) and the GUK domain, containing coiled-coil and α -helices respectively (Muller *et al.* 2005). Thus, ZO-1 acts as a linker protein and anchors occludin to the actin cytoskeleton (Fanning *et al.* 1998), although occludin can also bind directly to actin (Wittchen *et al.* 1999).

ZO-1 expression may be regulated at the post-transcriptional level by alternate

splicing. The C-terminal half of ZO-1 contains an 80 amino acid sequence termed the α -motif. Two splice variants of ZO-1 exist, ZO-1 α^+ and ZO-1 α^- , the latter lacking the 80 amino acid sequence found in ZO-1 α^+ (Willott *et al.* 1992). Epithelial and endothelial cells express both the α^+ and α^- isoforms, however, α^+ is the predominant form in epithelial cells, while α^- is preferentially expressed in endothelial cells (Balda and Anderson 1993). There is no correlation between ZO-1 isoforms and barrier function, however there is a correlation with junctional plasticity. ZO-1 α^- is associated with structurally dynamic junctions whilst α^+ is the predominant form in less dynamic junctions (Balda and Anderson 1993).

As there is a high degree of homology between the N-terminal half of ZO-1, -2 and -3, it is postulated that the C-terminal region is responsible for the specific functions of each of the three proteins at the tight junction. The C-terminal half of ZO-1 contains a proline rich domain with several PXXP motifs, which can bind to SH3 motifs (Katsube *et al.* 1998). Moreover, the C-terminal region of ZO-1 functions in binding to the actin cytoskeleton (Howarth and Stevenson 1995; Nybom and Magnusson 1996; Fanning *et al.* 1998), although the exact location and structure of the actin-binding motif is unknown. Furthermore, studies by Yamamoto *et al.* have shown that association of AF-6 with the tight junction is dependent on its interaction with ZO-1 (Yamamoto *et al.* 1997). In addition, the C-terminal region of ZO-1 binds to cingulin, a submembranous tight junction plaque protein, via its coiled-coil domain (Cordenonsi *et al.* 1999).

Thus, it would seem that ZO-1 is a multifunctional component of the tight junction. It acts as a scaffolding protein, forming a link between the transmembrane tight junction strands of occludin, claudins and JAM, and the actin cytoskeleton. Furthermore, the N-terminal of ZO-1 is involved in clustering of PDZ-expressing proteins at the submembranous tight junction plaque. Moreover, ZO-1 functions in trafficking of proteins, including occludin, to the tight junction, regulation of gene transcription via ZONAB and modulation of the cell cycle.

1.3.1.2.2 ZO-1 Regulation

ZO-1 contains several phosphorylation sites, and the post-translational regulation of its phosphorylation state impacts directly on its function and localization (Anderson *et al.* 1988; Balda *et al.* 1993; Collins *et al.* 2006).

Takeda and Tsukita demonstrated that in MDCK cells, tyrosine phosphorylation of ZO-1 correlated with a 30% reduction in electrical resistance (Takeda and Tsukita 1995). Further studies have shown that a VEGF-induced increase in rat retinal endothelial cell permeability was associated with the rapid tyrosine phosphorylation of ZO-1 (Antonetti *et al.* 1999). Moreover, studies using MDCK cells have shown that tyrosine phosphorylation of ZO-1 leads to its redistribution and decrease in barrier function (Staddon *et al.* 1995; Collares-Buzato *et al.* 1998). Therefore, it would seem that tyrosine phosphorylation of ZO-1 weakens junctional seals.

In contrast, phosphorylation of ZO-1 on serine/threonine residues increases tight junction formation and barrier function. Studies by Collins *et al.* in our laboratory have shown that following cyclic strain-induced tight junction formation, there is a significant increase in ZO-1 phosphorylation on both serine and threonine residues, which was accompanied by dramatic realignment of ZO-1 to the cell membrane. Moreover, inhibition of phosphorylation with rottlerin, a protein kinase inhibitor, completely abrogated the cyclic strain-induced ZO-1 localization (Collins *et al.* 2006). Furthermore, studies by Denisenko *et al.* have shown that inhibition of protein kinases by H-7, prevented the calcium switch-induced reorganization of ZO-1 in MDCK cells (Denisenko *et al.* 1994).

1.3.1.2.3 ZO-1 and Clinical Implications

Recent studies have shown that loss of ZO-1 is associated with poor prognosis in breast cancer. Studies by Hoover *et al.* showed that in normal breast

tissue ZO-1 staining is continuous along the epithelial cell periphery. However, in infiltrating duct carcinomas, there was a significant reduction in the amount of ZO-1 staining, and the amount of ZO-1 staining was positively correlated with tumor differentiation (Hoover *et al.* 1998).

Furthermore, *Helicobacter pylori*, a bacteria which is associated with the formation of stomach ulcers, duodenal ulcers and some forms of stomach cancer, has been shown to disrupt ZO-1 organization (Amieva *et al.* 2003). Following attachment of *H. pylori* to the cell surface, CagA protein is secreted from the bacterium into the host cell (Odenbreit *et al.* 2000). ZO-1 and JAM-1 within the cell are recruited to sites of bacterial attachment, thus leading to disruption of barrier function accompanied by alteration of the cell shape into the typical humming bird morphology associated with *H. pylori* infection (Amieva *et al.* 2003).

The faecal pellets of the common dust mite *Dermatophagoides pteronyssinus* contain both serine and cysteine peptidases. When inhaled, these peptidases cleave ZO-1 and occludin, thus leading to loss of the tight junction barrier, increased susceptibility to inhaled allergens and the induction of the immune response (Wan *et al.* 1999; Wan *et al.* 2000; Wan *et al.* 2001).

As ZO-1 is a direct target for several diseases, some of which are mentioned above, a greater understanding the diverse functions of ZO-1 and the factors which modulate it, may provide novel strategies for manipulating tight junctions.

1.4 Haemodynamics

Blood flowing through the vascular system exerts two distinct forces on the vessel wall, namely cyclic strain and shear stress. Cyclic strain is the circumferential stretch, exerted tangentially to the direction of flow on the vessel wall and is caused by the pulsatile nature of blood flow from the heart. Thus, cyclic strain is directly related to pressure and vessel dimensions. The cyclic strain force is

exerted on both the endothelium and the underlying cellular layers, i.e. smooth muscle cells in arteries and pericytes in arterioles. Shear stress is the drag force exerted on endothelial cells by the blood flowing through the vessel. The level of shear stress exerted is related to the velocity of the blood, vessel diameter and blood viscosity by the equation;

$$\tau = \frac{4\eta Q}{\pi R^3}$$

Where, τ = shear stress (dynes/cm²); η = viscosity (dyne sec/cm²); Q = flow rate (mL/sec) and R = vessel radius (cm) (Lehoux and Tedgui 2003).

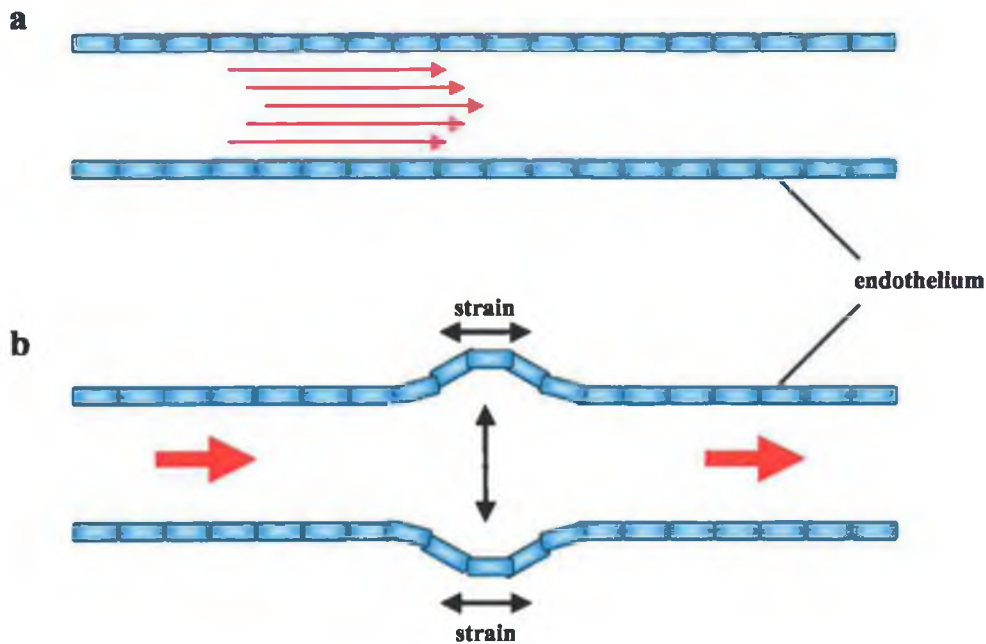


Figure 1.4.1: Schematic diagram depicting shear stress (a) and cyclic strain (b) with respect to the vascular endothelium. Red arrows indicate direction of flow.

Moreover, the forces exerted on the vessel are dependent on its position within the vascular tree. For example, major arteries, such as the aorta or pulmonary artery are exposed to high levels of both cyclic strain and shear stress, whilst veins, including

the vena cava, experience relatively high levels of shear stress but are not exposed to cyclic strain.

Cerebral capillaries, which give rise to the BBB, experience levels of shear stress ranging from 4 to 20 dynes/cm² (Desai *et al.* 2002). Although blood flow within capillaries is slow, the small vessel diameter (approx. 7 µm) results in relatively high level of shear being exerted on the endothelium. Moreover, these capillary vessels are not exposed to pulsatile cyclic strain. Extensive branching of the arteries into arterioles and then capillaries dulls the pulse pressure exerted on the vessel wall and hence, cyclic strain. Furthermore, precapillary sphincters, which encircle the capillary at the arteriole/capillary branch point, can open and close, thus regulating blood flow and pressure within the cerebral microvasculature.

Blood flow within the capillaries of the BBB is independent of perfusion pressure when autoregulation is intact (Wahl and Schilling 1993). That is, the rate of cerebral blood flow is regulated via changes in capillary resistance, rather than changes in overall systemic blood pressure. However, cerebral blood flow is not solely regulated by precapillary sphincters. On the contrary, cerebral circulation is determined by both endothelial-derived factors and paracrine interactions with astrocytes and pericytes, thus leading to the controlled dilation and constriction of the microvessels.

Nitric oxide synthase (NOS) causes the oxygen-dependent conversion of L-arginine into L-citrulline and nitric oxide (NO) (Fleming and Busse 1999). There are three known forms of NOS; neuronal NOS (nNOS), inducible NOS (iNOS) and endothelial NOS (eNOS). Both nNOS and eNOS are expressed in neurons and cerebral blood vessels, respectively (Bolanos and Almeida 1999; Benyo *et al.* 2000). NO^{*} production as a result of nNOS and eNOS activity causes dilation of cerebral vessels and increased blood flow, whilst its inhibition leads to vasoconstriction and decreases cerebral blood flow (Faraci 1991; Prado *et al.* 1992; You *et al.* 1999). Moreover, several substances including bradykinin, ATP/ADP and acetylcholine

induce dilation of cerebral blood vessels by activating G-protein coupled receptors on endothelial cells, thus leading to the production of NO, endothelium-derived hyperpolarization factor (EDHF) and/or prostanoids (You *et al.* 1997; Yamada *et al.* 2001; Bai *et al.* 2004). Furthermore, vasoconstricting substances such as endothelin-1 (ET-1), prostaglandin F_{2α} and thromboxane A₂ (TXA₂), decrease the vessel diameter and hence decrease cerebral blood flow (Patel *et al.* 1996; Smith *et al.* 1996; Pierre and Davenport 1999; Zhou *et al.* 2004). Under circumstances of compromise or loss of autoregulation within cerebral capillaries, blood flows into the vessels at high pressure and fluid passes out of the capillaries and into the interstitial space resulting in brain edema (Stamatovic *et al.* 2006).

1.4.1 Shear Stress and the BBB

Shear stress plays a pivotal role in determining endothelial cell functions. In particular, shear stress leads to profound changes in endothelial cell morphology. Early studies by Flaherty *et al.* showed that in a canine artery excised and then reinserted perpendicular to the original direction of flow, endothelial cells realigned in the direction of blood flow (Flaherty *et al.* 1972). Furthermore, shear stress has been shown to cause changes in endothelial morphology (Galbraith *et al.* 1998; Noria *et al.* 1999), gene expression (Patrick and McIntire 1995; Chien *et al.* 1998; Traub and Berk 1998) and function (Ballermann and Ott 1995; Ngai and Winn 1995; Ott and Ballermann 1995). Endothelial cells *in vivo* have a lifespan of 2.5 to 3 years (Denekamp 1993) and as such, have low rates of proliferation and apoptosis. Moreover, endothelial cells exposed to shear stress do not proliferate due to inhibition of cell cycle genes (Nagel *et al.* 1999; Akimoto *et al.* 2000; Lin *et al.* 2000).

Studies by Stannes *et al.* have indicated that shear stress is required for induction and maintenance of the BBB (Stannes *et al.* 1997). Ischemic events are associated with anoxia, aglycemia and loss of blood flow. Krizanac-Bengez *et al.* have demonstrated that loss of shear stress alone causes changes in endothelial/glial

signaling and suggest that the increase in BBB permeability associated with ischemia may be the result of a combination of factors including anoxia, loss of shear stress and aglycemia (Krizanac-Bengez *et al.* 2003). Moreover, shear stress has been shown to modulate both occludin expression and phosphorylation (DeMaio *et al.* 2001; Conklin *et al.* 2002; Pang *et al.* 2005). However, these studies were carried out on macrovascular cells and do not address the specific functions of the brain microvasculature.

Moreover, pathologies exhibiting reduced barrier function with associated leakage frequently manifest elevated or reduced hemodynamic loading and/or associated mechanotransduction, either of which may contribute to endothelial dysfunction/injury (leading to inflammation and vessel wall remodeling) or stem from changes in blood pressure and heart rate. Within the context of vascular health and pathology therefore, force-mediated regulation of tight junction assembly and function is extremely relevant, albeit very poorly understood.

1.4.2 Mechanotransduction

Mechanotransduction is the process by which cells detect physical stimuli, such as cyclic strain and shear stress, and translate them into signaling cascades, which in turn mediate a cellular response. Mechanotransduction of shear stress is a multi-faceted signaling event, with mechanical sensing of shear stress occurring on both the abluminal and luminal endothelial surfaces (Shyy and Chien 2002). However, the location of the mechanosensor responsible for translating cellular mechanical distortion into biological signals is somewhat controversial (Davies 1995). Mechanotransduction of shear stress involves many receptors including ion channels, G-proteins, integrins and the endothelial glycocalyx, among others, some of which are discussed below.

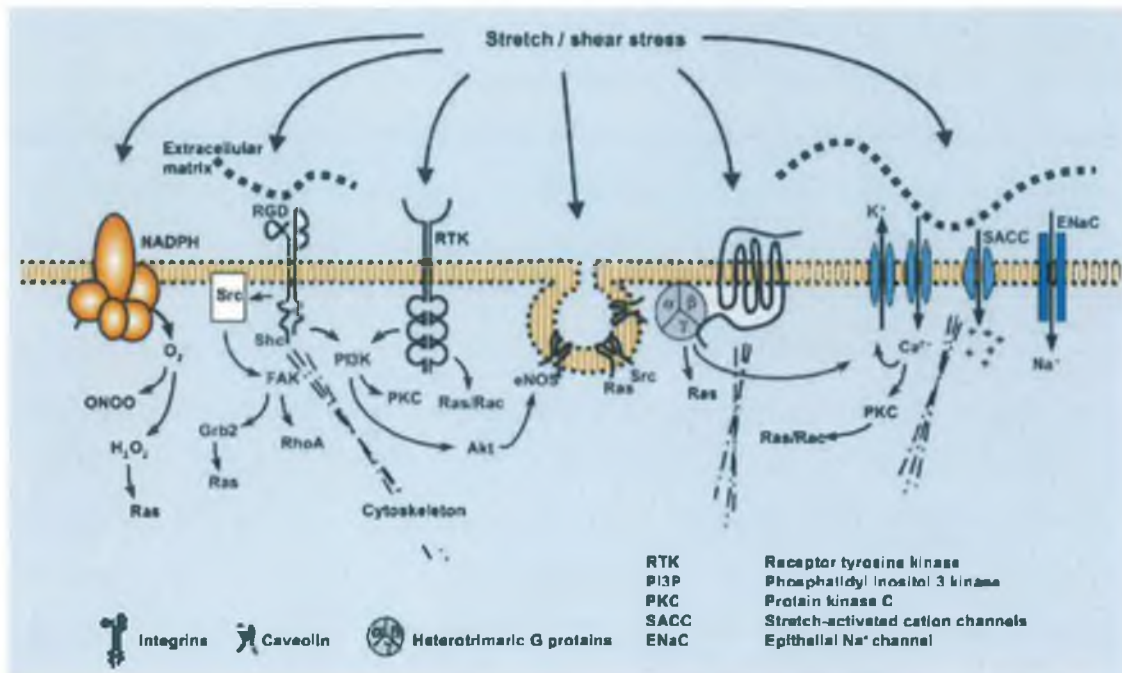


Figure 1.4.2.1: Schematic representation of receptors involved in initiating signaling cascades in endothelial cells stimulated by haemodynamic forces. (Originally published in *J Intern Med* (Lehoux *et al.* 2006))

1.4.2.1 Mechanosensitive Ion Channels

Mechanosensitive ion channels are one such potential mechanosensor. Located at the plasma membrane, ion channels are ideally situated to convert mechanical forces from shear stress into electrical or ion-dependent cellular responses (Gillespie and Walker 2001). Studies by Olesen *et al.* have shown that endothelial cells exposed to shear stress of ~ 20 dynes/cm² resulted in hyperpolarization of the cells as a result of an inward-rectifying K⁺ current (Olesen *et al.* 1988). Further studies have also shown that plasma membrane permeability to K⁺ increases in response to shear stress (Alevriadou *et al.* 1993; Hutcheson and

Griffith 1994). In addition, the nonselective cation channel has also been implicated in mechanotransduction, which would account for the influx of Ca^{2+} observed in endothelial cells under shear conditions (Schwarz *et al.* 1992b; Schwarz *et al.* 1992a; MacRobbie 1998). However, it is not yet clear whether the ion channels are merely mechanosensitive or the actual cellular mechanosensor. In the former case, a mechanosensor located elsewhere in the cell would detect shear stress and induce a signaling cascade resulting in the activation of the ion channel. In the latter case, it is plausible that ion channels are mechanosensors and that they are directly activated by shear stress.

1.4.2.2 The Role of G-Proteins in Mechanotransduction

G-proteins have also been implicated in modulating mechanotransduction in endothelial cells in response to shear stress (Berthiaume and Frangos 1992). G-protein coupled receptors (GPCR) are integral membrane proteins consisting of seven transmembrane domains. The extracellular loops are responsible for ligand binding, whilst the intracellular loops and cytoplasmic tail interact with heterotrimeric G-proteins consisting of α , β and γ subunits. Upon ligand binding, guanosine diphosphate (GDP) dissociates from the α -subunit and is replaced by guanosine triphosphate (GTP). Binding of GTP results in release of the $\beta\gamma$ and α components, which in turn bind to and activate effector molecules (Wieland and Mittmann 2003). Following hydrolysis of GTP by the α subunit, the heterotrimer reassociates.

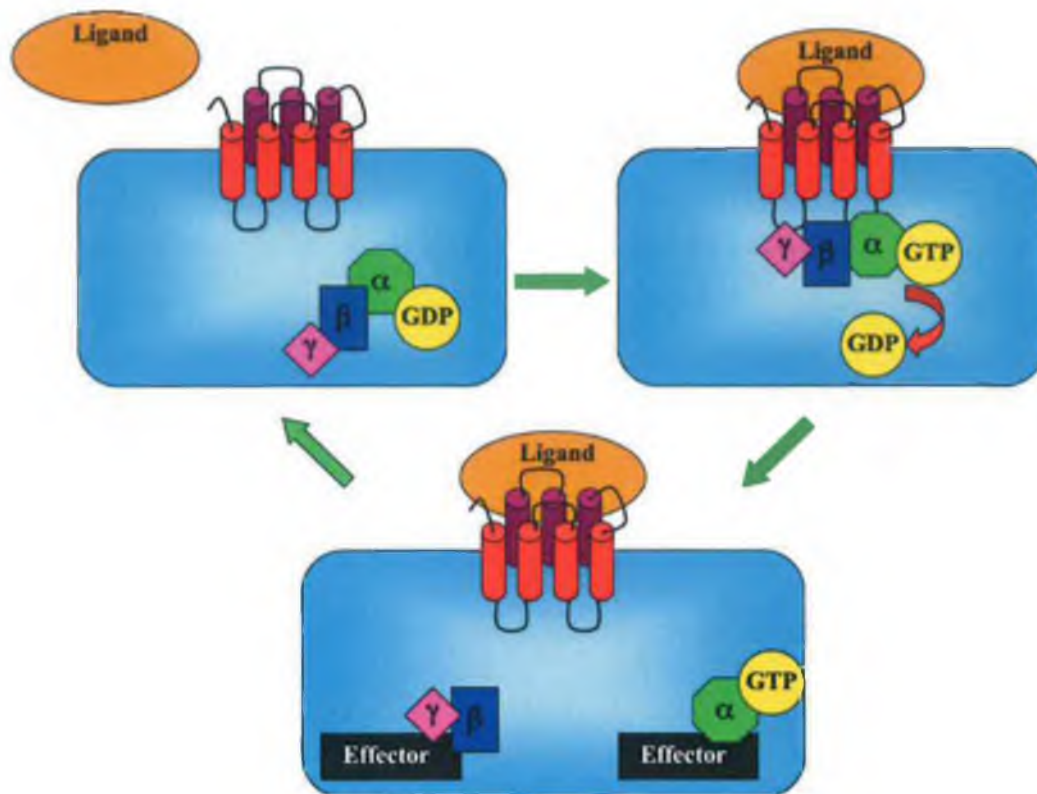


Figure 1.4.2.2.1: Schematic diagram depicting G-protein activation and hydrolyses.

G-proteins have been shown to mediate several signaling pathways in response to shear stress. Studies by Gudi *et al.* have shown that shear stress ranging from 0 – 30 dynes/cm² increased G-protein activity in a dose-dependent manner (Gudi *et al.* 1998). Additional studies by Gudi *et al.* have shown that rapid activation of Ras occurs following exposure of endothelial cells to shear stress, and that this activation is mediated by heterotrimeric G-protein subunits (Gudi *et al.* 2003). Furthermore, G proteins modulate both the activation of c-jun N-terminal kinase (JNK) and the mitogen-activated protein kinase (MAPK) pathway (Ishida *et al.* 1996; Takahashi and Berk 1996; Jo *et al.* 1997) in response to shear stress. However, although it is clear that G-proteins are involved in the early responses to mechanical stimuli, to date no endothelial mechanosensitive GPCR has been

identified. Thus, although G proteins are involved in mechanotransduction, their role as a mechanosensors is yet to be determined.

1.4.2.3 The Role of Integrins in Mechanotransduction

Integrins are membrane-associated glycoproteins composed of non-covalently linked α and β subunits. There are 18 α - and 8 β - subunits, which can form 24 unique heterodimeric complexes, 7 of which are expressed on endothelial cells (Rupp and Little 2001). Each of the subunits has a large extracellular domain, which binds directly to extracellular matrix (ECM) proteins such as fibronectin, laminin, collagen and vitronectin. The subunits' cytoplasmic domains interact with cytoskeletal proteins and signaling molecules where they regulate integrin affinity and avidity (Shyy and Chien 2002). Integrin affinity is modulated via changes in the heterodimer conformation that leads to increased ligand binding, whilst integrin avidity modulation involves clustering of integrins at focal adhesion sites (Giancotti and Ruoslahti 1999; Schoenwaelder and Burridge 1999). Findings that several signaling pathways activated by integrins are also activated by shear stress suggests that integrins may be involved in mechanotransduction in endothelial cells (Shyy and Chien 1997). Recent studies indicate that integrin affinity and avidity are modulated by shear stress (Jalali *et al.* 2001; Tzima *et al.* 2001). Furthermore, incubation of endothelial cells with integrin blocking antibodies prior to shear prevented shear-dependent activation of ERK, JNK and I κ B kinase (Li *et al.* 1997; Bhullar *et al.* 1998). Moreover, inhibition of integrins using Arg-Gly-Asp (RGD) peptides prevented shear stress-induced secretion of bFGF by endothelial cells (Gloe *et al.* 2002) and abolished the anti-apoptotic effect of shear stress (Urbich *et al.* 2000). Although shear stress leads to conformational activation of integrins and increased binding to the ECM (Jalali *et al.* 2001), it is not known if integrins are mechanosensors or just mechanosensitive complexes.

1.4.2.4 The Role of the Endothelial Glycocalyx in Mechanotransduction

One recent publication highlights the possible role of the endothelial glycocalyx (EG) as a mechanosensor (Thi *et al.* 2004). The EG is comprised of heparan sulfate, chondroitin and hyaluronan protein strands and is expressed on the apical surface of endothelial cells (Ihrcke *et al.* 1993; Henry and Duling 1999; Florian *et al.* 2003). Studies by Florian *et al.* demonstrated that partial removal of heparan sulphate proteoglycan from the EG prevented shear-induced NO in endothelial cells (Florian *et al.* 2003). The EG is anchored to a geodesic-like scaffold of hexagonally arranged filamentous actin (F-actin), which forms the actin cortical web (ACW) just below the cell membrane (Squire *et al.* 2001). Thi *et al.* propose a model in which proteins of the EG form stiff bristles, which transmit the fluid drag on their tips, caused by shear stress, to a bending motion that acts on the ACW (Thi *et al.* 2004). Moreover, disruption of the EG prevented shear stress induced F-actin realignment, thus it is plausible that the EG acts as a mechanosensor in endothelial cells exposed to shear stress.

1.5 Summary

The BBB constitutes a physical and metabolic barrier, preventing blood-borne solutes from entering into the brain ISF. Disruption of the BBB is associated with multiple disease states, whilst the tightness of the barrier proves a major obstacle for drug development and delivery. Regulation of occludin and ZO-1, two pivotal tight junction proteins are essential for the formation and function of the BBB. Brain microvascular endothelial cells forming the BBB are encircled at the basolateral membrane by astrocyte end feet in serum-free conditions and are exposed to shear stress, caused by the flow of blood through capillaries, on their apical surface. The purpose of this study is to examine how basolateral and apical conditions (serum, astrocytes and shear stress) collectively impact upon tight junction assembly and function within the brain microvasculature. Elucidation of how the BBB is regulated by physiological and pathological stimuli will greatly

enhance our understanding of BBB assembly and may provide novel therapeutic strategies to modulate barrier integrity, thus having profound clinical impact on several neurological diseases and facilitate drug delivery to the brain.

1.6 Thesis Overview

The research data presented in the following chapters examines the role of physiologically relevant factors on tight junction formation and barrier function in BBMvECs. Emphasis is placed on the expression, localization and association of the transmembrane tight junction protein, occludin and the peripheral tight junction plaque protein, ZO-1. Permeability and electrical resistance studies are employed to extrapolate if there is a correlation between occludin/ZO-1 regulation and endothelial barrier function. These findings are presented in the following manner:

Chapter 3 Optimisation of cell culture media and characterization of the model.

Chapter 4 Examination of the polar-specific effect of serum on endothelial tight junction formation and barrier function.

Chapter 5 Investigation of the role of C6 glioma in regulating BBMvEC occludin and ZO-1 and the effect of co-culture on BBMvEC permeability.

Chapter 6 Assessment of the role of laminar shear stress on BBMvEC tight junction formation and barrier function.

Chapter 2

Materials and Methods

2.0 Material & Methods:

All reagents used in this study were of the highest purity commercially available and were of cell culture standard when applicable.

2.1 Materials:

Acros Organics (New Jersey, USA)

Formaldehyde (37%)

AGB Scientific (Dublin, Ireland)

Whatmann Chromatography paper

Amersham Pharmacia Biotech (Buckinghamshire, UK)

Anti-mouse 2⁰ antibody, HRP-conjugated

Anti-rabbit 2⁰ antibody, HRP-conjugated

ECL Hybond nitrocellulose membrane

ECL Hyperfilm

Rainbow molecular weight marker, broad range (6-175kDa)

Bio Sciences Ltd (Dun Laoghaire, Ireland)

DEPC-treated water

Trizol® reagent

Cell Applications (San Francisco, USA)

Bovine Brain Microvascular Endothelial Cells

Chemicon International (CA, USA)

bFGF – Recombinant Human Fibroblast Growth Factor-Basic

Corning (Buckinghamshire, UK)

Transwell®-Clear Polyester (PET) Membrane inserts

DakoCytomation (Glostrup, Denmark)

Polyclonal Rabbit Anti-Human Von Willebrand Factor

Polyclonal Rabbit Anti-Glial Fibrillary Acidic Protein

Fluorescent Mounting Media

Fisher Scientific (Leicestershire, UK)

Buffer solution pH 4 (phthalate)

Buffer solution pH 7 (phosphate)

Buffer solution pH 10 (borate)

Gibco (Scotland, UK)

Fetal calf serum

UltraPURE™ Distilled Water DNase-, RNase-Free

Molecular Probes (Oregon, USA)

Alexa Fluor® 488 F(ab')₂ fragment of goat anti-mouse IgG (H+L)

Alexa Fluor® 488 F(ab')₂ fragment of goat anti-rabbit IgG (H+L)

MWG Biotech (Milton Keynes, UK)

GAPDH primer set

Occludin primer set

ZO-1 primer set

Nalgene

Cryogenic vials

Cryo freezing container

National Diagnostics (Georgia, USA)

Ecoscint-H

PALL Corporation (Dun Laoghaire, Ireland)

Biotrace nitrocellulose membrane

Pierce Chemicals (Cheshire, UK)

BCA protein assay kit

Supersignal West Pico chemiluminescent substrate

Sarstedt (Drinagh, Wexford, Ireland)

1.5 mL micro tube with safety cap

10, 200 and 1000 μ L pipette tips

15 and 50 mL falcone tubes

25 mL sterilin tubes

5, 10 and 25 mL serological pipettes

6 mL scintillation vials

6-well tissue culture plates

T-175 tissue culture flasks

T-25 tissue culture flasks

T-75 tissue culture flasks

Scientific Imaging Systems (Eastman Kodak Group, Rochester, NY)

Kodak 1D image analysis software

Sigma Chemical Company (Poole, Dorset, England)

2-propanol

Ammonium Persulfate

Agarose

Bovine Serum Albumin

Brightline Haemocytomoeter

Bromophenol Blue

Chloroform

Cycloheximide – C7698
DMEM – High glucose D5796
Glycine
Hanks Balanced Salt Solution
Heparin
Hydrochloric Acid
Lauryl Sulfate (i.e. Sodium Doecyl Sulphate (SDS))
Penicillin-Streptomycin (100x)
Phosphatase Inhibitor Cocktail
Ponceau S Solution
Protease Inhibitor Cocktail
Potassium Chloride
Potassium Phosphate
Potassium Phosphate-Dibasic Trihydrate
Potssium Hydroxide
Sodium Chloride
Sodium Orthovanadate
Sodium Phosphate-Dibasic anhydrous
Sodium Phosphate-Monobasic anhydrous
Triton® X-100
Trizma Base
Trypsin-EDTA (10x)
Tween® 20

Zymed Laboratories (CA, USA)

Mouse anti-Occludin monoclonal antibody
Mouse anti-ZO-1 monoclonal antibody

2.2 Cell Culture Methods

All cell culture procedures were carried out under clean, sterile conditions using a Bio Air 2000 MAC laminar flow unit. Cells were monitored daily using an Olympus CK30 phase contrast microscope.

2.2.1 Culture of Bovine Brain Microvascular Endothelial Cells (BBMvECs)

Cryopreserved passage two differentiated BBMvECs were obtained from Cell Applications Inc., California, USA (Cat No. B840-05). Brain tissue was acquired from Talone's Custom, a California Department of Food and Agriculture approved and licensed facility, which was derived from animals with no history of clinical signs of infectious diseases. The cell line was tested free from contamination with bacteria, mycoplasma or fungi and showed no signs, including cytopathic effects, of contamination with any adventitious microbial (including viral) contaminants prior to shipping. Cells were characterized as endothelial by positive Dil-Ac-LDL uptake. Upon delivery, cells were maintained in high glucose DMEM supplemented with 100 U/mL penicillin, 100 µg/mL streptomycin, 10% v/v FCS, 3 µg/mL Heparin and 3 ng/mL bFGF. Cells were cultured in T25 cm², T75 cm² and T175 cm² flasks and 6 well plates. For co-culture and serum studies, cells were grown on Transwell[®]-Clear, tissue culture treated polyester membrane filter inserts in the 6 well format with 0.4 µm pore size and 24 mm filter diameter. All experiments were carried out on cells between passage 5 – 15 and cells were maintained in a humidified atmosphere of 5% v/v CO₂ at 37⁰C.

2.2.2 Culture of C6 Glioma Astroglial Cells

Proliferating C6 glioma cells were a kind gift from Prof. Ciaran Regan, University College Dublin. The C6 glioma cell line is a rat brain glial cell, originally cloned by Benda *et al.* (Benda *et al.* 1968) from a rat glial tumor induced by N-nitrosomethylurea. Cells were maintained in high glucose DMEM

supplemented with 100 U/mL penicillin and 100 µg/mL streptomycin, 10% v/v FCS, 3 µg/mL Heparin and 3 ng/mL bFGF. Cells were cultured in T75 cm² and T175 cm² flasks. For co-culture studies, C6 glioma cells were grown 6 well plates for 24 h prior to addition of the Transwell®-Clear inserts on which the BBMvECs were grown. Cells between passage 30 – 37 were used for all experiments and were maintained in an humidified atmosphere of 5% v/v CO₂ at 37⁰C.

2.2.3 Preparation of C6 Glioma Astrocyte-Conditioned Media

To prepare C6 glioma astrocyte-conditioned media (C6 ACM), C6 glioma cells in a T75cm² flask at 80% confluence were washed twice in HBSS after which 15 mL of serum-containing or serum-free media was added to the flask. After 24 h, the conditioned media was removed and centrifuged at 1,000 g for 5 min at 4⁰C to remove any cell debris. Prior to usage, the conditioned media was mixed 50:50 with fresh media to reconstitute any nutrients, which may have been depleted by the C6 glioma. At this point, the C6 ACM was either used or stored at -80⁰C for up to 1 month.

2.2.4 Trypsinization of BBMvECs and C6 Glioma

As both BBMvECs and C6 gliomas are adherent cell lines, trypsinization was required for their sub-culture. Briefly, growth media was removed by aspiration and the cells washed in Hank's balanced salt solution (HBSS) to remove α-macroglobulin, a trypsin inhibitor present in FCS. An appropriate volume of trypsin/ethylenediamine tetracetic acid (10% v/v Trp/EDTA in HBSS) was subsequently added to the cells and incubated for 1 – 2 min at 37⁰C, until the cells were rounded, but not fully detached, and then tapped briefly to detach them from the growth surface. Growth media containing FCS was added to prevent further trypsinization and cells removed from suspension by centrifugation at 1,000 g for 5 min at 4⁰C. Cells were resuspended in growth media or freeze media and either,

counted using a bright line haemocytometer for experiments, split at a 1:5 ratio or cryopreserved.

2.2.5 Cryogenic Preservation and Recovery of Cells

For long-term storage of cells, BBMvECs and C6 glioma were stored in a cryofreezer unit (ThermoFisher Locator Jr. cryostorage system). Following trypsinization, cells were centrifuged at 1,000 g for 5 min at 4°C and supernatant was removed. The resultant pellet was resuspended in an appropriate volume of freezing media (high glucose DMEM supplemented with 20% v/v FCS, 10% DMSO (Dimethyl sulfoxide), 1% P/S, 3 µg/mL Heparin and 3 ng/mL bFGF) and transferred in 1 mL aliquots to Nalgene cryogenic vials and frozen in a -80°C freezer at a rate of -1°C/min in a Nalgene cryo freezing container. Cryovials were stored in the cryofreeze unit until required.

For recovery of cells, cryovials were heated rapidly in a 37°C water bath and added to a T 75cm² flask containing 15 mL of growth media to dilute the DMSO. After 24 h, the media was removed, the cells were washed in HBSS and fresh growth media was added.

2.2.6 Cell Counts

Following trypsinization, cell counts were performed using a brightline haemocytometer in conjunction with Trypan blue staining to assess cell viability. 20 µL of trypan blue was added to 100 µL of cell suspension and incubated at room temperature for 2 min. 20 µL of this suspension was added to the counting chamber of the haemocytometer and visualized under phase contrast microscopy. Dead cells stained blue, whilst viable cells excluded the dye and appeared colourless. The number of viable cells was calculated according to the equation:

$$\text{Avg. cell no.} \times 1.2 \text{ (dilution factor)} \times 1 \times 10^4 \text{ (area under coverslip)} = \text{Viable cells/mL}$$

2.2.7 Serum and Co-culture Studies

For serum and co-culture studies, BBMvECs were seeded at 1×10^4 cells/cm² on Transwell®-Clear, tissue culture-treated polyester membrane filter inserts in the 6 well format with 0.4 µm pore size and 24 mm filter diameter, and allowed to come to confluence, typically 5 – 7 days.

For serum studies, confluent inserts were washed twice with HBSS and transferred to 6 – well plates with serum-containing media in the apical compartment and either serum-containing or serum-free media in the basolateral compartment.

For co-culture studies, confluent inserts were washed twice and transferred to 6 – well plates containing C6 glioma which, had been seeded 24 h earlier at a density of 1×10^4 cells/cm², and the appropriate serum-containing or serum-free media in the basolateral compartment.

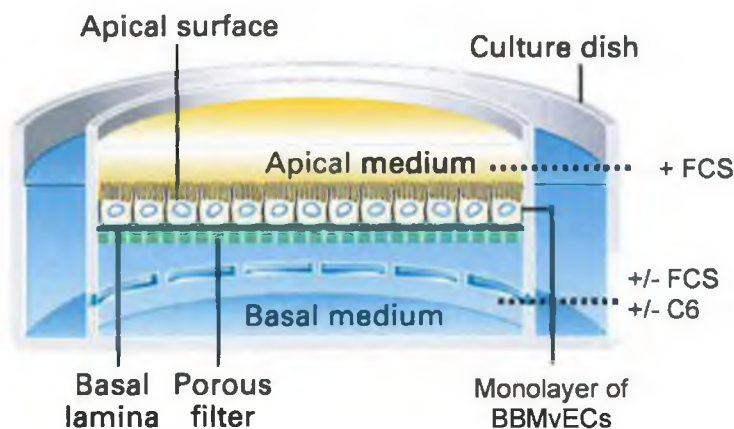


Fig. 2.2.7.1: Schematic diagram of the Transwell®-Clear culture system: Transwell®-Clear inserts have microscopically clear membranes with 0.4 µm pores, thus facilitating co-culture studies without mixing of the two cell types.

2.2.8 Non-pulsatile Laminar Shear Stress Studies

For laminar shear stress studies, BBMvECs were seeded at 1×10^4 cells/cm² in 6 well plates and allowed to come to confluency, typically 5 – 7 days. Following this, media was removed and replaced with 4 mL of fresh growth media. Cells were then sheared at 10 dyne/cm² for 24 h on an orbital shaker (Stuart Scientific Mini Orbital Shaker OS) set to the appropriate RPM as determined by the following equation (Hendrickson *et al.* 1999).

$$\text{ShearStress} = \alpha \sqrt{\rho n (2\pi f)^3}$$

Where

α = radius of rotation (cm)

ρ = density of liquid (g/L)

$n = 7.5 \times 10^{-3}$ (dynes/cm² at 37⁰C)

f = rotation per second

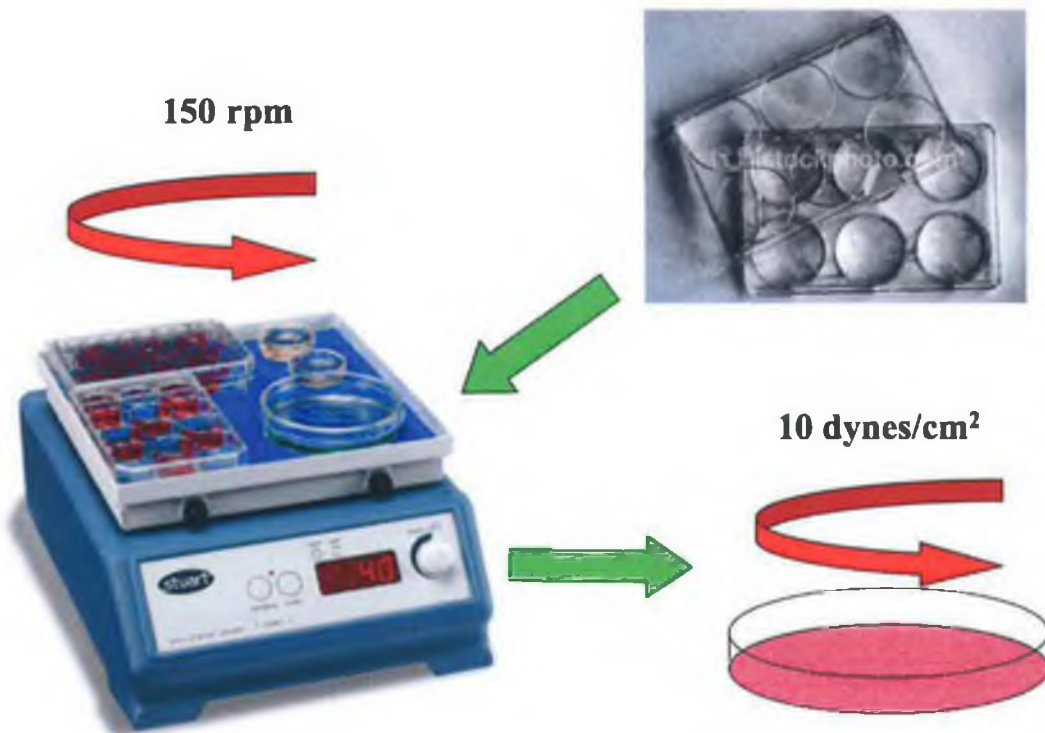


Figure 2.2.8.1: Apparatus used in non-pulsatile laminar shear stress studies.

2.2.9 Perfused Transcapillary System

The perfused transcapillary culture apparatus (Cellmax Quad™ artificial capillary culture system) consists of an enclosed bundle of 50 semi-permeable, Pronectin™ coated polypropylene capillaries (capillary length 13 cm; outer diameter 630 μm , wall thickness 150 μm , luminal area 70 cm^2 , outer surface area 100 cm^2 , extra-capillary volume 1.4 mL, 95% MWCO 0.5 μm) through which medium from a reservoir is pumped at a chosen flow rate via silicone rubber tubing. As the gear pump rotates, the motor shaft forces the pump pins to depress the pump tubing on the capillary module, thereby forcing culture media to flow in a pulsatile fashion through the gas-permeable silicone flow path tubing and through the capillary (Figure 2.2.9.1). By altering the flow rate using an electronic control unit housed outside the humidified incubator, varying pulsatile flow rates and hence pulse heights (pressure) can be achieved in this system.

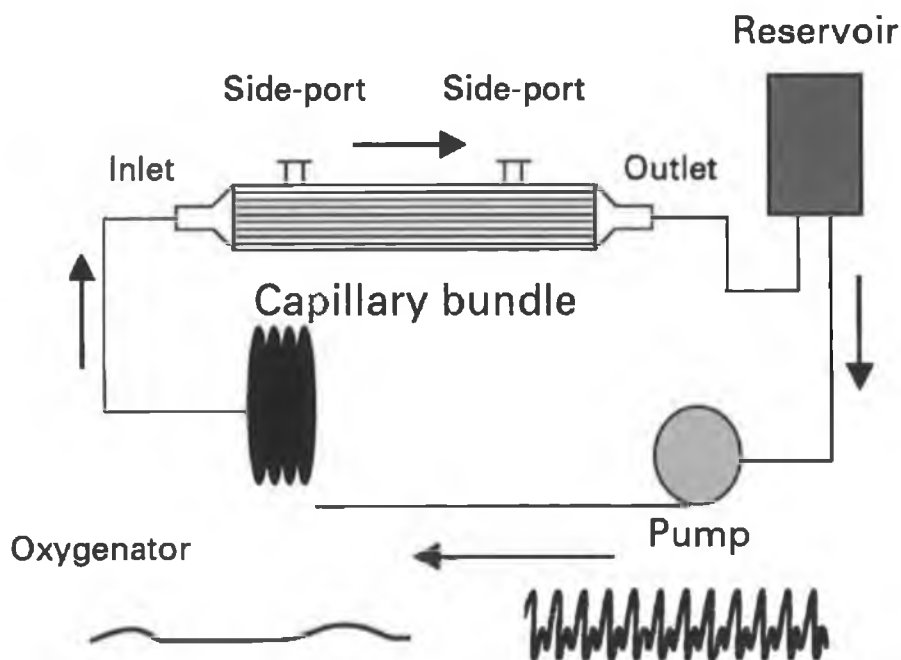


Figure 2.2.9.1 Schematic of the Perfused Transcapillary system: demonstrating the normal flow path of the perfusing medium via inlet and outlet ports and through the luminal spaces. Below: wave forms generated at 'low' (left) and 'high' flow (right).

Flow rate (mL/min) was converted to shear stress (dynes/cm²) according to the following equation:

$$\tau = \frac{4\eta Q}{\pi R^3}$$

Where: η = Fluid viscosity (0.008 dyne sec/cm², media + 10% FCS)
 Q = Fluid flow rate per fiber (mL/sec)
 R = Internal fiber radius (cm)

To maintain pH, pCO₂, and pO₂ of the culture media at constant levels, the perfused transcapillary culture system was housed in a humidified atmosphere in a standard CO₂ incubator, thereby allowing gaseous exchange to occur through the silicone rubber tubing. Prior to the addition of cells, the module is equilibrated for 3 days by circulation of culture media through the capillaries and tubing.

For perfused capillary studies, BBMvECs from culture flasks of equivalent or greater surface area were trypsinized according to the methods outlined in section 2.2.4, suspended in 10 mL of growth medium and injected into the luminal compartment using a double syringe method. Briefly BBMvECs are introduced with a syringe into one luminal port and triturated gently through the lumen three times to ensure even distribution of the cells. Displaced media is drawn off using a syringe through one of the extracapillary space (ECS) ports. Cells are allowed to adhere for 3 hours, after which the pump is set to low flow (0.3 mL/min; pulse pressure of 6mmHg; shear stress of 0.2 dynes/cm²) and returned to the incubator for 10 days. The number of cells that did not adhere were routinely counted to measure seeding density and adherence after the pump has been turned back on to ensure maximal coverage of each capillary. The harvested cells were then routinely counted at the end of each experiment to confirm uniform seeding density and adherence. To obtain 'high flow' the flow rate is increased steadily over approximately 5 hours until the desired high flow rate of 19 mL/min (14 dynes/cm²) is reached (t = 0). After completion of the experimental time-course, cells are harvested by first washing

both the luminal and extracapillary space with Hanks Balanced Salt Solution (HBSS) using the double syringe method, and removing the remaining cells by treatment with trypsin-EDTA.

2.2.10 Inhibitor Studies

In order to inhibit new protein synthesis at the ribosomal level, cycloheximide was used at a final concentration of 1 µg/mL. Cells were incubated for 1 h in the presence of cycloheximide prior to treatment (i.e. shear, co-culture or serum removal).

2.2.11 Immunocytochemistry

In order to visually monitor the expression and/or subcellular localization of proteins, cells were prepared for immunocytochemical analysis as previously described (Groarke *et al.* 2001) with minor modifications. Cells were washed twice in phosphate buffered saline (PBS) and fixed with 3% formaldehyde for 15 min. Cells were subsequently washed, permeabilised for 15 min with 0.2% Triton X-100 and blocked for 30 min in 5% BSA solution. Following blocking, cells were incubated with the appropriate primary antiserum or stain as indicated in table 2.2.11.1, followed by 1 h incubation with 1:400 dilution of either Alexa Fluor 488 anti-mouse or anti-rabbit fluorescent secondary antiserum. Nuclear DAPI staining was routinely performed by incubating cells with 0.5×10^{-6} µg/mL DAPI for 3 min. Cells were sealed with coverslips using DAKO mounting media (DAKO Cytomation, Cambridgeshire UK) and visualized by standard fluorescent microscopy (Olympus BX50).

Primary Antiserum/Stain	Concentration/Dilution	Time (h)
GFAP	1:1000	3
Occludin	8 µg/mL	3
Rhodamine Phalloidin	1:200	1
Von-Willebrand	1:1000	3
ZO-1	0.25 µg/mL	2

Table 2.2.11.1: Tabulated data for specific primary antisera and protein stain parameters.

2.2.12 Transendothelial Electrical Resistance

Transendothelial electrical resistance (TEER) is routinely used to monitor endothelial proliferation and barrier function (Francis *et al.* 1999; Grant *et al.* 1999; Liu *et al.* 1999). As a cellular monolayer forms there is a sharp increase in TEER. Moreover, when tight junctions are formed between adjacent endothelial cells, barrier function increases concomitant with an increase in TEER.

TEER was measured in BBMvEC monolayers using an EVOM™ Epithelial Voltohmmeter (WPI, Sarasota) and ENDOHM-24 Snap measurement chamber. The EVOM™ Epithelial Voltohmmeter produces an AC current, which avoids the adverse effects of DC currents, and measures the amount of resistance provided by the monolayer. The amount of resistance detected is proportional to endothelial barrier function.

In order to measure TEER, Transwell® inserts were placed in the ENDOHM-24 Snap measurement chamber with 1 mL of electrolyte in the apical compartment and 3.5 mL in the basolateral compartment. The resistance of each insert was assessed in triplicate. For all TEER studies, serum-free DMEM, without antibiotics, was used as the electrolyte solution.

2.2.13 Permeability Studies

To measure barrier function in BBMvECs, tracer studies using ^{14}C sucrose were employed. In the case of Transwell® studies, 0.1 μCi of ^{14}C sucrose was added to the apical compartment and diffusion of sucrose allowed to proceed for 60 – 120 minutes as previously described (Berezowski *et al.* 2004). Media samples (100 μL) were collected every 15 min from the basolateral compartment. % Trans Endothelial Exchange (%TEE) of ^{14}C sucrose is expressed as the total subluminal concentration of ^{14}C sucrose at a given time point (from 0-120 min) expressed as a percentage of total abluminal concentration of ^{14}C sucrose at $t=0$ min.

Following laminar shear stress studies in 6-well plates, cells were trypsinized and replated into Transwell®-Clear plates at 2.5×10^5 cells/cm². After 24 h when cells were confluent, transendothelial permeability was measured as previously described (Collins *et al.* 2006). At $t=0$, fluorescein isothiocyanate (FITC)-labelled dextran (40 kDa, Sigma-Aldrich) was added to the abluminal chamber (to give a final concentration of 250 $\mu\text{g}/\text{mL}$) and diffusion of dextran across the monolayer allowed to proceed at 37°C for 2 h. Media samples (30 μL) were collected every 30 min from the subluminal compartment and monitored in triplicate (7 μL sample + 93 μL media) for FITC-dextran fluorescence at excitation and emission wavelengths of 490 and 520 nm, respectively (Perkin-Elmer Luminescence Spectrometer LS50B with microplate reader attachment). % Trans Endothelial Exchange (%TEE) of FITC-dextran 40 kDa is expressed as the total subluminal fluorescence at a given time point (from 0-120 min) expressed as a percentage of total abluminal fluorescence at $t=0$ min.

For perfused capillary studies, after 24 h of either high or low shearing, the pumps were stopped and 2 μCi of ^{14}C sucrose was added to each reservoir. The pumps were returned to their high and low settings and the diffusion of ^{14}C sucrose was allowed to proceed for 3 h. Media samples (approximately 100 μL) were collected every 15 minutes by briefly stopping the pumps, applying clamps to the luminal inlet

and outlet tubing, inserting a syringe needle into the ECS port and removing a media sample. All samples were subsequently assessed in triplicate for ^{14}C -sucrose concentrations by scintillation counting as outlined in section 2.2.14. % Trans Endothelial Exchange (%TEE) of ^{14}C sucrose is expressed as the total ECS concentration of ^{14}C sucrose at a given time point expressed as a percentage of total reservoir concentration of ^{14}C sucrose at $t=180$ min. Due to difference in flow rates used, the ^{14}C -sucrose in the high flow system comes into contact with the capillary bundle approximately 60 minutes prior to the low flow system. Therefore, for scintillation permeability studies, it was necessary to adjust the time scale for low flow from “actual time” to a “comparative time scale” (i.e. time ^{14}C -sucrose is first detected in the ECS). No significant difference in permeability was found in capillaries without cells under low and high flow rates (Fig. 2.2.13.1).

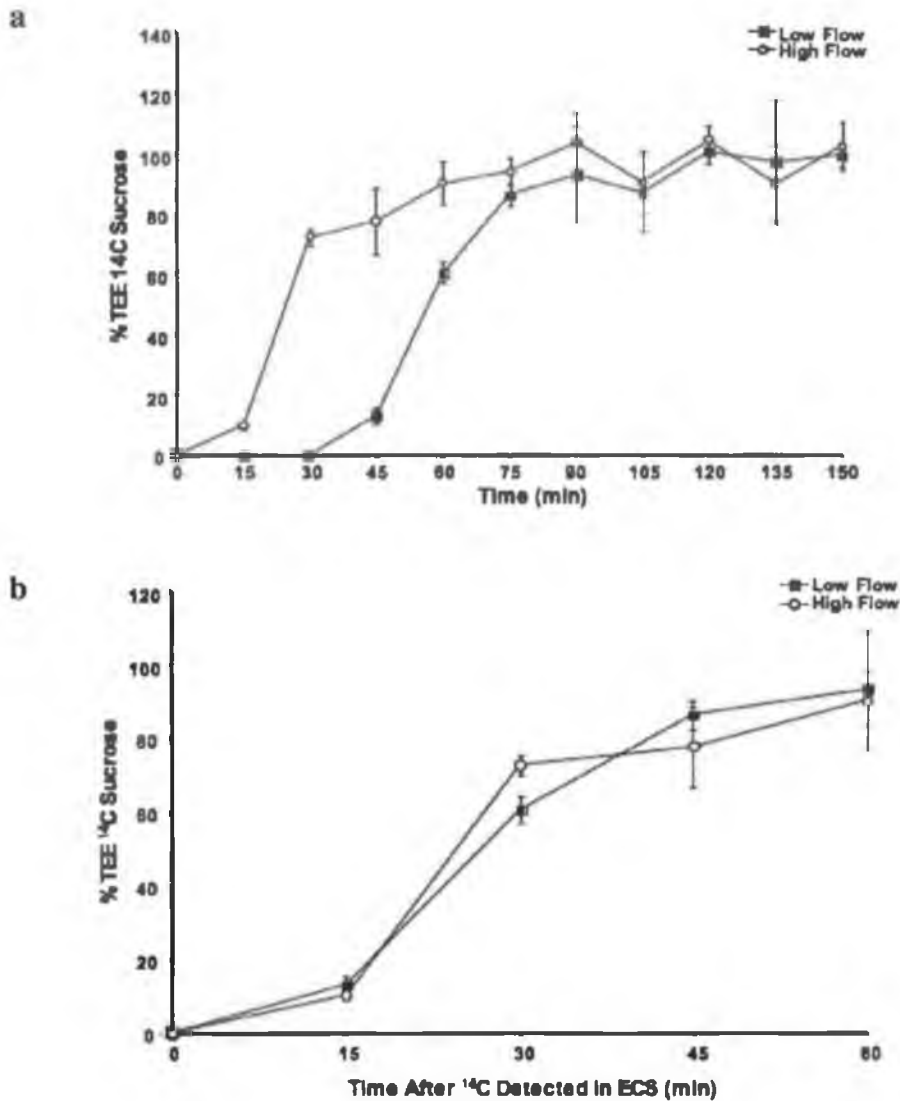


Fig. 2.2.13.1: Low and high flow rates do not affect ¹⁴C Sucrose permeability in the perfused capillary system without cells. Empty capillaries were exposed to pulsatile laminar shear stress (low – 0.2 dynes/cm²; high – 14 dynes/cm², 24 h) and monitored for permeability to ¹⁴C sucrose. In the cartridge with high flow, the concentration of ¹⁴C sucrose in the ECS reaches it's max at 60 min, and the low at 90 min (a). However, when the time scales are adjusted to correct for the time that the ¹⁴C first comes into contact with the capillary bundle, there is no significant difference between the low and high flow paradigms in the rate of permeability of ¹⁴C sucrose (b).

2.2.14 ¹⁴C Scintillation Counts

For scintillation counts, 25 µL of ECS media was added to 2 mL of Ecoscint H fluid in 6 mL scintillation vials and vortexed for 3 seconds to ensure even mixing. Each sample was analysed in triplicate. Samples were assessed for ¹⁴C concentrations by scintillation counting each sample for 5 minutes in a Beckman LS 6500 Multi-Purpose Scintillation Counter.

2.2.15 Preparation of Whole Cell Lysates

BBMvECs were washed twice in HBSS before being harvested using a cell scraper for Transwell and laminar plate shear experiments, or by trypsinization for perfused capillary studies and centrifuged at 1000 g for 5 minutes at 4⁰C. Pelleted cells were subsequently lysed in a modified RIPA buffer (50 mM HEPES, 150 mM NaCl, 10 mM EDTA, 10 mM sodium pyrophosphate, 1 mM sodium orthovanadate, 100 mM NaF and 1% Triton X supplemented with 1/100 dilution of protease and phosphatase inhibitor cocktails (Sigma)). Cells were rotated gently for 1 h at 4⁰C and subsequently centrifuged at 13,000 g for 20 min at 4⁰C to sediment any triton-insoluble material and generate a triton-soluble supernatant fraction. Pelleted triton-insoluble material was subsequently resuspended according to the method of Sakakibara *et al.* (Sakakibara *et al.* 1997) in SDS-IP buffer (25 mM HEPES, 4 mM EDTA, 25 mM NaF, 1% SDS and 1 mM sodium orthovanadate) and homogenized using a Kontes homogenizer before being passed ten times through a 27-gauge needle. Following gentle rotation at 4⁰C for 30 min, lysates were centrifuged at 10,000 g for 30 min at 4⁰C to generate an SDS-soluble fraction, which was combined with the triton soluble fraction to yield a total BBMvEC lysate. All lysates were aliquoted into working volumes and stored at -80⁰C.

2.2.16 Bicinchoninic Acid (BCA) Protein Microassay

In this assay, Cu⁺ reacts with the protein under alkaline conditions to

produce Cu', which in turn reacts with BCA to produce a coloured product. Two separate reagents were supplied in this commercially available assay kit (Pierce Chemicals), **A**; an alkaline bicarbonate solution and **B**; a copper sulphate solution. 1 part solution B is mixed with 49 parts solution A; 200 μ L of this mixture is added to 5 μ L of protein lysate or BSA standards (standard curve in the range 0-2 mg/mL). The plate is incubated at 37°C for 30 min and the absorbance read at 570 nm using a Bio-TEK® ELx800 microtitre plate reader.

2.2.17 Preparation of Immunoprecipitates

Following preparation of whole cell lysates as outlined in section 2.2.15, lysates were monitored by immunoprecipitation (IP) analysis as previously described (Ferguson *et al.* 2000) for occludin content and association of occludin/ZO-1. 60 μ g of lysate was incubated with 1.5 μ g of the appropriate monoclonal antibody, 6 μ L of 10% BSA, 7.5 μ L of Protein G Sepharose beads and lysis buffer to give a final volume of 500 μ L. Incubation proceeded overnight at 4°C with continuous eppendorf rotation. Following incubation, beads were washed twice in lysis buffer + 1% Triton-X and twice in lysis buffer, resuspended in 30 mL of SDS-PAGE sample solubilization buffer and heated for 10 min at 90°C. Samples were then spun for 25 sec using a Capsulefuge (Tomy, Freemont, CA) to pellet beads. The supernatant, containing solubilized proteins, was removed to a fresh tube for Western blotting as described in section 2.4.

2.3 RNA Preparation Methods

2.3.1 RNA isolation

Trizol is a ready-to-use reagent for the isolation of total RNA, DNA and/or protein from cells and tissues and employs the methods of RNA isolation developed by Chomczynski and Sacchi (Chomczynski and Sacchi 1987). Trizol maintains the integrity of the RNA while disrupting the cells and dissolving the cell components.

Cells were lysed directly in culture plates by the addition of 1 mL of Trizol per 10 cm². A volume less than this can result in contamination of the RNA with DNA. To ensure complete homogenization, cells were lysed by passing through a pipette a number of times. The samples were then incubated for 5 min at room temperature to allow complete dissociation of nucleoprotein complexes. 0.2 mL of chloroform was added per mL of Trizol used and was then mixed vigorously for 15 seconds before being incubated for 5 min at room temperature. Samples were subsequently centrifuged at 12,000 g for 15 min at 4⁰C. The mixture separated into a lower red, phenol-chloroform phase, an interphase and an upper colourless aqueous phase. RNA remains exclusively in the aqueous phase. The aqueous phase was carefully removed and transferred to a fresh, sterile tube. The RNA was precipitated out of solution by the addition of 0.5 ml of isopropanol per 1 mL of Trizol used. Samples were incubated for 15 min at room temperature and then centrifuged at 12,000 g for 10 min at 4⁰C. The RNA precipitate forms a gel-like pellet on the side of the tube. The supernatant was removed and the pellet washed in 1 mL of 75% ethanol per mL of Trizol used followed by centrifugation at 7,500 g for 5 min at 4⁰C. The resultant pellet was air-dried for 5-10 min before being resuspended in DEPC-treated water. The sample was then stored at -80⁰C until use. RNA concentration was determined by UV spectrophotometry as outlined in section 2.3.2.

2.3.2 Spectrophotometric Analysis of Nucleic Acids

The concentration and purity of the isolated RNA was determined by measuring the absorbance of a 1:100 dilution of the sample in Shimadzu UV-160A dual spectrophotometer at 260 nm and 280 nm. DEPC water in a quartz cuvette was used to blank the machine. The RNA concentration was determined as follows;

$$Abs_{@260nm} \times 40 \times dilution\ factor = Concentration\ of\ RNA\ (\mu g/mL)$$

The purity of RNA samples was established by reading the absorbance at 260 nm and the absorbance at 280 nm and then determining the ratio between the two (ABS₂₆₀/ABS₂₈₀). Pure RNA has a ratio of 2.0, lower ratios indicate the presence of proteins, higher ratios imply the presence of organic reagents such as phenols.

2.3.3 Reverse Transcription (RT) Reaction

Copy DNA (cDNA) was synthesized from messenger RNA (mRNA) using an iScript™ cDNA synthesis kit (Bio-Rad Laboratories, California, USA). For each RT reaction, 4 µL 5x buffer, 1 µL reverse transcriptase enzyme and 1 µg of RNA were mixed and subjected to one RT cycle consisting of three phases; i) 25°C for 5 min, ii) 42°C for 30 min and iii) 85°C for 5 min in a PCR Sprint thermo cycler (Thermo Electron Corporation – Massachusetts, USA). The resultant cDNA of interest was amplified by real-time PCR as described in section 2.3.4.

2.3.4 Real-Time Polymerase Chain Reaction (PCR)

Quantitative real-time PCR was carried out using SYBR Green dye and a Real time Rotor-GeneRG-3000™ lightcycler (Corbett Research). SYBR Green is a fluorescent dye which, when bound to the minor groove of double stranded DNA, emits fluorescence. The fluorescence is directly proportional to the amount of product formed. cDNA, as outlined in section 2.3.3 was amplified for the target sequences of interest, namely occludin, ZO-1 and GAPDH. Primer sets specific for the product of interest are detailed in table 2.3.4.1.

Target Gene	Primer Sequence	Anneal Temp	Product Size
Occludin	For 5' AGT GGC TCA GGA GCT GCC ATT GAC TTC ACC 3' Rev 3' AGG TGG ATA TTC CCT GAT CCA GTC GTC GTC 5'	61°C	220 bp
ZO-1	For 5' AGG CGC AGC TCC ACG GGC TTC AGG AAC TTG 3' Rev 3' TCA GCC GTG GAG GAA GAT GAA GAC GAA GAC 5'	59°C	290 bp
GAPDH	For 5' TGC TGA GTA TGT CGT GGA GT 3' Rev 3' GCA TTG CTG ACA ATC TTG AG 5'	53°C	186 bp

Table 2.3.4.1: Tabulated data for specific primer sequences for real-time PCR products

Each reaction was set up in triplicate as follows:

SYBR Green total reagent	12.5 μ L
DEPC Water	8.5 μ L
Forward Primer	1.0 μ L
Reverse Primer	1.0 μ L
cDNA	2.0 μ L

Each sample was mixed briefly and spun down for 6 seconds using a Capsulefuge (Tomy, Freemount, CA). The Real-time PCR cycle program used for product amplification was as follows:

Denature		95 ⁰ C	15 min	} 45 cycles
Cycling	Denature	95 ⁰ C	20 s	
	Annealing	59 ⁰ C	30 s	
	Extension	72 ⁰ C	30 s	
Hold		60 ⁰ C	1 min	
Melt		50 – 100 ⁰ C		

Although the optimum annealing temperature for each of the primers was different, all three functioned at an annealing temperature of 59⁰C, therefore, this was used as the annealing temperature for all real-time PCR product amplifications. All primer pairs used were routinely screened for non-specific primer-dimer products by melt curve analysis and agarose gel electrophoresis as outlined in section 2.3.5. For the purpose of quantification, GAPDH (glyceraldehyde phosphate dehydrogenase) a house-keeping gene, was used for normalization.

2.3.5 Agarose Gel Electrophoresis

Real-time PCR products were examined to ensure that the PCR product was the correct size and that primer-dimers were not formed. All DNA gel

electrophoresis was carried out using a GibcoBRL Horizon 20.25 Gel Electrophoresis Apparatus. Before use the gel box was cleaned with ethanol and the gel cast was set up as described in the manufacturers instruction manual. A 2.5% agarose gel was made up by dissolving 12.5 g of agarose in 500 mL of 1x Tris Acetate EDTA (50x TAE, Eppendorf, Hamburg, Germany). The agarose was dissolved by heating in a microwave (700 MHz) at full power for 5 min. 100 mL of the liquid agarose was then transferred to a fresh glass beaker. To this 250 mL of 200 mg/mL of Ethidium Bromide (EtBr) solution was added and mixed thoroughly to give a final concentration of 0.5 mg/mL EtBr. The agarose was then poured into the cast, the comb put into place and the gel allowed to set. Once set, the comb was removed and the apparatus filled with 1x TAE buffer. The samples were prepared as follows: 15 mL of PCR product + 5 mL of 4x loading dye. 8 mL was loaded into each well, with duplicate wells for each sample. The gel was run at 80 V, 110 mA and 150 W until the dye front had migrated the length of the gel. When finished the gel was placed on an Ultra Violet Products UV transilluminator for visualization and an image captured using a Kodak DC290 digital camera for documentation. The gel was then disposed of in the appropriate EtBr waste container.

2.4 Western Blotting

2.4.1 Preparation of SDS PAGE Gels

For all protein electrophoresis and Western blotting, an Atto AE-6450 Dual Mini Slab Kit was used. Prior to usage glass plates, gaskets and combs were swabbed with ethanol as per manufactures instructions (AHO, Tokyo Japan). BBMvEC lysate and IP samples were resolved under reducing conditions according to the methods of Laemmli (*Laemmli 1970*). Resolving gels 12% (occ IP and co-IP) and 6% (ZO-1) and stacking gels 5% (occ IP and co-IP) and 3% (ZO-1) were prepared as outlined in table 2.4.1.1.

	Resolving Gel		Stacking Gel	
	12%	6%	5%	3%
Acrylamide/Bis Acrylamide	4.2 mL	2.36 mL	500 μ L	300 μ L
Gel Buffer	3.5 mL	157 μ L	1 mL	40 μ L
10% SDS (w/v)	140 μ L	3.94 mL	40 μ L	1 mL
UPH ₂ O	6.16 mL	9.3 mL	2.46 mL	2.66 mL
10% Ammonium Persulphate (w/v)	70 μ L	79 μ L	20 μ L	20 μ L
TEMED	21 μ L	24 μ L	6 μ L	6 μ L

Table 2.3.4.1: SDS PAGE gel formulations. Resolving gel buffer and stacking gel buffers have a pH of 8.8 and 6.8 respectively.

The resolving gel was poured, overlaid with ethanol and allowed to polymerize for 20 min at which point the ethanol was poured off and any traces of ethanol were removed by washing with stacking gel buffer. 2 mL of stacking gel was then overlaid on the resolving gel, the comb inserted and allowed to polymerize for 20 min. The electrophoresis chamber was then filled with approximately 200 mL reservoir buffer (25 mM Tris, 192 mM Glycine, 0.1% SDS). When the gels had polymerized, the combs, clamps and gaskets were removed and gel plates inserted into the electrophoresis chamber. The space between the two gels was then filled with reservoir buffer and wells flushed to remove any unpolymerized acrylamide.

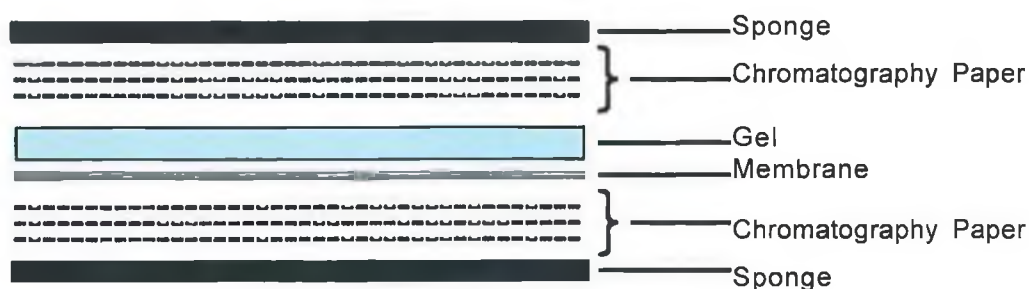
2.4.2 SDS PAGE Sample Preparation and Electrophoresis

In order to measure occludin expression and occludin/ZO-1 association, IPs were prepared as outlined in section 2.2.15. For ZO-1 Western blotting, total lysate, 4X sample solubilization buffer (SSB – 8% SDS, 40% glycerol, 4% β -mercaptoethanol, 0.008% Bromophenol blue and 0.25M TrisCl, pH 6.8) and lysis buffer were mixed to give a final concentration of 8 μ g protein and 1X SSB in 20 μ L. The sample was then incubated for 5 min in a 95^oC heating block and cooled rapidly on ice. The lysate or IP samples were then slowly added to the stacking gel

wells. 2 μ L of Rainbow Protein Molecular Marker (Amersham Lifesciences) was added to the first lane of the gel. The samples and markers were then separated electrophoretically at 150 V, 90 mA, 150 W for 2 h (IPs) or 4 h (ZO-1).

2.4.3 Wet Transfer and Ponceau S Staining

A BIO-RAD Mini-PROTEAN® 3 Cell wet transfer chamber was used for all wet transfers. Following gel electrophoresis, gels were removed from glass plates, the stacking gel discarded and the resolving gel soaked for 10 min in transfer buffer (25 mM Tris, 192 mM Glycine, 20% methanol, 0.1% SDS). Whatmann chromatography paper and nitrocellulose membrane (PALL Biotrace) were cut to the size of the resolving gel (7 x 9 cm) and pre-soaked in transfer buffer. The transfer cassette was assembled as follows:



Proteins were transferred at 100 V, 500 mA, 150 W for 1 h 30 min. After completion of the transfer, membranes were soaked in Ponceau S solution (Sigma) for 3 min to ensure even protein loading. The stain was subsequently removed by gentle washing in 1X PBS, 0.05% Tween-20 (PBS-Tween).

2.4.4 Immunodetection

Following removal of the Ponceau S stain, membranes were blocked either overnight (ZO-1) or for 1 h (occ or occ/ZO-1 IPs) in 5% BSA solution. Membranes were rinsed gently in PBS-Tween to remove excess blocking solution and incubated

either overnight (occludin) or for 3 h (ZO-1) with the appropriate primary monoclonal antisera (Zymed) at 1:1000 dilution. Membranes were washed vigorously for 30 min in PBS-Tween prior to incubation with a 1:4000 dilution of HRP-conjugated goat anti-mouse secondary antisera (Amersham Biosciences – Buckinghamshire, UK) for 2 h. Membranes were then washed vigorously for 30 min in PBS-Tween prior to detection of immunoreactive proteins by enhanced chemiluminescence. Supersignal® West Pico chemiluminescent substrate (Pierce) was prepared according to the manufacturers instructions and incubated with membranes for 5 min. Excess substrate was removed and chemiluminescent signal was detected in a dark room using Amersham Hyperfilm autoradiography film and developed in an Amersham hyperprocessor automatic developer. Immunoblot images were captured using a Kodak DC290 digital camera and a quantitative comparison between bands carried out using Kodak 1D (version 3.5.4) densitometry imaging software.

2.5 Statistical Analysis

Results are expressed as mean \pm SEM of a minimum of three independent experiments (n=3) unless otherwise stated. Statistical comparisons were performed using unpaired Student's *t*-test or Two-Way ANOVA with replication, where applicable. A value of $P \leq 0.05$ was considered significant.

Chapter 3

*Optimisation of cell culture media and
characterization of the model*

3.1 Introduction

Endothelial cells forming the BBB *in vivo* are highly differentiated, displaying a distinct phenotype associated with low permeability and high electrical resistance, caused by the presence of tight junctions sealing the paracellular pathway between adjacent endothelial cell (Crone and Olesen 1982; Butt *et al.* 1990). However, many of these characteristics are lost *in vitro* due to the ongoing de-differentiation of the cells when passaged (Meresse *et al.* 1989; Mischeck *et al.* 1989; Fukushima *et al.* 1990; Meyer *et al.* 1990; Mizuguchi *et al.* 1994). For this reason, it is essential to optimize the endothelial culture medium in order to maintain the BBB characteristics of BBMvECs and lower the rate of de-differentiation.

BBMvECs received from Cell Applications, Inc. displayed typical microvascular endothelial phenotype as defined by viability, morphology and doubling time. However, the media components, including serum content and growth factors, were undefined (and proprietary information). Furthermore, due to licencing difficulties in importing bovine-derived products (serum in media) from a non-EU source and the associated cost involved, it was neither cost or time-efficient to continue usage of Cell Applications, Inc. media. As such it was necessary to develop a defined in-house media that induced the same phenotype and growth characteristics in BBMvECs as the Cell Applications media.

Moreover, for co-culture and serum studies outlined in section 2.2.7, it is necessary to culture C6 glioma cells in serum free-media for 24 h. As the C6 glioma were responsible for the co-culture conditioning of the BBMvECs, it is of paramount importance that they remain viable in serum-free conditions, and maintain their astrocyte properties.

In this chapter, we describe the optimization of a growth media suitable for the culture of both BBMvECs and C6 glioma and to characterize the two cell types. Moreover, it was necessary to ensure the viability of C6 glioma in the serum-free conditions required by the co-culture experimental paradigm.

3.2 Results

3.2.1 Media- and serum-dependent proliferation, morphology and viability of BBMvECs

BBMvECs were plated at 1×10^4 cells/cm² in either high glucose DMEM (Fig. 3.2.1 c and d), Medium 199 (Fig. 3.2.1 e and f) or Ham's F12 Medium (Fig. 3.2.1 g and h) containing 1% P/S and either 10% v/v Sigma or Gibco FCS. BBMvECs were also plated in Cell Applications BBMvEC Cell Growth Medium (Day 0, Fig. 3.2.1 a), as a positive control. Cells were monitored by phase contrast microscopy every 24 h for cell proliferation, morphology and viability. Following 6 days in culture, the BBMvECs in Cell Applications media became confluent (Fig. 3.2.1 b). BBMvECs grown in DMEM with 10% Gibco FCS most closely resembled cells grown in Cell Applications media for rate of proliferation, cell morphology and cell viability (Fig. 3.2.1 d).

3.2.2. Basic Fibroblast Growth Factor (bFGF) is required for maintained BBMvEC proliferation, morphology and viability *in vitro*

BBMvECs were plated at 1×10^4 cells/cm² in either Cell Applications BBMvEC Cell Growth Medium (as control) or high glucose DMEM with 1% P/S and Gibco FCS, containing recombinant human bFGF ranging in concentration from 0 to 6 ng/mL. Cells were monitored by phase contrast microscopy every 24 h for cell proliferation, morphology and viability. Following 6 days in culture, the BBMvECs in Cell Applications media became confluent (Fig. 3.2.2 blue border). BBMvECs grown in the presence of 3 ng/mL bFGF (Fig. 3.2.2 red border) most closely resembled cells grown in the Cell Applications media for rate of proliferation, cell morphology and cell viability.

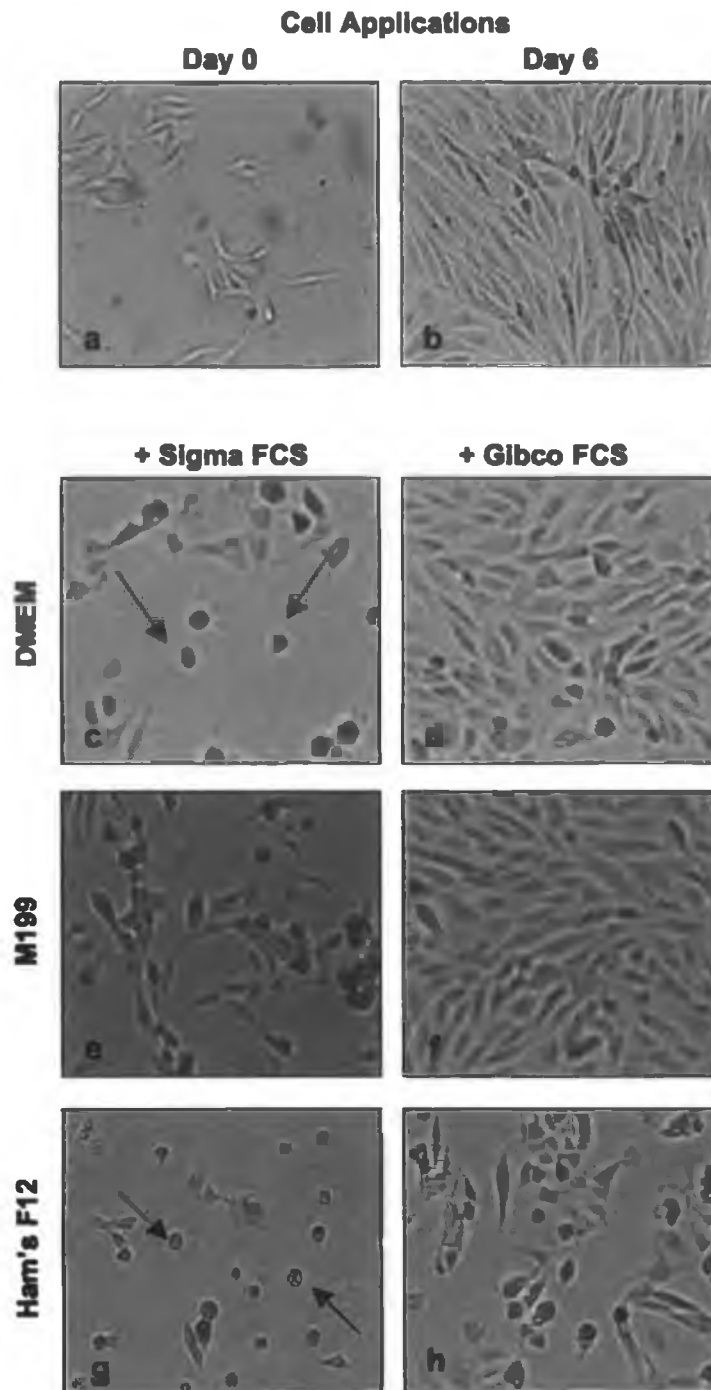


Fig. 3.2.1: Optimization of Basal Media and Fetal Calf Serum for BBMvEC Growth Media: BBMvECs were seeded at 1×10^4 cells/cm² in either Cell Applications complete media (day 0, (a) and at confluence, day 6, (b)), high glucose DMEM (b and c), M199 (d and e) or Ham's F12 (f and g) with 1% P/S and 10% FCS from either Sigma or Gibco. BBMvEC proliferation, viability and morphology were assessed daily by phase contrast microscopy. Images b-h shown are 6 days post seeding (i.e. time required for cells to reach confluency in Cell Applications Media). Black arrows indicate cells which failed to flatten or proliferate following adherence..

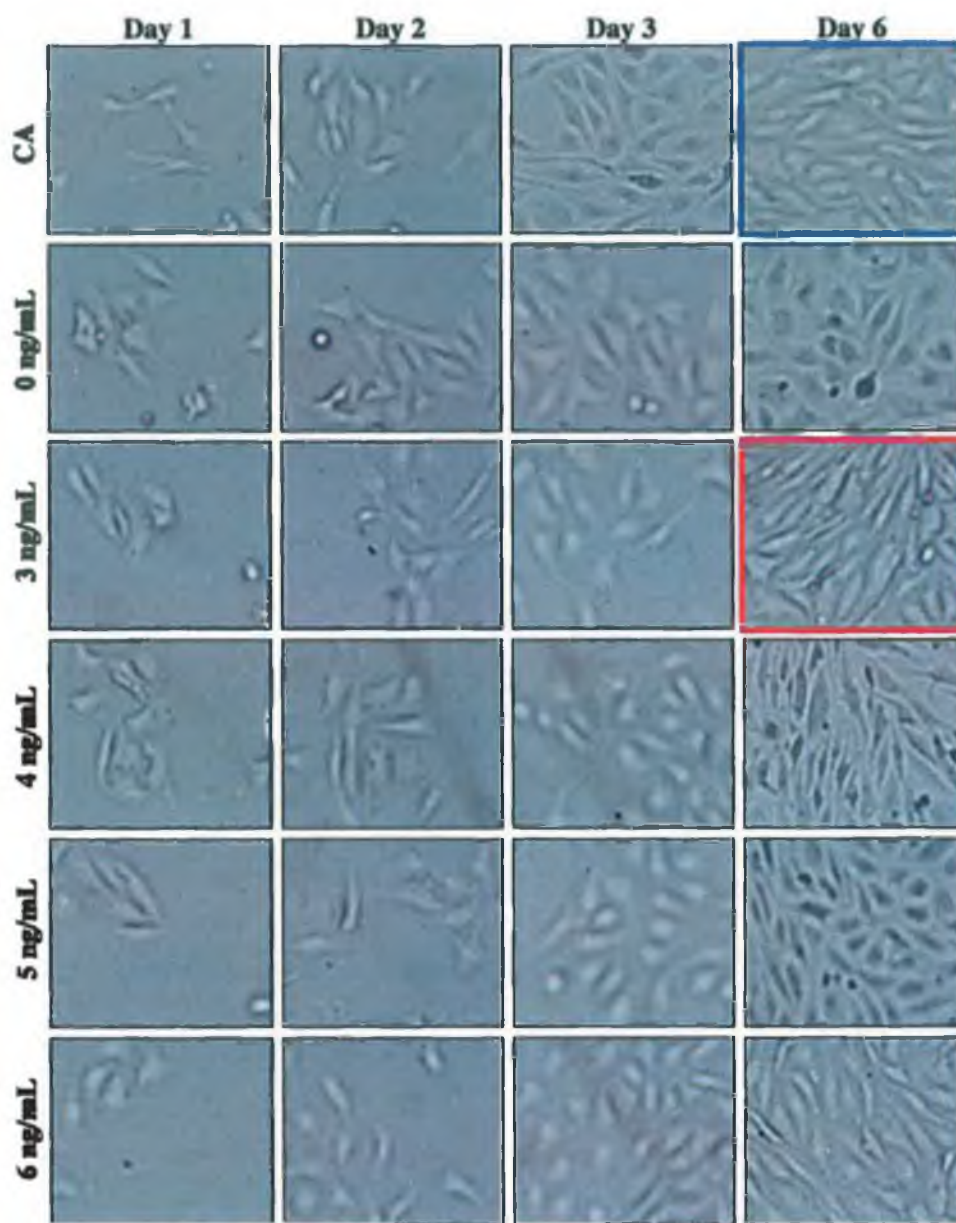


Fig. 3.2.2: Optimization of Growth Factors in BBMvEC Growth Media: BBMvECs were seeded at 1×10^4 cells/cm² in either Cell Applications complete media (CA) or high glucose DMEM containing 1% P/S, 10% Gibco FCS and bFGF ranging from 0 to 6 ng/mL. BBMvEC proliferation, viability and morphology were assessed daily by phase contrast microscopy. Images shown are 1, 2, 3 and 6 days post seeding (i.e. time required for cells to reach confluency in Cell Applications Media). Blue frame indicates confluent BBMvECs in Cell Applications complete media, red frame indicates optimum bFGF concentration in DMEM media.

3.2.3 Heparin is required for maintained BBMvEC proliferation, morphology and viability *in vitro*

BBMvECs were plated at 1×10^4 cells/cm² in either Cell Applications BBMvEC Cell Growth Medium (as control) or high glucose DMEM containing 1% P/S and Gibco FCS, 3 ng/mL recombinant human bFGF and heparin ranging in concentration from 0 to 6 µg/mL. Cells were monitored by phase contrast microscopy every 24 h for cell proliferation, morphology and viability. Following 144 h in culture, the BBMvECs in Cell Applications media became confluent (Fig. 3.2.3 a). BBMvECs grown in the presence of 3 µg/mL heparin (Fig. 3.2.3 b) most closely resembled cells grown in the Cell Applications media for rate of proliferation, cell morphology and cell viability.

3.2.4 Characterization of BBMvECs grown in in-house media by expression of Von-Willebrand Factor VIII antigen

BBMvECs were plated at 1×10^4 cells/cm² on sterile coverslips using in-house media (high glucose DMEM, 1% P/S, 10% Gibco FCS, 3 ng/mL bFGF and 3 µg/mL heparin) and grown for 72 h to 80% confluence. Von Willebrand Factor VIII expression was monitored by immunocytochemistry as described in section 2.2.11. BBMvECs were found to be positive for Von Willebrand Factor VIII (Fig. 3.2.4 b) and negative for control cells without primary anti-serum (Fig. 3.2.4 a).

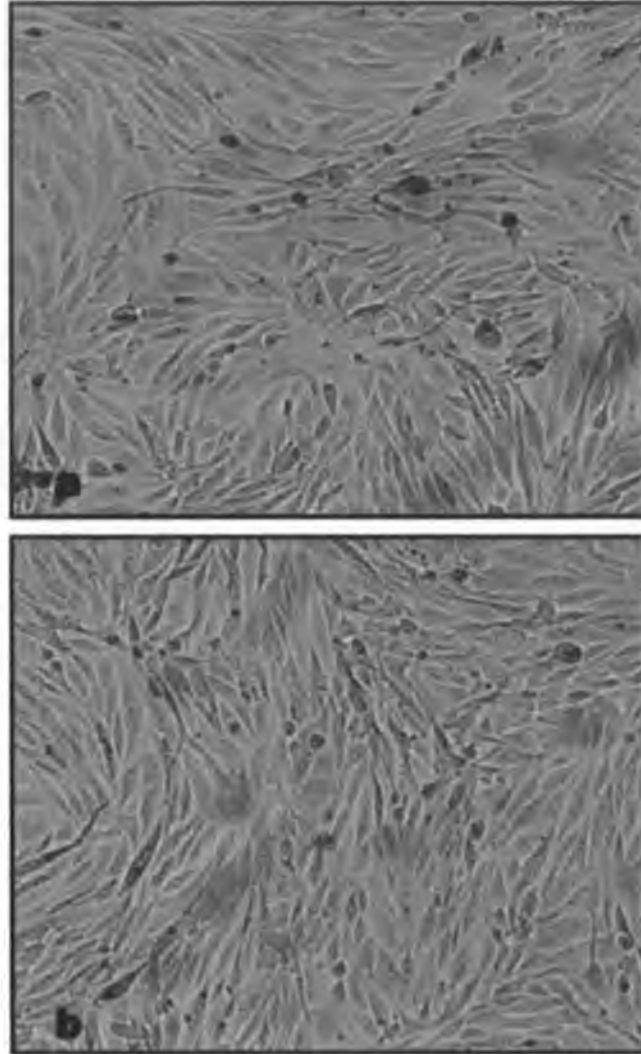


Fig. 3.2.3: Optimization of Heparin in BBMVEC growth media: BBMVECs were seeded at 1×10^4 cells/cm² in either Cell Applications complete media (a) or high glucose DMEM containing 1% P/S, 10% Gibco FCS, 3 ng/mL bFGF and 3 µg/mL Heparin (b). BBMVEC proliferation, viability and morphology were assessed daily by phase contrast microscopy. Images shown are 6 days post seeding (i.e. time required for cells to reach confluency in Cell Applications Media)



Fig. 3.2.4: Characterization of BBMVECs by Von Willebrand Staining: BBMVECs were seeded at 1×10^4 cells/cm² in high glucose DMEM containing 1% P/S, 10% Gibco FCS, 3 ng/mL bFGF and 3 μ g/mL Heparin. Expression of endothelial-specific Von Willebrand Factor VIII (green, b) was monitored by immunocytochemistry using standard fluorescence microscopy (1000x). Control cells incubated without primary anti-serum show no fluorescence (a).

3.2.5 Characterization of C6 Glioma by expression of Glial Fibrillary Acidic Protein (GFAP) antigen and assessment of viability in serum-free media

C6 Glioma were plated at 1×10^4 cells/cm² on sterile coverslips in high glucose DMEM, 1% P/S, 10% Gibco FCS, 3 ng/mL bFGF and 3 µg/mL heparin and grown for 48 h to 80% confluence. GFAP expression was monitored by immunocytochemistry as described in section 2.2.11. C6 Glioma were found to be positive for GFAP (Fig. 3.2.5 b) and negative for controls without primary anti-serum (Fig. 3.2.5 a). For co-culture studies, as described in section 2.2.7, it was necessary to culture C6 Glioma for 24 h in serum-free media. Therefore, it was necessary to assess C6 Glioma viability in serum-free media. C6 Glioma cells were plated at 1×10^4 cells/cm² in 6-well plates and allowed to adhere overnight. Cells were subsequently washed in HBSS and 2 mL of either serum-containing or serum-free was added to each well. After 24 h cells were assessed by phase-contrast microscopy for cell morphology and viability. Cells grown in serum-containing media displayed typical C6 glioma fibroblast-like morphology (Fig. 3.2.5 c). The cells grown in serum-free media displayed a slightly elongated morphology after 24 h (Fig. 3.2.5 d), but maintained good cell viability and proliferation for up to five days in serum-free media (data not shown).

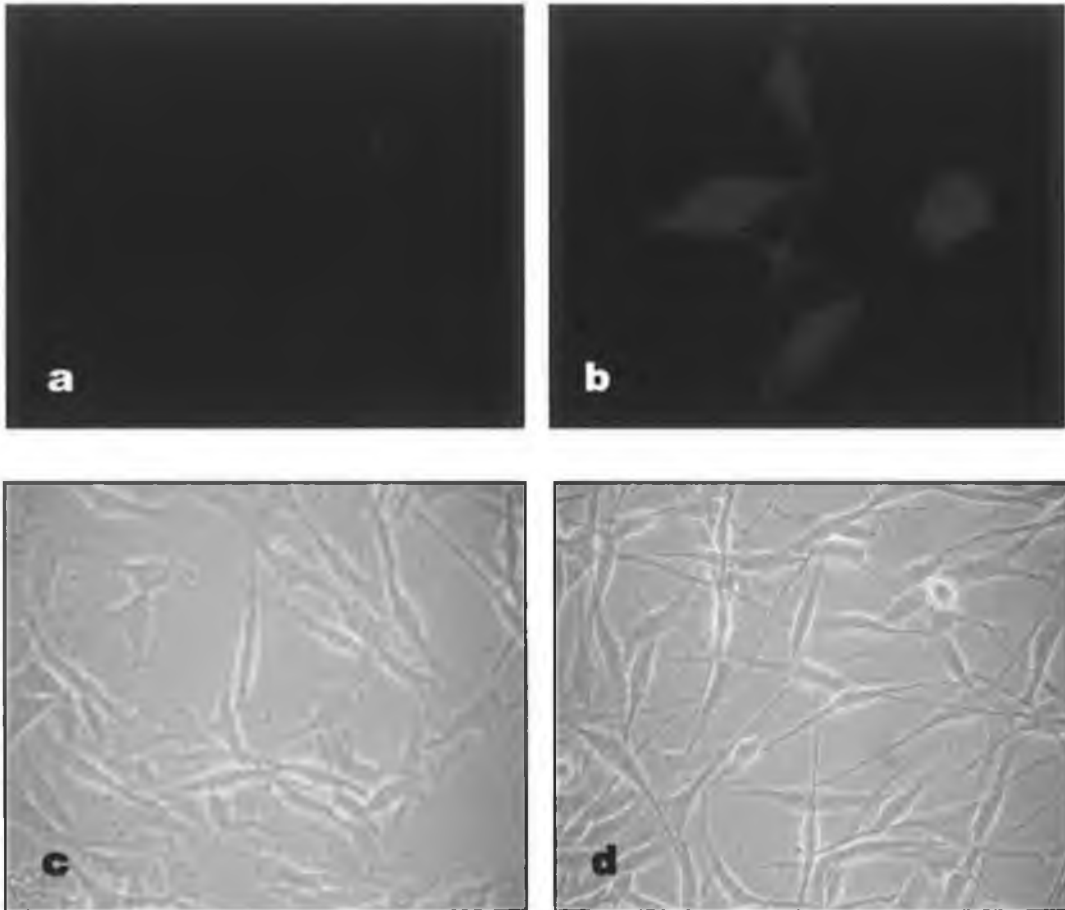


Fig. 3.2.5: Characterization of C6 Glioma: C6 Glioma were seeded at 1×10^4 cells/cm² in high glucose DMEM containing 1% P/S, 10% Gibco FCS, 3 ng/mL bFGF and 3 μ g/mL Heparin. Expression of astrocyte specific Glial Fibrillary Acidic Protein (GFAP) (green) was monitored using standard fluorescent microscopy (b, 1000x). Control cells incubated without primary anti-serum show no fluorescence (a, 1000x). Cell proliferation, morphology and viability in serum-containing (c) and serum-free media (d) were monitored by phase contrast microscopy (400x).

3.3 Discussion

In order to study BBB permeability and the etiology of tight junction formation and regulation, it is necessary to develop a cell-based model of the BBB. As the barrier function of the BBB can be completely attributed to the endothelial cells, it stands to reason that these cells are the most essential component of any BBB model. Primary cultured brain microvascular endothelial cells retain some of their *in vivo* characteristics, but lose BBB specific markers such as γ -glutamyl transpeptidase (γ -GTP) and alkaline phosphatase (ALP) within a few days of their isolation (Meresse *et al.* 1989; Mischeck *et al.* 1989; Fukushima *et al.* 1990; Meyer *et al.* 1990; Mizuguchi *et al.* 1994). Moreover, with rats yielding between 1-2 million cells per brain (Mizuguchi *et al.* 1997), many animals must be sacrificed in order to produce quantities of cells adequate for extensive experimentation, thus raising both ethical issues and batch-to-batch variations within the cells. For this reason, it is often adventitious to use a continuous cell line for experimental procedures, thus eliminating dissimilarities between batches of cells and reducing the ethical issues associated usage of animal cells. However, continuous passaging of brain endothelial cells can lead to their de-differentiation and loss of BBB specific phenotype. For example, TEER of the BBB *in vivo*, is typically in the region of 1000 – 2000 Ω .cm² (Butt 1995), but when isolated and grown *in vitro* may drop as low as 10 Ω .cm² (Butt *et al.* 1990). Therefore, it is essential to maintain cells under optimum culture conditions to minimize de-differentiation and retain BBB characteristics *in vitro*.

As BBMvECs are routinely grown in a variety of media (Audus and Borchardt 1987; Prasadarao *et al.* 1999; Zhang *et al.* 2000; Zysk *et al.* 2001), it was necessary to establish the optimum basal media and serum required for growth of the BBMvEC continuous cell line purchased from Cell Applications, Inc.. Initial investigation revealed that the BBMvECs grown in high glucose DMEM, containing 10% (v/v) Gibco FCS, most closely reflected, but was not the same as, the growth rate, morphology and viability observed in BBMvECs grown in Cell Applications

media. Furthermore, cells grown in the presence of Sigma FCS had a lower rate of adherence, flattening and proliferation. Further studies investigating the effect of bFGF revealed that a concentration of 3 ng/mL was optimum for cell growth and viability, but that the addition of 3 µg/mL heparin resulted in a culture media, which induced the same BBMvEC rate of proliferation, viability and morphology as Cell Applications media. Immunocytochemical analysis indicated that the BBMvECs retained their endothelial characteristics when grown in our in-house media as shown by anti-Von-Willebrand Factor VIII antigen staining.

The co-culture experimental paradigm outlined in section 2.2.7 requires firstly that both C6 glioma and BBMvEC be cultured in the same growth media and secondly that the C6 glioma could be cultured in serum-free media for 24 h. Therefore, it was necessary to ensure that the C6 glioma retained their viability and characteristics in the in-house media in both the presence and absence of serum. Immunocytochemical analysis confirmed that C6 glioma express GFAP following growth and passaging in our in-house media and that the C6 glioma continued to proliferate in serum-free media for up to 5 days.

In conclusion, these observations indicate that the BBMvECs are sensitive to the type of basal medium and serum they are grown in and that both bFGF and heparin are required for sustained BBMvEC proliferation and viability. Furthermore, these findings show that C6 glioma can be sustained in both serum-containing and serum-free media. This information provided the basal components required for our BBB model.

Chapter 4

*Examination of the polar-specific
effect of serum on endothelial tight
junction formation and barrier
function.*

4.1 Introduction

The BBB acts as a selective barrier preventing blood-borne solutes from entering the brain ISF, where they can act as neurotransmitters and disrupt normal neuronal function. The BBB is formed by brain microvascular endothelial cells, which line cerebral capillaries, and are sealed by tight junctions. These tight junctions form continuous contacts between adjacent endothelial cells, thus sealing the intercellular space and preventing paracellular flux from the blood to the brain (Balda and Matter 1998; Rubin and Staddon 1999). Moreover, tight junctions function in maintaining cell polarity by preventing the lateral diffusion of membrane proteins and lipids (Citi 1993; Cereijido *et al.* 1998; Madara 1998). Therefore, due to the action of the BBB, the ISF is devoid of serum proteins.

Altered function and/or integrity of the BBB is associated with a variety of disease states including multiple sclerosis, meningitis, encephalitis, ischaemic stroke, Parkinson's disease, Alzheimer's disease and AIDS related dementia (PML - progressive multifocal leukoencephalopathy) (Tunkel and Scheld 1993; Mattila *et al.* 1994; Williams *et al.* 1994; Poland *et al.* 1995). Moreover, recent studies have shown that serum prevents new barrier formation and disrupts previously formed barriers, as assessed by TEER, in a highly polar-specific manner (Hoheisel *et al.* 1998; Nitz *et al.* 2003). That is, serum contacting endothelial cells from the basolateral aspect reduced monolayer electrical resistance, indicative of loss of tight junctions, whilst apically applied serum had no such effect. However, the mechanisms by which serum disrupts barriers, and the biochemical events which take place, are poorly understood.

Therefore, the aim of this chapter was to investigate the polar-specific effects of serum on tight junction formation and barrier function in BBMvECs and to elucidate the underlying biochemical processes with respect to occludin and ZO-1 expression, association and subcellular localization.

4.2 Results

4.2.1 Apically applied serum-dependent subcellular localization of occludin and ZO-1 in BBMvECs

Following 24 h culture of BBMvECs in the presence or absence of apical serum, subcellular localization of occludin and ZO-1 within BBMvEC monolayers was monitored by immunocytochemistry as described in section 2.2.11. In the BBMvEC monolayer with apical serum, occludin was found solely in the cytoplasm (Fig. 4.2.1 a). Following removal of serum from the apical compartment, there was no significant difference in subcellular localization of occludin (Fig. 4.2.1 c). Moreover, in monolayers with apical serum present, ZO-1 immunoreactivity was discontinuous, with jagged finger-like projections at the cell membrane (Fig. 4.2.1 b) and again, no significant difference in ZO-1 subcellular localization was seen following the removal of apical serum for 24 h (Fig. 4.2.1 d).

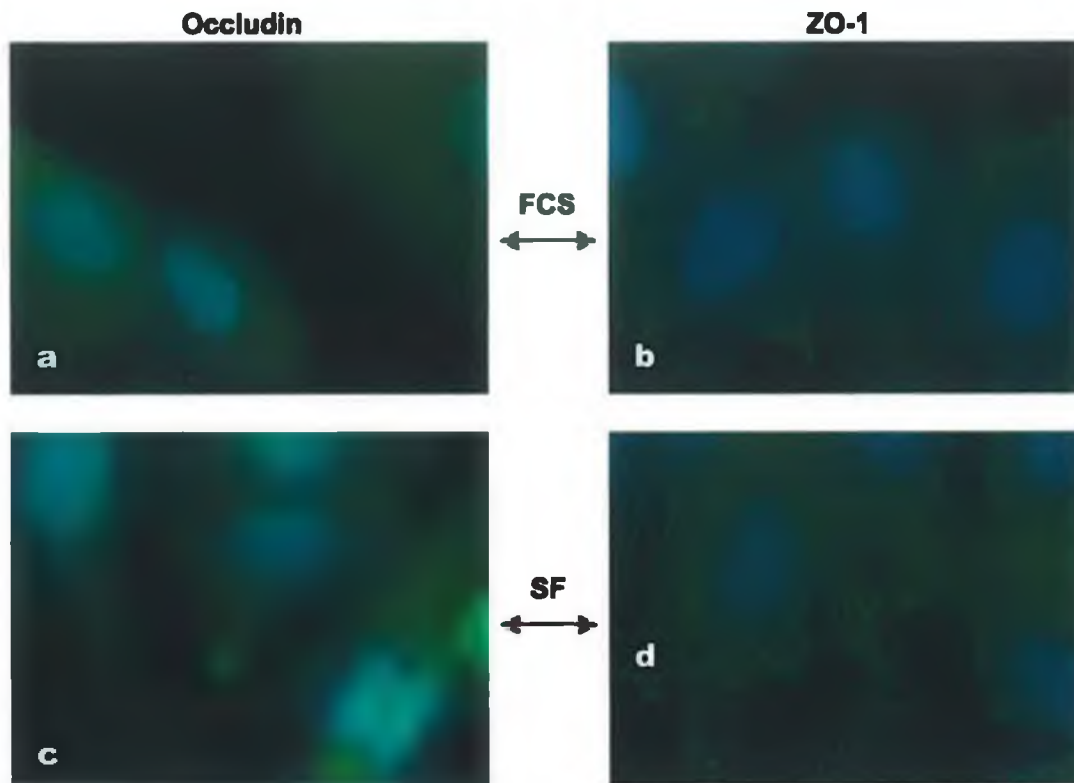


Fig. 4.2.1: Effect of apically applied serum on Occludin and ZO-1 Subcellular Localization. Following 24 h incubation of fully confluent BBMvEC in the absence or presence of serum on the apical side of the endothelial cells, subcellular localization of occludin and ZO-1 was monitored by immunocytochemistry. Occludin protein (green a and c), ZO-1 protein (green b and d, clearly visible in a disjointed pattern at cell-cell borders) and nuclear DAPI staining (blue a-d) were monitored using standard fluorescent microscopy (1000x).

4.2.2 Basolaterally applied serum-dependent expression of occludin in BBMvECs

Following 24 h culture of BBMvECs in the presence or absence of basolateral serum, occludin protein expression was monitored by IP/Western blot as described in sections 2.2.16 and 2.4 respectively, and mRNA expression by Real-time PCR as described in section 2.3.4. Following 24 h culture of BBMvEC without basolateral serum (SF), occludin protein expression increased by 1.9 ± 0.2 fold (Fig. 4.2.2 a) concomitant with a 1.7 ± 0.2 fold increase in occludin mRNA (Fig. 4.2.2 b).

4.2.3 Basolaterally applied serum-dependent expression of ZO-1 in BBMvECs

Following 24 h culture of BBMvECs in the presence or absence of basolateral serum, ZO-1 protein expression was monitored by Western blot as described in sections 2.2.16 and 2.4 respectively, and mRNA expression by Real-time PCR as described in section 2.3.4. Following 24 h culture of BBMvEC without basolateral serum (SF), ZO-1 protein expression increased significantly by 1.8 ± 0.2 fold (Fig. 4.2.3 a), which was accompanied by a small but significant increase in ZO-1 mRNA (1.2 ± 0.1 fold, Fig. 4.2.3 b).

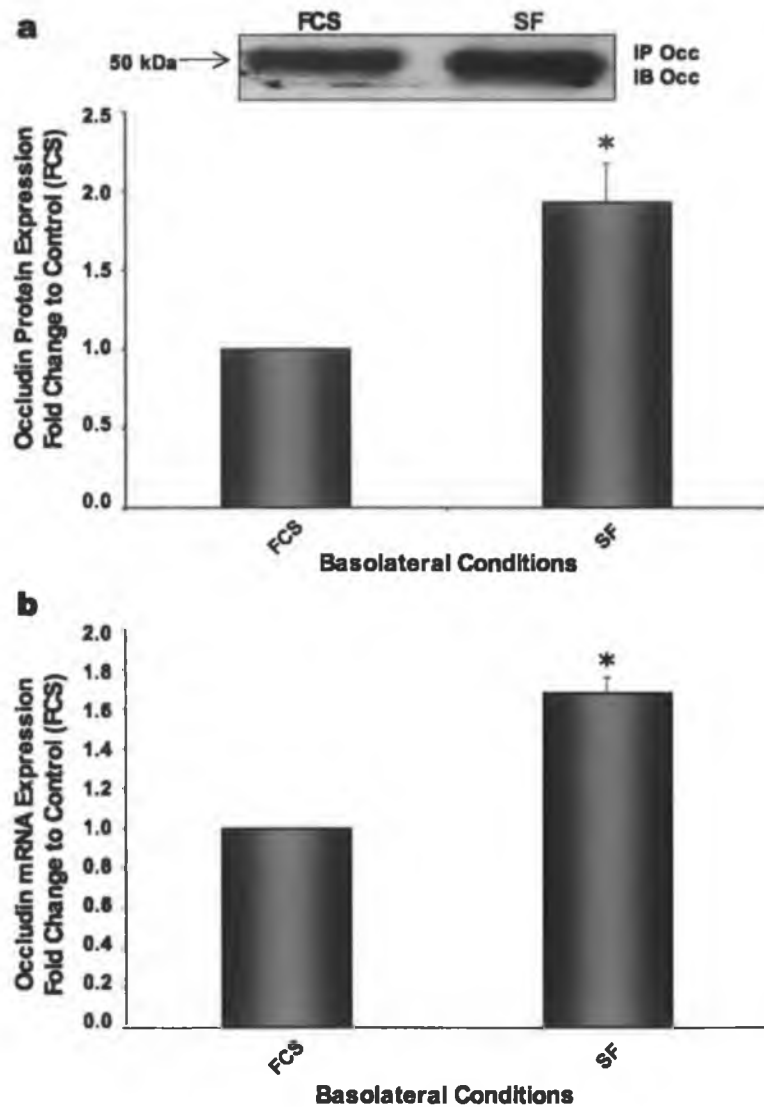


Fig. 4.2.2: Effect of basolateral serum on occludin expression in BBMvECs. Confluent BBMvEC monolayers in Transwell inserts were incubated for 24 h with either serum-containing (FCS) or serum-free (SF) basolateral media and monitored for Occludin protein expression (a) by immunoprecipitation/Western blot and for mRNA (b) by Real-Time PCR. Histograms represent fold change in product formation relative to control (FCS) and are averaged from three independent experiments (a) or seven independent experiments (b) \pm SEM. * $P < 0.05$ relative to FCS.

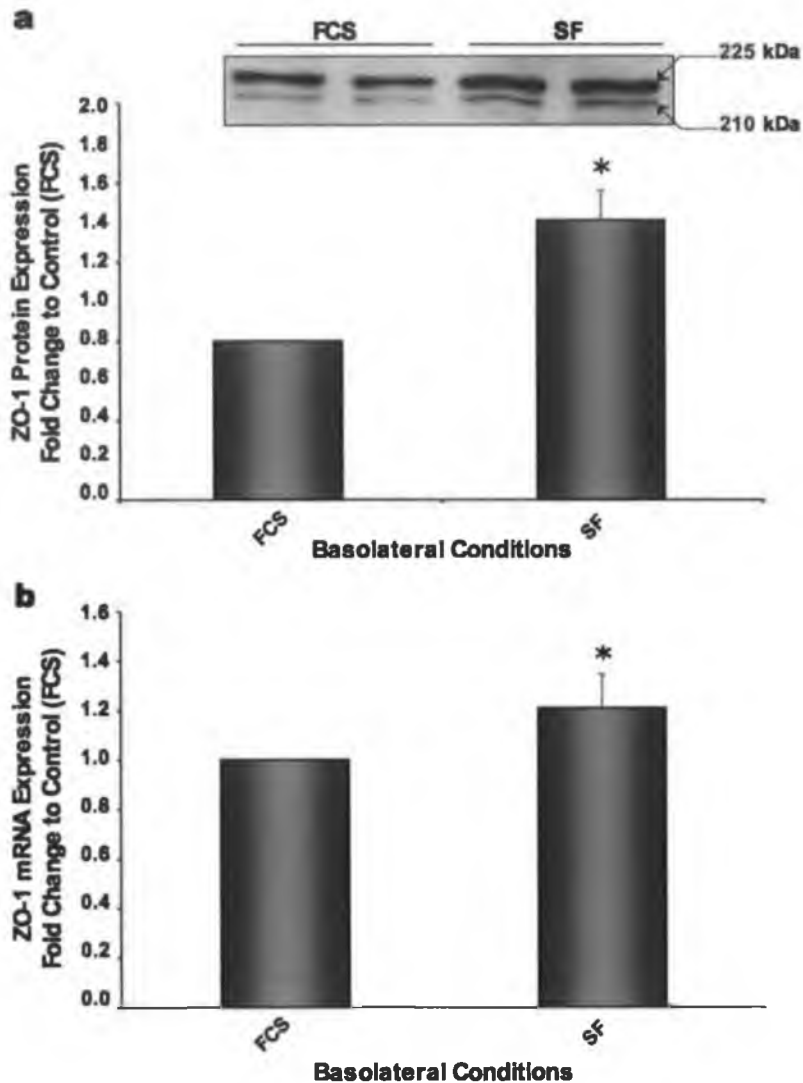


Fig. 4.2.3: Effect of basolateral serum on ZO-1 expression in BBMvECs. Confluent BBMvEC monolayers in Transwell inserts were incubated for 24 h with either serum-containing (FCS) or serum-free (SF) basolateral media and monitored for Occludin protein expression (a) by Western blot and for mRNA (b) by Real-Time PCR. Histograms represent fold change in product formation relative to control (FCS) and are averaged from three independent experiments (a) or seven independent experiments (b) \pm SEM. * $P \leq 0.05$ relative to FCS.

4.2.4 Basolaterally applied serum-dependent association of occludin/ZO-1

Following 24 h culture of BBMvECs in the presence or absence of basolateral serum, association of occludin with ZO-1 was monitored in total BBMvEC lysates by IP as described in section 2.2.16. In response to the removal of basolateral serum, the level of occludin detected in anti-ZO-1 immunoprecipitates was seen to increase by 2.4 ± 0.3 fold (Fig. 4.2.4).

4.2.5 Basolaterally applied serum-dependent subcellular localization of occludin and ZO-1

Following 24 h culture of BBMvECs in the presence or absence of basolateral serum, subcellular localization of occludin and ZO-1 within BBMvEC monolayers was monitored by immunocytochemistry as described in section 2.2.11. In the BBMvEC monoculture with basolateral serum, occludin was found solely in the cytoplasm (Fig. 4.2.5 a), but became significantly more concentrated at the cell membrane in response to serum removal (Fig. 4.2.5 c). Moreover, with serum in both the apical and basolateral media, ZO-1 immunoreactivity was discontinuous, with jagged finger-like projections at cell-cell contacts (Fig. 4.2.5 b). However, following removal of serum from the basolateral compartment for 24 h, ZO-1 immunoreactivity became significantly more continuous along the membrane periphery (Fig. 4.2.5 d).

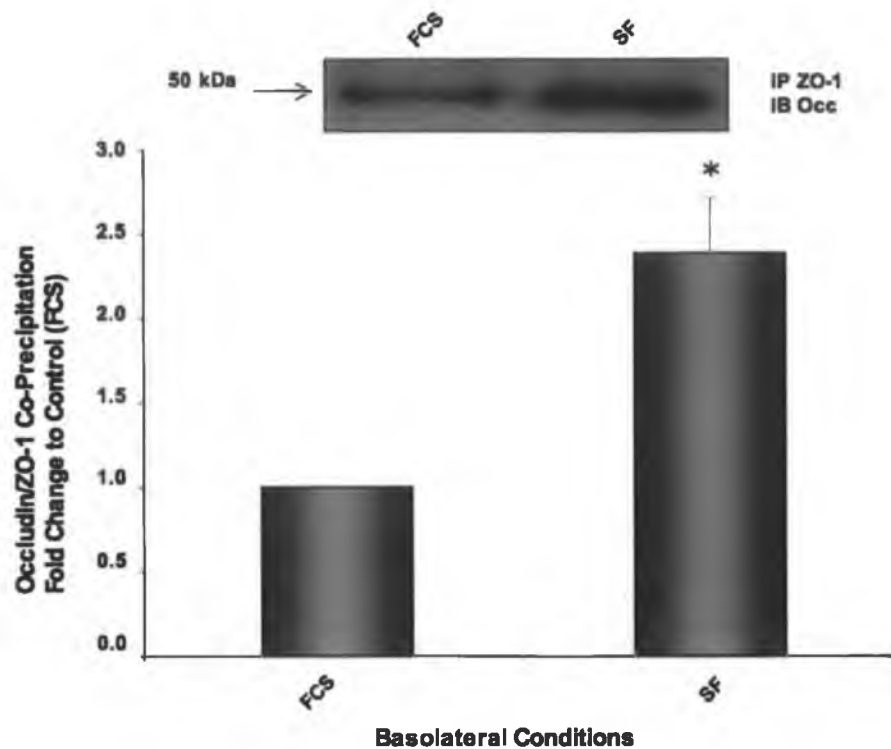


Fig. 4.2.4: Effect of basolateral serum on occludin/ZO-1 association in BBMvECs. Following 24 h incubation of fully confluent BBMvEC monolayers with either serum-containing (FCS) or serum-free (SF) basolateral media, co-association of occludin and ZO-1 was monitored by immunoprecipitation and Western blotting. Histogram represents fold change in band intensity relative to serum-containing control (FCS) and is averaged from six independent experiments \pm SEM. * $P < 0.05$ relative to FCS.

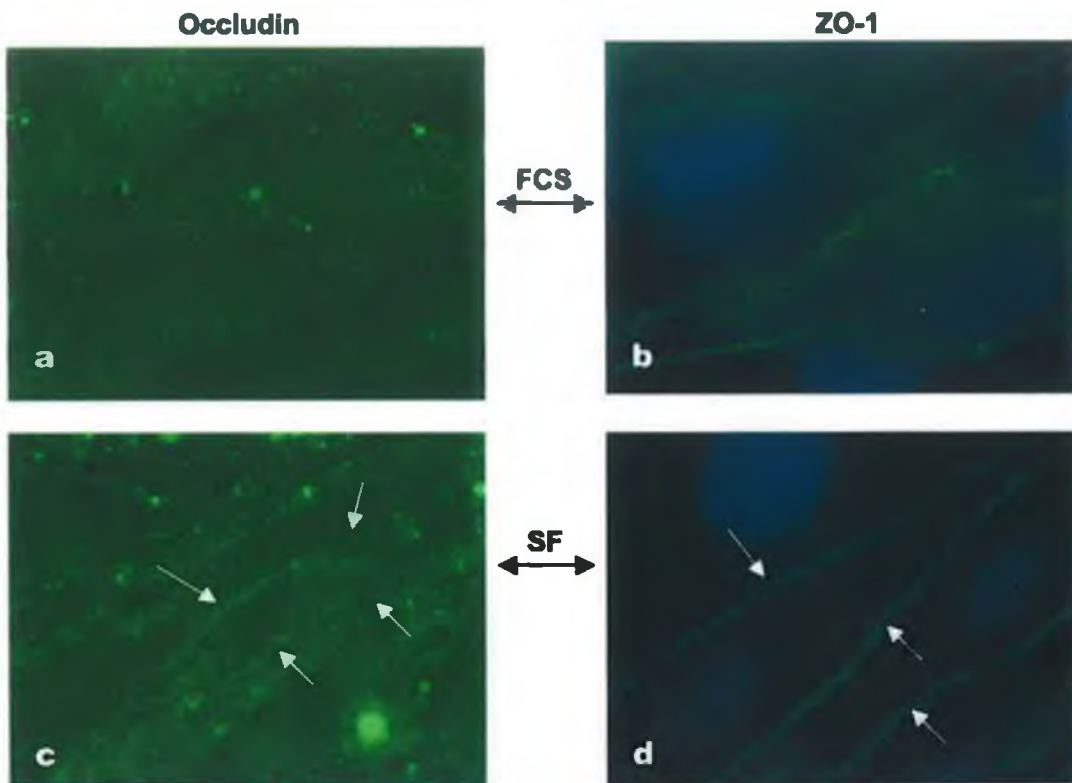


Fig. 4.2.5: Effect of basolateral serum on occludin and ZO-1 subcellular localization in BBMvECs. Following 24 h incubation of fully confluent BBMvEC monolayers, with either serum-containing or serum-free basolateral media, subcellular localization of occludin and ZO-1 was monitored by immunocytochemistry. Occludin protein (green a and c), ZO-1 protein (b and d) and nuclear DAPI staining (blue b and d) were monitored using standard fluorescent microscopy (1000x). White arrows indicate cell-cell border localization. Images are representative of at least three individual sets of experiments.

4.2.6 Basolaterally applied serum-dependent transendothelial permeability of BBMvECs to ¹⁴C-sucrose

Transendothelial permeability of ¹⁴C-sucrose was assessed in fully confluent monolayers of BBMvECs and cells were subsequently treated with either serum-containing or serum-free basolateral media for 24 h as described in section 2.2.7. Permeability was re-assessed after 24 h and expressed as a percentage of the ¹⁴C-sucrose concentration in the apical compartment at t=0 (see section 2.2.13 for details). In monolayers with both apical and basolateral serum (open circles), permeability at t=60 was 10.5 ± 0.6 %TEE. Removal of basolateral serum (shaded squares) significantly decreased permeability to 8.2 ± 0.8 %TEE (Fig. 4.2.6).

4.2.7 Basolaterally applied serum-dependent transendothelial electrical resistance (TEER) of BBMvECs

TEER of BBMvEC monolayers was assessed at confluence as described in section 2.2.12 and cells were subsequently treated with either serum-containing or serum-free basolateral media for 24 h as described in section 2.2.7. After 24 h, TEER was reassessed. The TEER for the monolayer with basolateral serum (FCS) was set to 100% and the TEER of the monolayer without basolateral serum (SF) expressed relative to this. Removal of serum from the basolateral compartment for 24 h significantly increased TEER to 142 ± 6.3 % (Fig. 4.2.7).

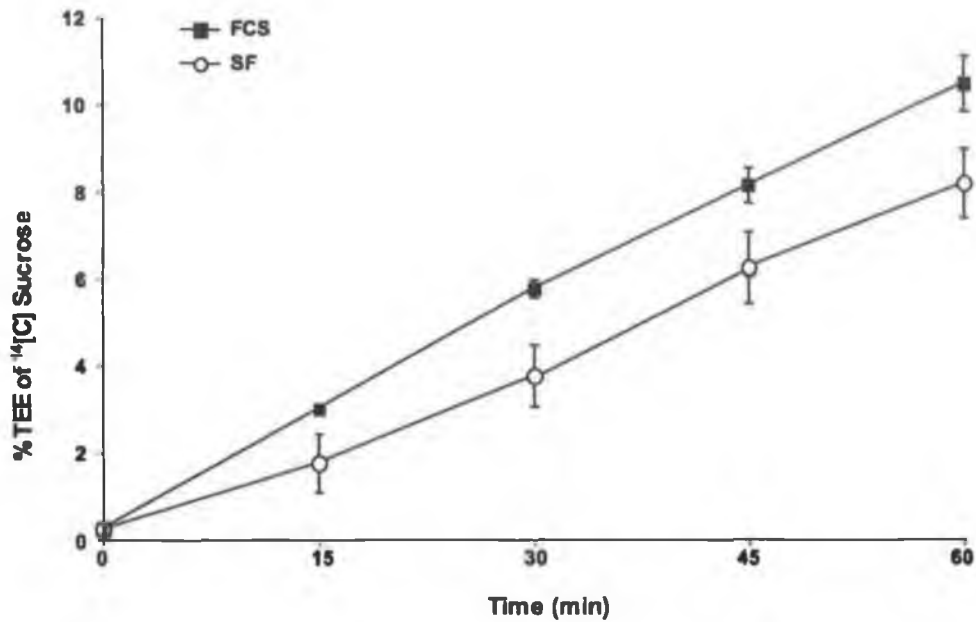


Fig. 4.2.6: Effect of basolateral serum on BBMvEC transendothelial permeability. Prior to and following 24 h incubation of fully confluent BBMvEC monolayers, with either serum-containing (FCS) or serum-free (SF) basolateral media, BBMvECs were monitored for permeability to ¹⁴C-sucrose. Data points are expressed as a percentage of the initial concentration of ¹⁴C-sucrose in the apical chamber at t=0. Results are averaged from three individual experiments ±SEM. $P < 0.0005$ (Two-Way ANOVA, FCS versus SF).

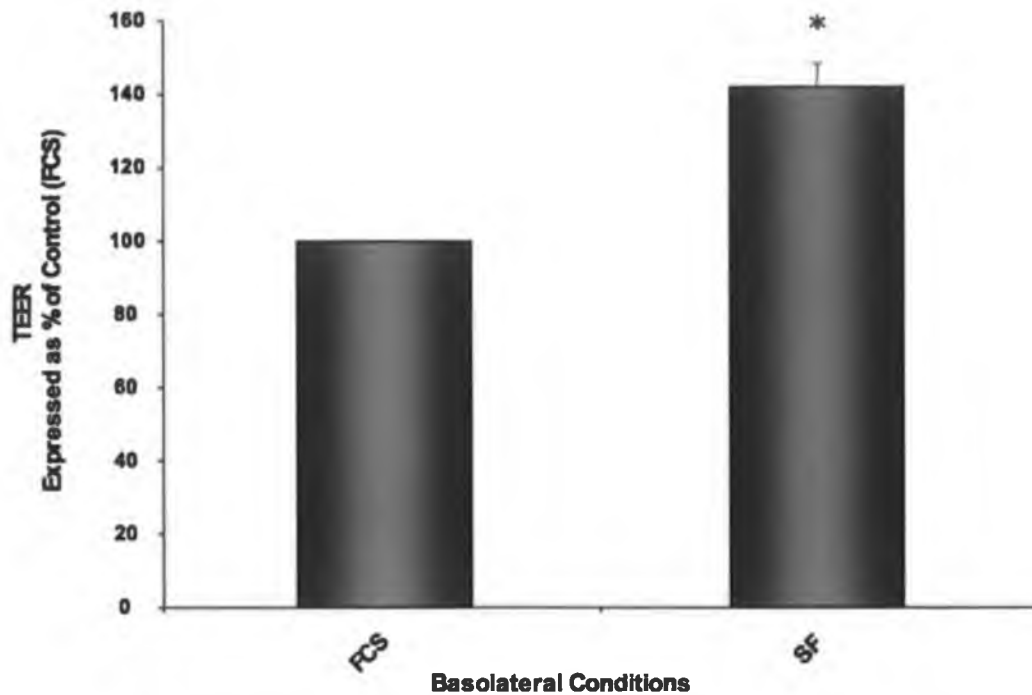


Fig. 4.2.7: Effect of basolateral serum on BBMvEC transendothelial electrical resistance. Prior to and following 24 h incubation of fully confluent BBMvEC monolayers, with either serum-containing (FCS) or serum-free (SF) basolateral media, TEER was assessed. TEER of the BBMvEC monolayer after 24 h with serum in the basolateral compartment (FCS) was set to 100% and the TEER of the monolayer without basolateral serum (SF) expressed relative to this. Histogram represents percentage change in TEER and is averaged from five independent experiments \pm SEM. * $P \leq 0.05$ relative to FCS.

4.3 Discussion

In continuous cell culture, serum is frequently used to promote cell proliferation, however proliferation and cell differentiation are often opposing cell fate decisions. Moreover, the majority of *in vitro* BBB models use serum-containing media on both the apical and basolateral sides, which is contrary to the *in-vivo* situation where the ISF bathing the basolateral side of the ECs is void of serum. Previous publications have shown that serum can lower TEER and increase paracellular permeability (Hoheisel *et al.* 1998; Nitz *et al.* 2003; Lohmann *et al.* 2004), however the mechanisms by which this occurs are poorly understood. This study sought to elucidate the effects of serum on the biochemical etiology of tight junction formation and barrier function with specific emphasis on occludin and ZO-1, two pivotal tight junction proteins and to examine if these effects are polar-specific.

Initial observations revealed that removal of serum from the basolateral compartment of Transwell plates significantly increased TEER, similar to findings by Nitz *et al.*, and significantly lowered transendothelial permeability in BBMvECs. We then sought to further elucidate the subcellular biochemical events responsible for the increase in barrier functionality (Nitz *et al.* 2003). These findings show that removal of basolateral serum from the BBMvEC monolayer leads to increased occludin and ZO-1 protein and mRNA expression. Similar to findings by Collins *et al.*, the increase in ZO-1 mRNA was significantly lower than the observed increase in protein expression, thus indicating a role for post-translational modification of the ZO-1 protein, inducing stabilization and reducing the levels of protein turnover within the cell (Collins *et al.* 2006) or potentially a role for increased mRNA stability thus facilitating increased protein production. Furthermore, removal of basolateral serum for 24 h led to a significant increase in the association of occludin/ZO-1. We therefore postulate a putative role for co-association of occludin/ZO-1 inducing stabilization of the protein complex, thus leading to an apparent increase in protein expression caused by decreased protein degradation.

Further studies employing pulse-chase technique to monitor new protein synthesis would aid in clarifying the processes involved. Also, it is possible that any increase in ZO-1 mRNA occurs before the 24 h time-point, therefore a time-course measuring mRNA production, ranging from 0 – 24 h, would help to definitively clarify if the observed increase in ZO-1 protein expression is in fact due to increased mRNA synthesis or indeed to a yet unidentified post-translational modification.

Immunocytochemical analysis revealed that ZO-1 localization in monolayers with serum in both the apical and basolateral compartments was characterized by the presence of extrusions and invaginations typical of leaky junctions. Following the removal of serum from the basolateral compartment, a profound redistribution of ZO-1 was observed, from discontinuous finger-like projections to a smooth and continuous localization at points of cell-cell contact. In addition, occludin staining, which is localized mainly in the cytoplasm when both apical and basolateral serum are present, re-localized to the membrane periphery upon removal of basolateral serum. The increased co-localization of both occludin and ZO-1 to the membrane periphery, in conjunction with the increased co-association of the two is indicative of functional tight junctions. Moreover, removal of serum from the apical compartment alone caused no redistribution of either occludin or ZO-1, and led to reduced viability of the cells as assessed by phase-contrast microscopy (data not shown). These data indicate a robust role for serum in modulating BBMvEC tight junction formation and function in a highly polar-specific manner.

The effects of serum on barrier function and tight junction formation in both endothelial and epithelial cells are shown to be exerted in a highly polar-specific manner either from the apical or basolateral aspect depending on cell phenotype (Marmorstein *et al.* 1992; Chang *et al.* 1997; Nitz *et al.* 2003). Moreover, the preference for one cell surface over the other indicates a role for specific membrane-standing receptors in modulating the effect of serum on barrier function. Thus, it appears that the polar-specific effect of serum is dependent on cell physiology and phenotype. Furthermore, serum, although widely used in cell culture, remains

largely undefined, containing plasma proteins, hormones, growth factors and fatty acids among others, which induce a variety of cell fate decisions ranging from proliferation, to angiogenesis, to differentiation.

Vascular endothelial growth factor (VEGF) is a heat-stable cytokine found in serum, which is known to induce endothelial cell proliferation, angiogenesis, permeability and motility (Ferrara *et al.* 1991; Houck *et al.* 1992) and is essential for the growth and survival of endothelial cells *in vivo*. VEGF is ubiquitously expressed by most cell types, but not endothelial cells. However, endothelial cells are the sole target for VEGF activity. Originally identified in 1983 as vascular permeability factor (Senger *et al.* 1983), a large family of VEGF splice variants and receptors have now been identified. The most widely studied form, VEGF-A₁₆₅ (hereafter termed VEGF) is the most predominant form, containing a heparin-binding domain involved in anchoring to the extracellular matrix and presentation to VEGF receptors. There are three receptors in the VEGF family, known as VEGF-R1, -R2 and -R3, which contain tyrosine kinase activity and multiple IgG-like domains (Shibuya *et al.* 1999). VEGF-R1 and VEGF-R2 both bind VEGF, however VEGF-R1 is of a higher affinity than VEGF-R2 (Waltenberger *et al.* 1994), and is primarily associated with endothelial mobility and permeability (Seetharam *et al.* 1995; Neufeld *et al.* 1999; Shibuya *et al.* 1999). VEGF-R2 on the other hand is implicated in cell proliferation (Millauer *et al.* 1993; Waltenberger *et al.* 1994). Previous studies by Nitz *et al.* have demonstrated the ability of VEGF to decrease barrier function of primary porcine brain capillary endothelial cells and that this effect is seen only when VEGF is added to the basolateral compartment (Nitz *et al.* 2003). We, therefore, postulate that VEGF may be one serum component responsible for increasing BBMvEC permeability. These data suggest that if the increased permeability caused by the presence of basolateral serum is due to the action of VEGF, that there is polar-specific expression of VEGF receptors in BBMvECs. That is, that the VEGF-R2 may be expressed primarily on the apical cell surface, and the VEGF-R1 receptor (primarily associated with mobility and permeability) on the basolateral surface. Thus, in this transwell model, with apical serum-rich and basolateral serum-free

media, VEGF contained in serum could stimulate cell proliferation via the apical VEGF-R2, without activation of the basolateral VEGF-R1, which would cause increased permeability. Further investigations using VEGF antagonists to block receptors, in conjunction with confocal immunocytochemistry distinguishing between the two receptors is required for clarification.

Lysophosphatidic acid (LPA) is another serum factor, which has been shown to increase endothelial permeability (Schulze *et al.* 1997; Nitz *et al.* 2003). Produced by activated platelets, fibroblasts and several carcinomas, LPA is found in serum as an amphiphilic molecule bound to albumin and gelsolin (Tigyi and Milei 1992; Goetzl *et al.* 2000). Studies by Nitz *et al.* have shown that purified LPA, in its unbound form, disrupts endothelial barriers but does not display any polar specificity. In contrast to these findings, the ability of serum to weaken endothelial barriers has been shown to be highly polar-specific, thus indicating that either LPA is not the component responsible for serum-induced barrier breakdown, or that in its native form, i.e. bound to albumin, it is unable to interact with apical receptors, but may bind to basolateral receptors. Future work investigating the effect of purified and bound LPA on tight junction formation and barrier function are required to elucidate if LPA is one serum component responsible for the polar-specific serum-induced barrier breakdown in BBMvECs.

In summary, this work describes the role of serum in endothelial tight junction regulation. These data clearly indicate that removal of basolateral serum modulates the expression, association and localization of occludin and ZO-1, which are integral tight junction proteins. Furthermore, these subcellular events correlate with increased electrical resistance and decreased paracellular flux across the BBMvEC monolayer. Further studies are required to explicate both the serum components and the exact mechanisms by which these events occur. This information may be invaluable in the development of a superior *in vitro* BBB model and greatly enhances our overall understanding of how serum factors regulate microvascular endothelial barrier formation and function.

Chapter 5

*Investigation of the role of C6 glioma
in regulating BBMvEC occludin and
ZO-1 and the effect of co-culture on
BBMvEC permeability.*

5.1 Introduction

The blood-brain barrier (BBB) is a selective barrier, which functions to maintain homeostasis of the central nervous system (CNS) by preventing potentially harmful blood-borne solutes entering the brain microenvironment. The endothelial cells comprising the BBB exhibit many specialized properties including extremely low permeability, high transendothelial electrical resistance (TEER) (Crone and Olesen 1982; Butt *et al.* 1990; Jones *et al.* 1992) and low occurrence of pinocytotic vessels. Adjacent endothelial cells are bound by three types of intercellular contacts, namely desmosomes, adherens junctions and tight junctions, with barrier function solely attributed to the tight junction (Anderson and Van Itallie 1995).

Although the barrier function of the BBB is attributed solely to endothelial cells, astrocytes, which encircle the basolateral aspect of the endothelium have been implicated in the up-regulation of BBB function both *in vitro* (Jeliazkova-Mecheva and Bobilya 2003; Gee and Keller 2005) and *in vivo* (Saunders *et al.* 1991), albeit via poorly understood mechanisms. As discussed previously in chapter 4, exposure of the basolateral surface of the endothelium to serum inhibits tight junction formation and increases paracellular permeability. Collectively, these observations have led us to hypothesize that basolateral endothelial conditions directly modulate endothelial barrier function by altering the expression and assembly of apical tight junction components.

Thus, the aim of this chapter is to investigate the role of non-contacting co-culture with C6 glioma on BBMvEC tight junction formation and barrier function in basolaterally serum-containing or serum-free environment, with particular emphasis on the tight junction proteins occludin and ZO-1. That is, BBMvECs grown on transwell inserts are co-cultured with C6 glioma grown on the plate bottom in either the presence or absence of basolateral serum (see fig. 2.2.7.1) and are monitored for changes in tight junction formation and function.

5.2 Results

5.2.1 C6 Glioma astrocyte-conditioned media- and serum-dependent subcellular localization of occludin in BBMvECs

Following 24 h incubation of BBMvECs with C6ACM \pm serum in the apical compartment, subcellular localization of occludin within BBMvEC monolayers was monitored by immunocytochemistry as described in section 2.2.11. In the BBMvEC monolayer with apical serum, occludin was found solely in the cytoplasm (Fig. 5.2.1 a). Following removal of serum, there was no significant difference in subcellular localization of occludin (Fig. 5.2.1 c). Moreover, monolayers incubated in the presence of C6ACM, either with or without serum, showed no significant difference in occludin subcellular localization (Fig. 5.2.1 b and d, respectively).

5.2.2 C6 Glioma astrocyte conditioned media- and serum-dependent subcellular localization of ZO-1 in BBMvECs

Following 24 h incubation of BBMvECs with C6ACM \pm serum in the apical compartment, subcellular localization of ZO-1 within BBMvEC monolayers was monitored by immunocytochemistry as described in section 2.2.11. In the BBMvEC monolayer with apical serum, ZO-1 distribution at the cellular membrane was discontinuous with long finger like projections (Fig. 5.2.2 a), indicative of weak tight junctions. Neither removal of serum from the culture media (Fig. 5.2.2 c) nor incubation in C6ACM with or without serum (Fig. 5.2.2 b and d, respectively) led to changes in ZO-1 distribution at the cellular membrane.

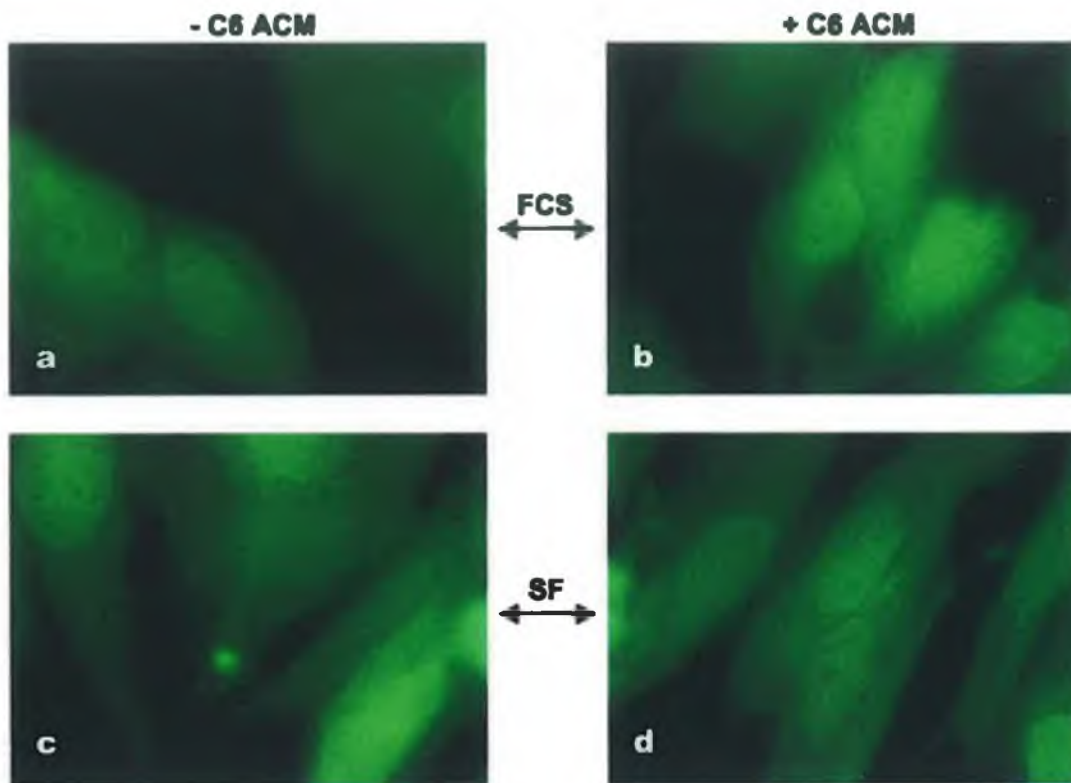


Fig. 5.2.1: Effect of apically applied C6 glioma astrocyte-conditioned media and serum on occludin subcellular localization. Following 24 h incubation of fully confluent BBMvEC in the absence or presence of C6 glioma astrocyte conditioned media (C6ACM), and/or serum in the apical compartment, subcellular localization of occludin was monitored by immunocytochemistry. Occludin protein (green a – d) was monitored using standard fluorescent microscopy (1000x).

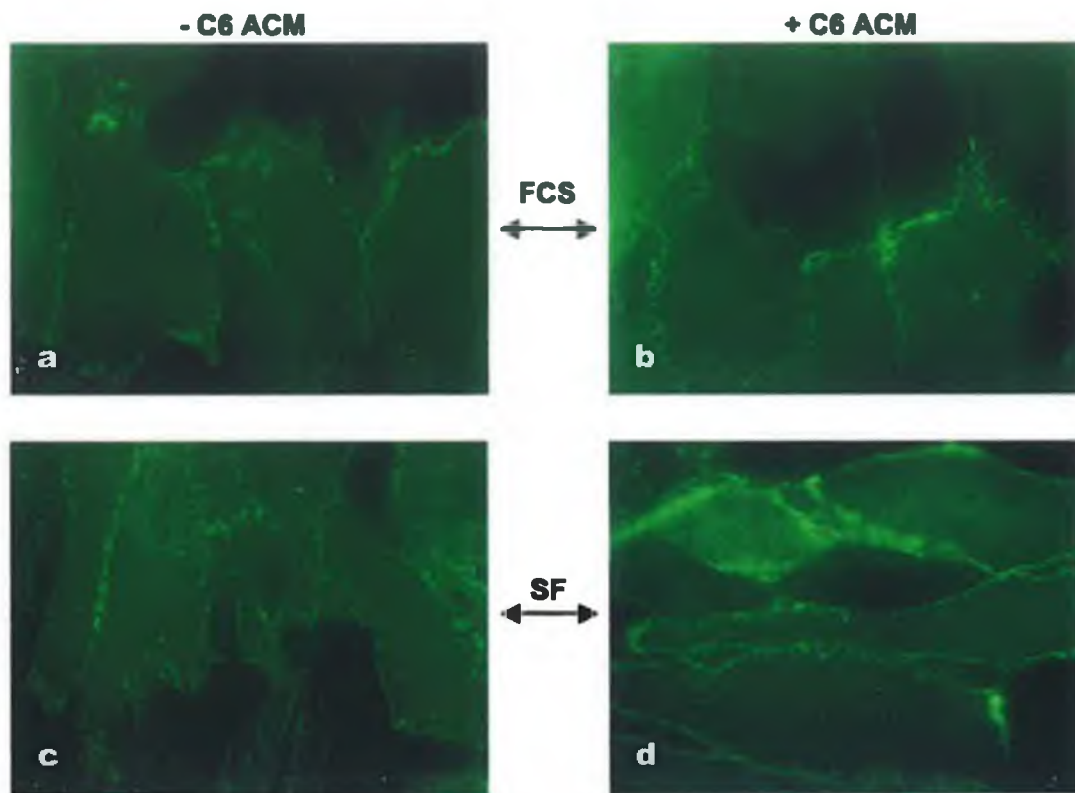


Fig. 5.2.2: Effect of apically applied C6 glioma astrocyte-conditioned media and serum on ZO-1 subcellular localization. Following 24 h incubation of fully confluent BBMV-EC in the absence or presence of C6 glioma astrocyte conditioned media (C6ACM), and/or serum in the apical compartment, subcellular localization of ZO-1 was monitored by immunocytochemistry. ZO-1 protein (green a – d) was monitored using standard fluorescent microscopy (1000x).

5.2.3 Co-culture- and serum-dependent subcellular localization of occludin in BBMvECs

Following co-culture and/or removal of serum from the basolateral compartment of fully confluent BBMvECs for 24 h, subcellular localization of occludin within BBMvEC monolayers was monitored by immunocytochemistry as described in section 2.2.11. In the BBMvEC monoculture with basolateral serum, occludin was found solely in the cytoplasm (Fig. 5.2.3 a), but became significantly more concentrated at the cell membrane in response to serum removal (Fig. 5.2.3 c). Co-culture with C6 glioma, in the presence of basolateral serum, also increased occludin localization at points of cell-cell contact (Fig. 5.2.3 b), however, the combination of C6 glioma without basolateral serum led to the most continuous occludin localization at the cell (Fig. 5.2.3 d)

5.2.4 Co-culture- and serum-dependent subcellular localization of ZO-1 in BBMvECs

Following co-culture and/or removal of serum from the basolateral compartment of fully confluent BBMvECs for 24 h, subcellular localization of ZO-1 within BBMvEC monolayers was monitored by immunocytochemistry as described in section 2.2.11. With serum in both the apical and basolateral media, ZO-1 immunoreactivity was discontinuous, with jagged finger-like projections at cell-cell contacts (Fig. 5.2.4 a). However, following removal of serum from the basolateral compartment, ZO-1 immunoreactivity became significantly more continuous along the membrane periphery (Fig. 5.2.4 c). Co-culture with C6 glioma, in the presence of basolateral serum, also increased ZO-1 immunoreactivity at the cell membrane (Fig. 5.2.4 c), however, the combination of C6 glioma without basolateral serum appears to give the most continuous ZO-1 localization at the cell membrane (Fig. 5.2.4 d).

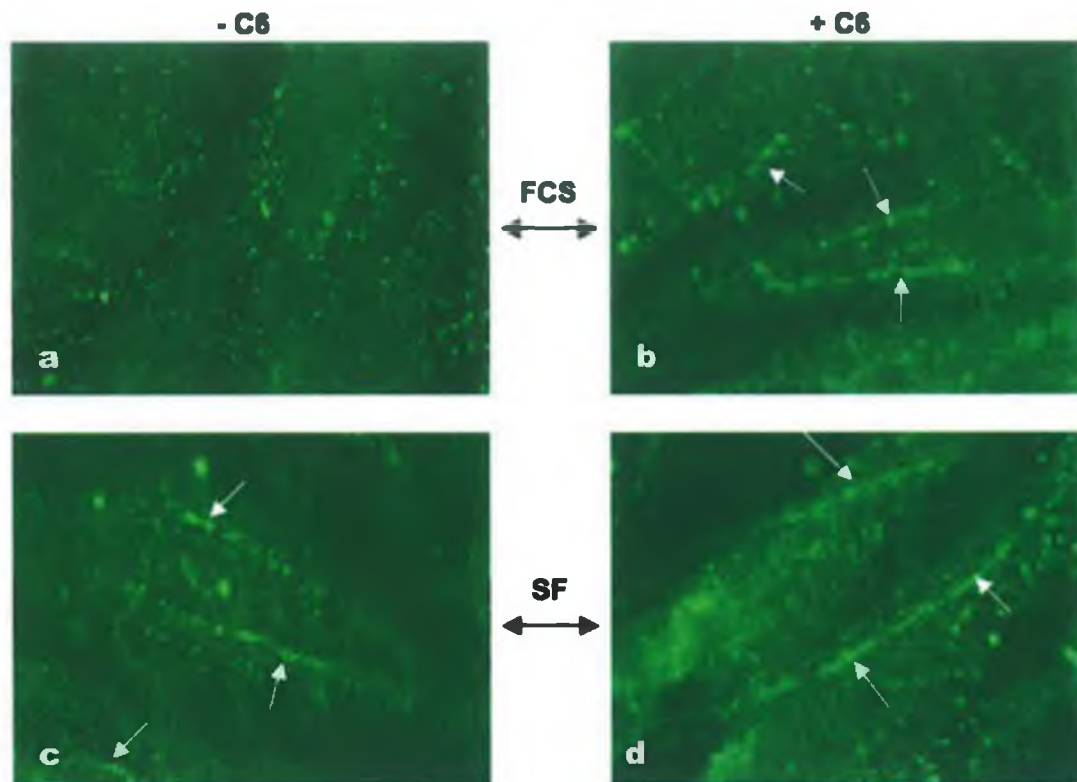


Fig. 5.2.3: Effect of co-culture and serum on ocludin subcellular localization in BBMvECs. Following 24 h incubation of fully confluent BBMvEC in either serum-containing or serum-free basolateral media and/or co-culture with C6 glioma, subcellular localization of ocludin was monitored by immunocytochemistry. Ocludin protein (green a–d) was monitored using standard fluorescence microscopy (1000x). White arrows indicate cell-cell border localization. Images are representative of at least three individual sets of experiments.

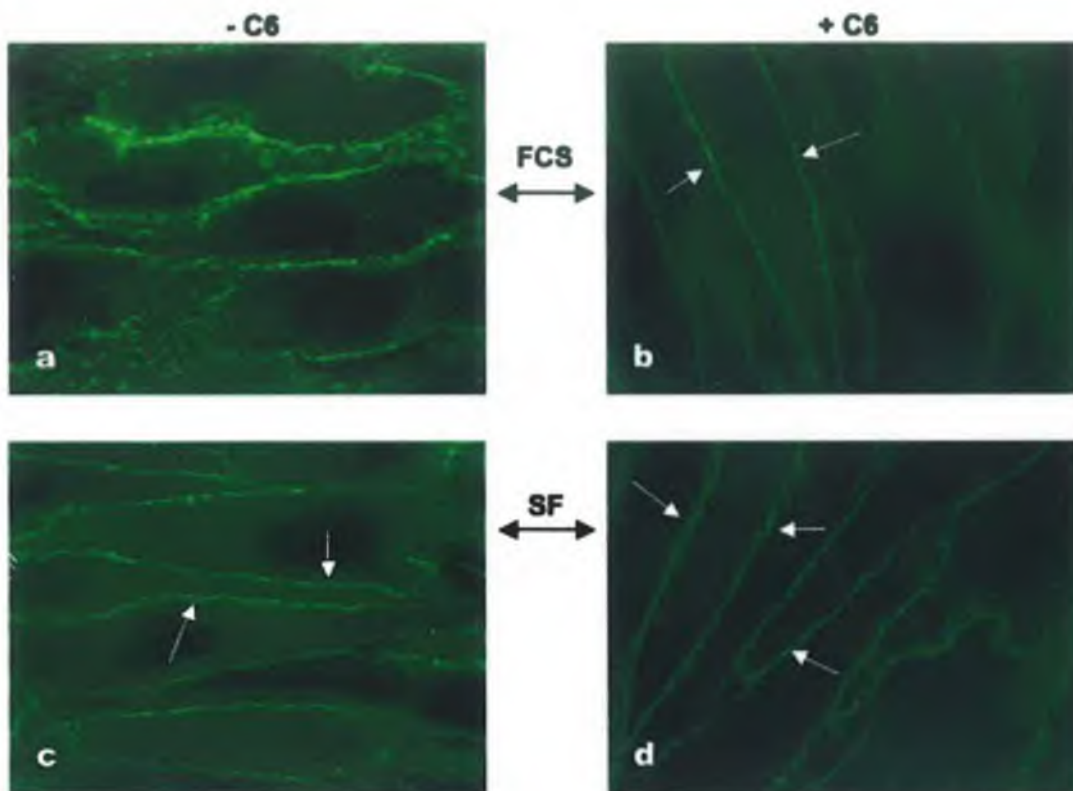


Fig. 5.2.4: Effect of co-culture and serum on ZO-1 subcellular localization in BBMvECs. Following 24 h incubation of fully confluent BBMvEC in either serum-containing or serum-free basolateral media and/or co-culture with C6 glioma,, subcellular localization of ZO-1 was monitored by immunocytochemistry. ZO-1 protein (green a-d) was monitored using standard fluorescence microscopy (1000x). White arrows indicate cell-cell border localization. Images are representative of at least three individual sets of experiments.

5.2.5 Co-culture- and serum-dependent expression of occludin in BBMvECs

Removal of basolateral serum from the BBMvEC monoculture for 24 h resulted in 1.9 ± 0.2 and 1.6 ± 0.1 fold increases in occludin protein and mRNA expression, respectively (Fig. 5.2.5 a and b). Co-culture in the presence of basolateral serum (C6 FCS) increased occludin protein expression by 2.4 ± 0.0 fold (Fig. 5.2.5 a) whilst exhibiting no significant effect on occludin mRNA expression (Fig. 5.2.5 b). Moreover, co-culture of BBMvEC and C6 glioma without basolateral serum (C6 SF) significantly increased both occludin protein and mRNA expression (2.9 ± 0.2 and 1.9 ± 0.1 fold respectively) (Fig. 5.2.5 a and 1b).

5.2.6 Co-culture- and serum-dependent expression of ZO-1 in BBMvECs

Removal of basolateral serum from the BBMvEC monoculture for 24 h resulted in 1.6 ± 0.2 and 1.5 ± 0.1 fold increases in ZO-1 protein and mRNA expression, respectively (Fig. 5.2.6 a and b). Co-culture in the presence of basolateral serum (C6 FCS) increased ZO-1 protein expression by 2.0 ± 0.1 fold (Fig. 5.2.6 a) whilst exhibiting no significant effect on ZO-1 mRNA expression (Fig. 5.2.6 b). Moreover, co-culture of BBMvEC and C6 glioma without basolateral serum (C6 SF) significantly increased both ZO-1 protein and mRNA expression (1.7 ± 0.0 and 1.3 ± 0.2 fold respectively) (Fig. 5.2.6 a and b).

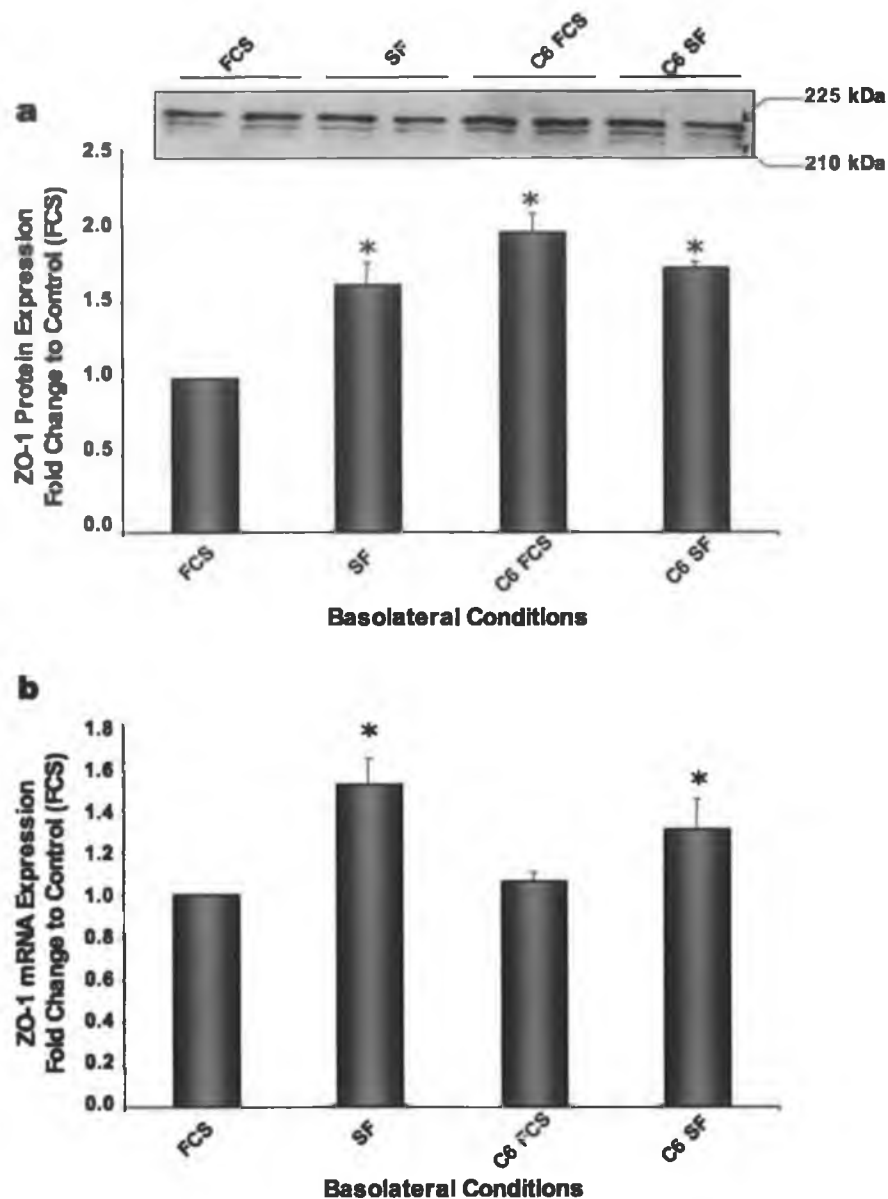


Fig. 5.2.6: Effect of co-culture and serum on ZO-1 expression in BBMvECs. Confluent BBMvEC monolayers in transwell inserts were incubated for 24 h with either serum-containing or serum-free basolateral media and/or C6 glioma, which had been growing on the plate bottom for 24 h. BBMvECs were then monitored for ZO-1 protein expression (a) by Western blot and for mRNA (b) by Real-Time PCR. Histograms represent fold change in product formation relative to control (i.e. FCS - monoculture with serum) and is averaged from three independent experiments \pm SEM. * $P \leq 0.05$ relative to FCS. Gels are representative.

5.2.7 Co-culture- and serum-dependent association of occludin/ZO-1

Following co-culture and/or removal of serum from the basolateral compartment of fully confluent BBMvECs for 24 h, association of occludin with ZO-1 was monitored in total BBMvEC lysates by IP as described in section 2.2.16. In response to the removal of serum (SF), the level of occludin detected in anti-ZO-1 immunoprecipitates was seen to increase by 2.2 ± 0.1 fold. Co-culture of BBMvECs and C6 glioma, in the presence of basolateral serum (C6 FCS) led to a 3.1 ± 0.2 fold increase in occludin/ZO-1 association, and 3.8 ± 0.2 fold increase when basolateral serum was removed (C6 SF) (Fig. 5.2.7).

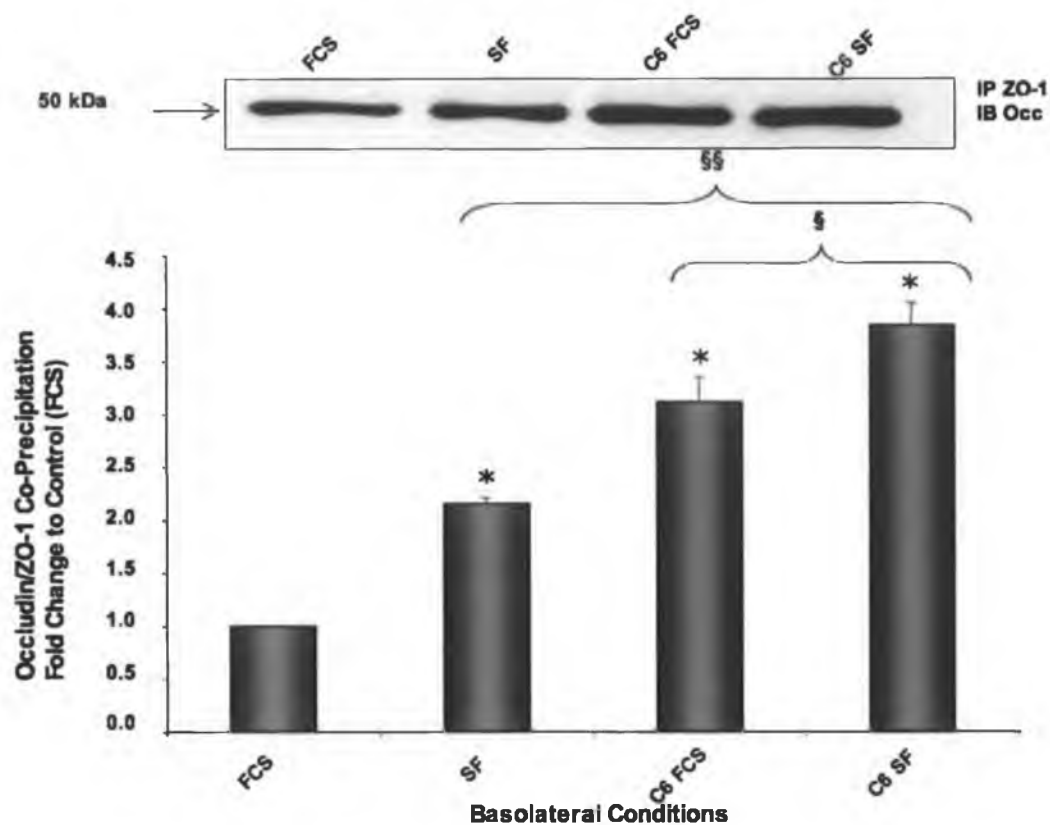


Fig. 5.2.7: Effect of co-culture and serum on occludin and ZO-1 association in BBMvECs. Following 24 h incubation of fully confluent BBMvEC in either serum-containing or serum-free basolateral media and/or co-culture with C6 glioma, co-association of occludin and ZO-1 were monitored by IP and Western blotting. Representative blot is shown above graph. Histogram represents fold change in band intensity relative to serum-containing control (FCS) and is averaged from three independent experiments \pm SEM; * $P \leq 0.005$ relative to FCS; § $P \leq 0.01$ relative to C6 FCS; §§ $P \leq 0.005$ relative to SF.

5.2.8 Co-culture- and serum-dependent transendothelial permeability of BBMvECs to ¹⁴C-sucrose

Transendothelial permeability of ¹⁴C-sucrose was assessed in fully confluent monolayers of BBMvECs and cells were subsequently treated with either serum-containing or serum-free basolateral media and/or co-culture with C6 glioma as described in section 2.2.7. Permeability was re-assessed after 24 h and expressed as a percentage of the ¹⁴C sucrose concentration in the apical compartment at t=0 (i.e. % TEE of ¹⁴C sucrose or % Trans Endothelial Exchange of ¹⁴C sucrose) as described in section 2.2.13. In control cells (i.e. monolayer with basolateral serum, FCS) permeability at t=60 was 11.3 ± 0.3 %TEE. Removal of basolateral serum (SF) significantly decreased permeability to 9.7 ± 0.2 %TEE, whilst co-culture with C6 glioma in the presence of basolateral serum (C6 FCS) also led to a significant decrease in permeability to 10.6 ± 0.3 %TEE. Co-culture without basolateral serum (C6 SF) also reduced permeability to 10.0 ± 0.5 %TEE (Fig. 5.2.8).

5.2.9 Co-culture- and serum-dependent transendothelial electrical resistance (TEER) of BBMvEC

TEER of BBMvEC monolayers was assessed at confluence as described in section 2.2.12 and cells were subsequently treated with either serum-containing or serum-free basolateral media and/or co-culture with C6 gliomas, as described above. The TEER for the monolayer without serum in the basolateral compartment (SF) increased significantly to $148 \pm 4.6\%$ of the control after 24 h. Co-culture in the presence of serum (C6 FCS) resulted in a $128 \pm 6.0\%$ increase in TEER, whilst co-culture without basolateral serum (C6 SF) led to a $160 \pm 7.1\%$ increase in TEER (Fig. 5.2.9).

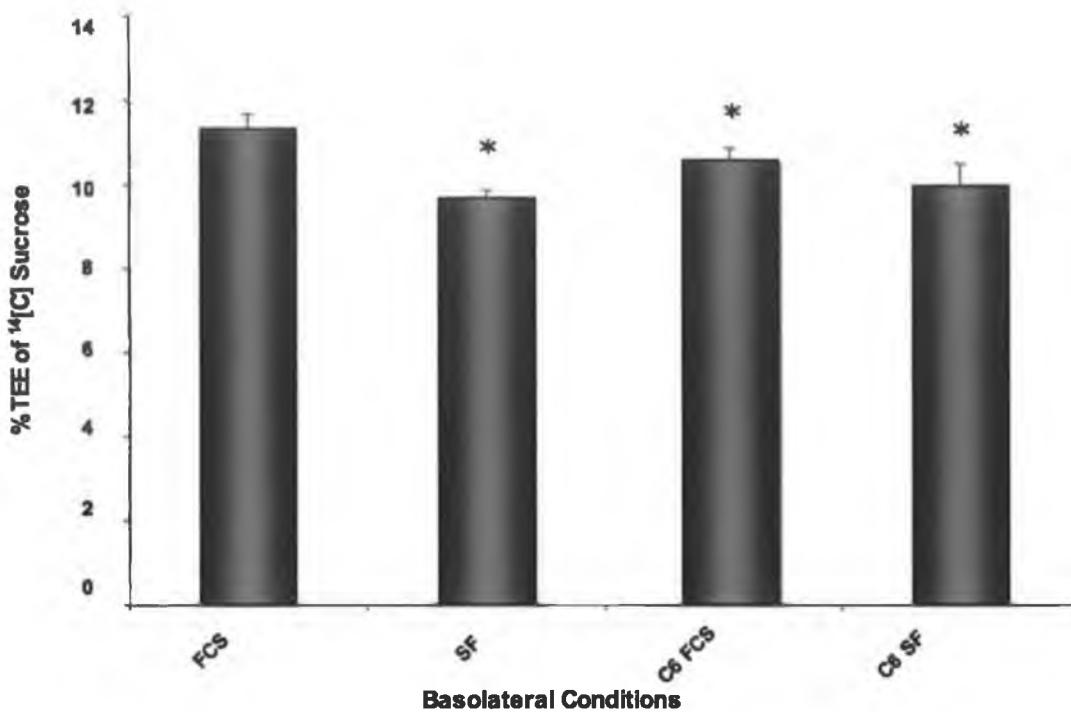


Fig. 5.2.8: Effect of co-culture and serum on BBMvEC transendothelial permeability. Prior to and following 24 h incubation of fully confluent BBMvECs in either serum-containing or serum-free basolateral media and/or co-culture with C6 glioma, BBMvECs were monitored for permeability to ¹⁴C-sucrose. Data points shown are expressed as a percentage of the initial concentration of ¹⁴C-sucrose in the apical chamber at t=0. Histogram represents percentage change in basolateral ¹⁴C-sucrose concentration at t=60 and is averaged from three independent experiments \pm SEM. * $P \leq 0.05$ relative to FCS.

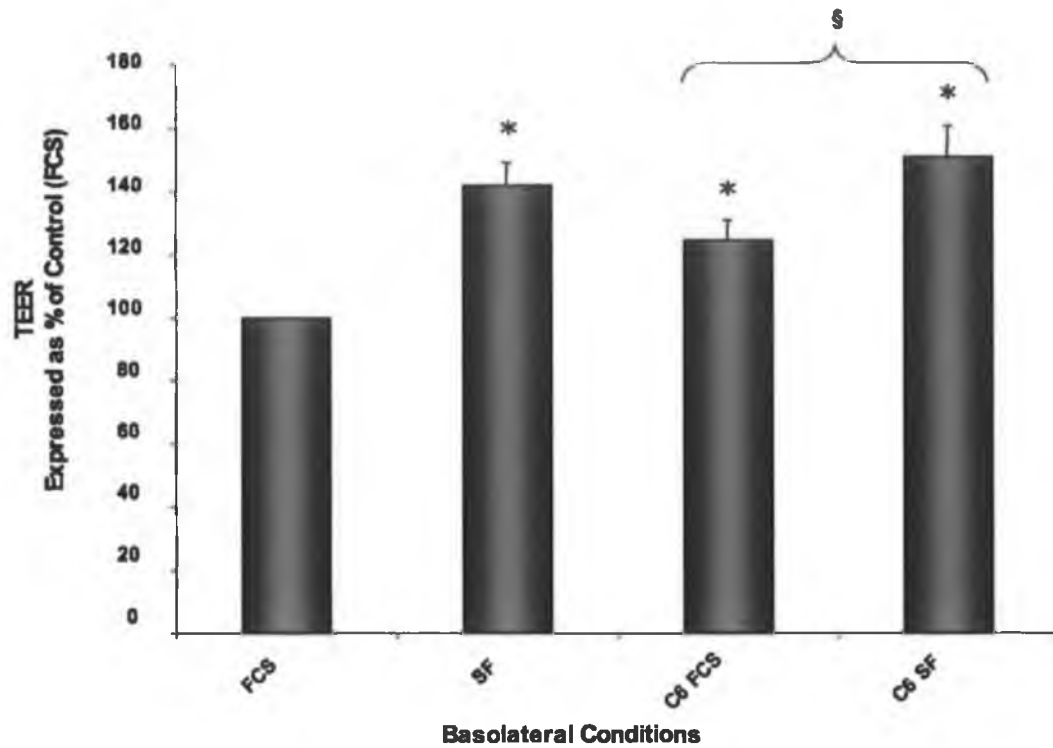


Fig. 5.2.9: Effect of co-culture and serum on BBMvEC transendothelial electrical resistance. Prior to and following 24 h incubation of fully confluent BBMvEC in either serum-containing or serum-free basolateral media and/or co-culture with C6 glioma, TEER was assessed. TEER of BBMvEC monoculture after 24 h with serum in both the apical and basolateral compartments (FCS), was set to 100% and the TEER of the serum-free (SF) and co-cultures with (C6 FCS) and without (C6 SF) basolateral serum expressed relative to this. Histogram represents percentage change in TEER and is averaged from four independent experiments \pm SEM; * $P \leq 0.005$ relative to FCS; § $P \leq 0.01$ relative to C6 FCS.

5.2.10 Serum-dependent, but not co-culture-dependent, subcellular localization of occludin is attenuated by cycloheximide in BBMvECs

Following co-culture and/or removal of serum from the basolateral compartment of fully confluent BBMvECs in the absence or presence of cycloheximide for 24 h, subcellular localization of occludin within BBMvEC monolayers was monitored by immunocytochemistry as described in section 2.2.11. The increased localization of occludin to the cell membrane following removal of basolateral serum was completely abolished by the addition of cycloheximide to the culture media (Fig. 5.2.10 a-d). The co-culture-dependent increase in occludin membrane localization in the presence of basolateral serum (Fig. 5.2.10 e) was unaffected by the addition of cycloheximide (Fig. 5.2.10 f). However, the increases in occludin localization to the cell membrane seen following co-culture in the absence of basolateral serum (Fig. 5.2.10 g) were only partially attenuated by the addition of cycloheximide (Fig. 5.2.10 h).

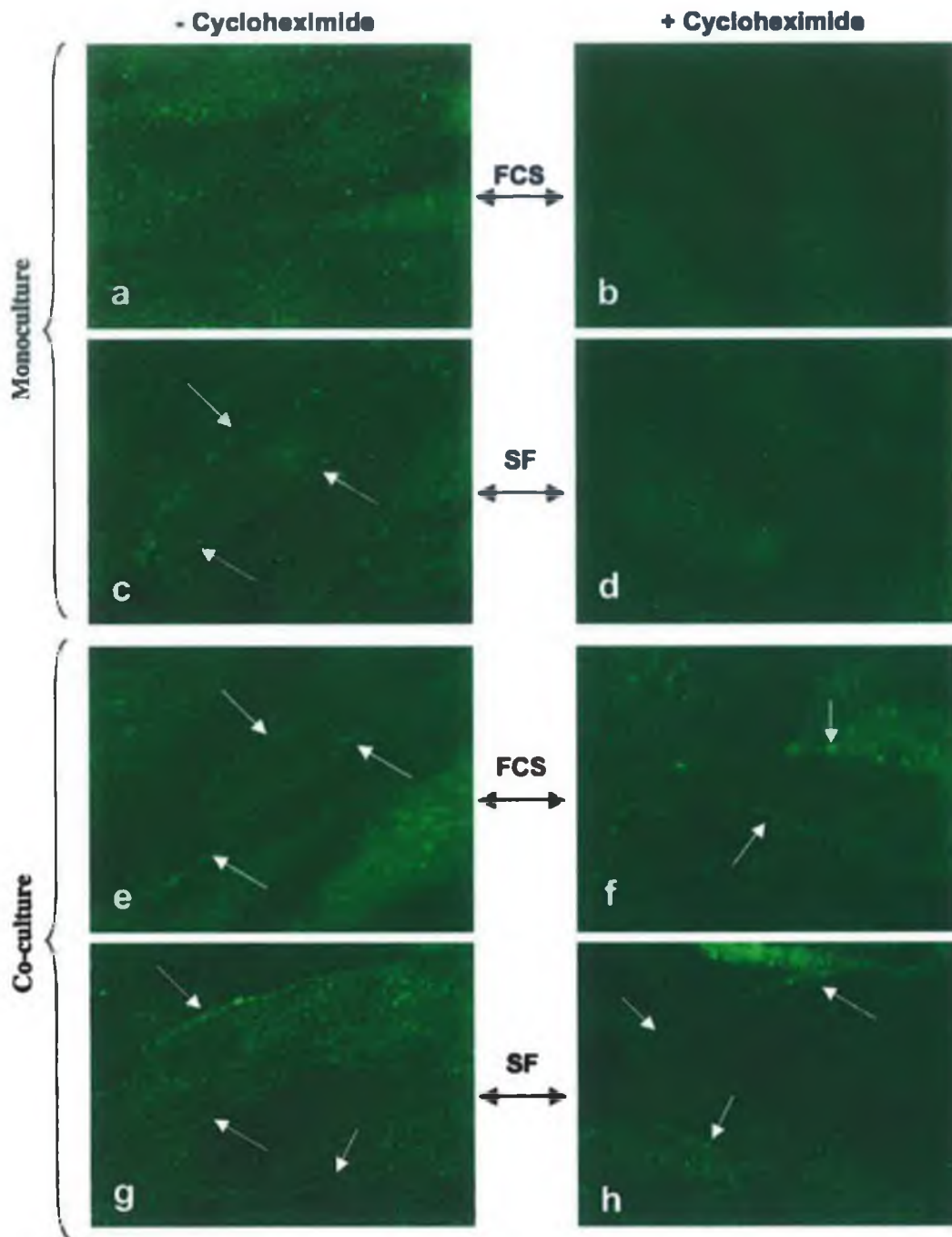


Fig. 5.2.10: Effect of cycloheximide on co-culture- and serum-dependent subcellular localization of occludin in BBMvECs. Following co-culture and/or removal of serum from the basolateral compartment of fully confluent BBMvECs in the absence or presence of cycloheximide for 24 h, subcellular localization of occludin was monitored by immunocytochemistry. Images b,d,f and h indicate the effect of cycloheximide on occludin localization. Occludin protein (green a–h) was monitored using standard fluorescence microscopy (1000x). White arrows indicate cell-cell border localization. Images are representative of at least three individual sets of experiments.

5.2.11 Serum-dependent, but not co-culture-dependent, subcellular localization of ZO-1 is attenuated by cycloheximide in BBMvECs

Following co-culture and/or removal of serum from the basolateral compartment of fully confluent BBMvECs in the absence or presence of cycloheximide for 24 h, subcellular localization of ZO-1 within BBMvEC monolayers was monitored by immunocytochemistry as described in section 2.2.11. The continuous localization of ZO-1 at the cell periphery seen following removal of basolateral serum was significantly reduced by the addition of cycloheximide to the culture media (Fig. 5.2.11 a-d). The increase in ZO-1 localization observed in the co-culture model with basolateral serum (Fig. 5.2.11 e) was not significantly altered following the addition of cycloheximide to the culture media (Fig. 5.2.11 f). However, addition of cycloheximide to the co-culture model without basolateral serum had no apparent effect on ZO-1 subcellular localization (Fig. 5.2.11 g and h).

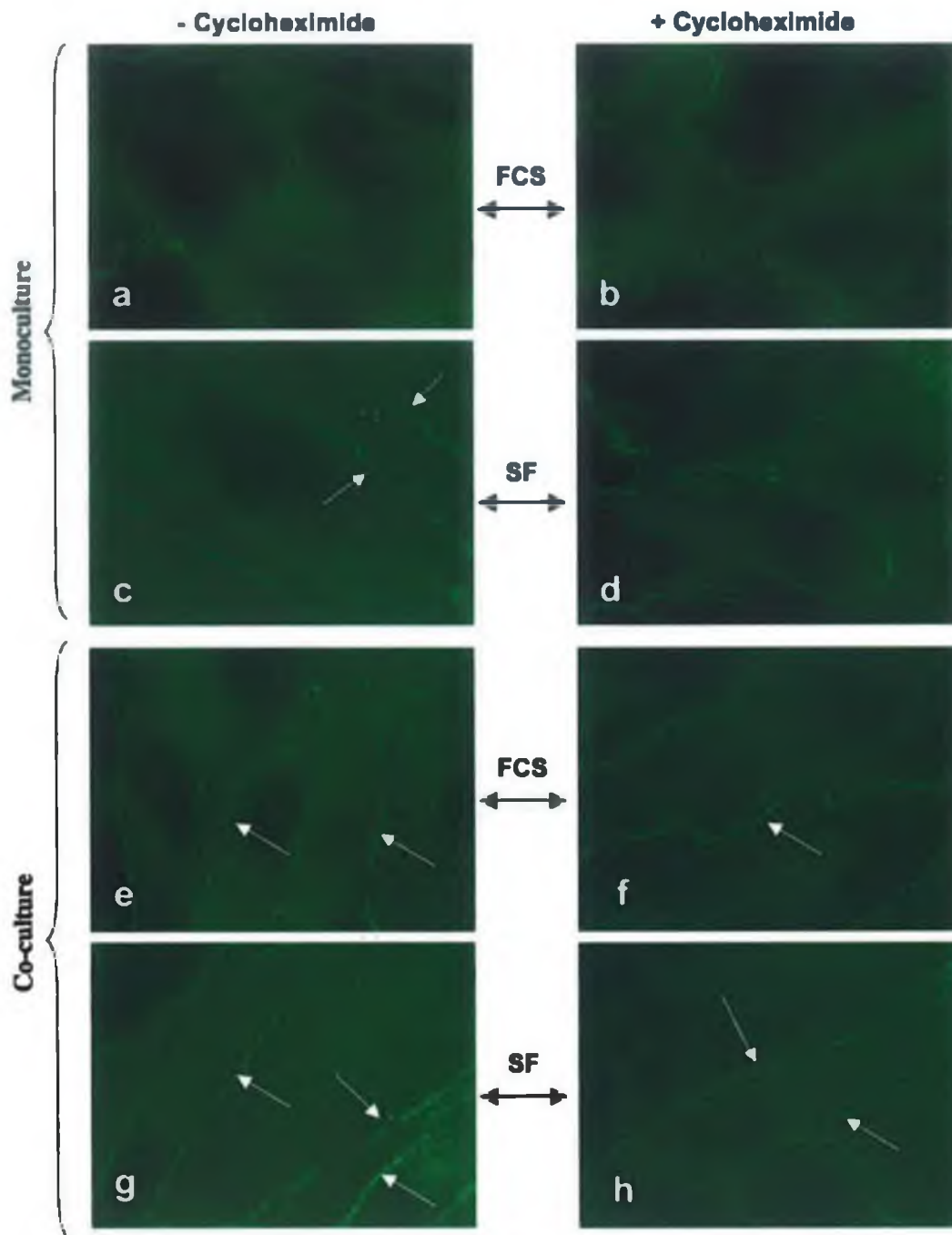


Fig. 5.2.11: Effect of cycloheximide on co-culture- and serum-dependent subcellular localization of ZO-1 in BBMvECs. Following co-culture and/or removal of serum from the basolateral compartment of fully confluent BBMvECs in the absence or presence of cycloheximide for 24 h, subcellular localization of ZO-1 was monitored by immunocytochemistry. Images b,d,f and h indicate the effect of cycloheximide on occludin localization. ZO-1 protein (green a–h) was monitored using standard fluorescence microscopy (1000x). White arrows indicate cell-cell border localization. Images are representative of at least three individual sets of experiments.

5.3 Discussion

Development of a reproducible *in vitro* BBB model, which exhibits low permeability and high electrical resistance, is essential for increasing our knowledge of tight junction formation at the molecular level and to understand the physiological factors which modulate barrier function. The development of such a model would enable high throughput screening of neurotherapeutic agents and potentially elucidate the mechanisms of barrier breakdown associated with a variety of neurological diseases (*see chapter 1 for details*). Furthermore, *in vivo* the basolateral aspect of the cerebral microvascular endothelium is ensheathed by astrocyte endfeet and bathed in ISF, which is completely devoid of serum proteins. Thus, in developing a model of the BBB, the role of these physiological basolateral conditions must be addressed.

We sought to investigate the effect of co-culturing C6 glioma with endothelial cells. Initial co-culture experiments, with *C6 glioma in the presence of basolateral serum*, showed no significant change in occludin or ZO-1 mRNA expression, but did cause significant increase in protein expression of both. Moreover, association of occludin/ZO-1 increased significantly following co-culture with C6 glioma. These data indicate that the increase in protein is not at the transcriptional level, but is perhaps due to decreased protein degradation and again suggests a putative role in the association of the two proteins leading to post-translational stabilization. Immunocytochemical analysis revealed that both occludin and ZO-1 became more continuous at points of cell-to-cell contact under co-culture conditions. In parallel with these biochemical changes, permeability to ¹⁴C-sucrose decreased and TEER increased following co-culture. Furthermore, incubation of the endothelial cells in the presence of cycloheximide during co-culture caused no significant change in the co-culture-dependent localization of occludin and ZO-1 to the cell membrane. These findings, in conjunction with the mRNA data, indicate that the increase in tight junction formation and barrier function associated with co-culture of

BBMvECs with C6 glioma is a result of post-translational modification of existing proteins rather than new protein synthesis.

In this chapter we observed that removal of basolateral serum from the BBMvEC monolayer decreased paracellular permeability and increased TEER, concomitant with an increase in occludin and ZO-1 expression, co-association and localization to the membrane (consistent with the findings of chapter 4). Furthermore, inhibition of new protein synthesis by cycloheximide abolished the serum free-dependent localization of both occludin and ZO-1 to the cell periphery, thus indicating that the removal of basolateral serum increases tight junction formation via *de novo* protein synthesis.

In view of these findings, we further sought to investigate if a combination of these two conditions, i.e. a *co-culture of BBMvECs and C6 glioma without basolateral serum*, would have an additive effect in relation to barrier formation and function. We found that under these conditions, occludin protein and mRNA expression was increased significantly, relative to both the serum-free monoculture and the co-culture model with serum. However, ZO-1 protein and mRNA expression was not significantly different to either the serum-free monoculture and the co-culture model with serum. In parallel immunocytochemical analysis of occludin and ZO-1 localization suggests that the C6 glioma cause increased expression at cell-cell contacts, an observation that was intensified by removal of serum. This model exhibited significantly increased TEER compared to the co-culture model with serum, but not to the serum-free monoculture, with a similar trend reflected in permeability to ¹⁴C sucrose. In addition, cycloheximide only partially abrogated the localization of occludin and ZO-1 to the cell membrane in the serum-free co-culture model, thus indicating that the increase in tight junction formation is partly due to new protein synthesis and partly due to modification of existing protein.

These data indicate that both removal of serum and the co-culture effects of C6 glioma increase tight junction formation, but that these effects are *not* additive with

respect to barrier function. Moreover, the mRNA and cycloheximide data shown indicate that removal of serum and co-culture with C6 glioma increase tight junction formation and barrier function via two separate pathways. That is, removal of serum leads to increased tight junction protein synthesis via *de novo* mRNA production, whilst co-culture with C6 glioma leads to post-translational modification of already existing protein pool.

Furthermore, incubation of BBMvECs with apically applied C6 ACM, in either the presence or absence of serum, led to no significant change in occludin or ZO-1 subcellular localization, thus indicating a polar-specific nature of the inducing properties of astrocytes on endothelial cell barrier function. Growth factors such as the bFGF and TGF- β which, are released by astrocytes, bind to endothelial cell surface receptors and induce tight junction formation. Thus, the polar-specific effect of C6 glioma on endothelial tight junction formation may be due to polar-specific expression of such receptors on the endothelial surfaces. However, further studies are required to elucidate which astrocyte-derived factors and associated receptors are responsible for induction of barrier properties in endothelial cells.

This BBB model reflects the *in-vivo* situation, with respect to the absence of basolateral serum and the presence of astrocytes. However, even though the co-culture is assessed visually for viability in the serum free-media, it is possible that the C6 glioma enter a quiesced state, and as such released lower levels of signaling molecules responsible for the induction of tight junction formation, which would explain why the potentially additive barrier effect of co-culturing in the absence of basolateral serum was not seen. Furthermore, C6 glioma may produce increased levels of VEGF or other barrier-disrupting cytokines under serum-free conditions, thus reducing the endothelial barrier. Further studies measuring VEGF, bFGF and TGF- β production would help to clarify this point.

Moreover, *in-vivo* the spatial relationship between endothelial cell bodies and astrocyte end-feet is in the magnitude of angstroms, whereas in this model it is

approximately 1 mm. We therefore hypothesize that a synergistic contact-dependent relationship may exist between astrocytes and endothelial cells; that is, that astrocytes may require contact (or near contact) with endothelial cells to maintain viability in serum-free conditions. However, in contrast to Garcia *et al.*, who propose that astrocyte-endothelial contact is required for induction of BBB properties (Garcia *et al.* 2004), our data indicate that under non-contact co-culture conditions, C6 glioma release a soluble factor, which increases endothelial barrier function by up-regulating tight junction formation.

In conclusion, this chapter describes, in part, the polar-specific effect of serum and of astrocytes on barrier function in endothelial cells. Our findings indicate that removal of basolateral serum increases occludin and ZO-1 expression, association of tight junction proteins and their subcellular distribution, concomitant with an increase in TEER and reduction in paracellular permeability, thus indicating that basolaterally applied serum inhibits tight junction formation. It also investigates the feasibility of combining a C6 co-culture model with serum-free conditions. We have shown that C6 glioma can cause increased barrier function in BBMvECs in both the presence and absence of basolateral serum, and that this functional change is accompanied by biochemical changes including the expression, localization and association of occludin and ZO-1. Further studies are required to fully elucidate the exact mechanisms by which these events occur, however this information may be invaluable in the development of a superior *in vitro* BBB model.

Chapter 6

Assessment of the role of laminar shear stress on BBMvEC tight junction formation and barrier function.

6.1 Introduction

The vascular endothelium is a dynamic cellular interface between the vessel wall and bloodstream, which regulates vessel tone and remodelling. Haemodynamic forces, namely cyclic strain and shear stress modulate endothelial gene expression, morphology and function (*see section 1.4 for details*). Furthermore, areas in the macrovasculature associated with low or turbulent shear stress, such as arterial bifurcations, show increased monocyte infiltration and a predisposition to the formation of atherosclerotic plaques (Dzau *et al.* 2002). Moreover, shear stress plays a significant role in maintaining homeostasis of the cerebral microvasculature and may have a protective effect in the pathophysiology of several neurological disorders (for review, see Krizanac-Bengez *et al.* 2004). Therefore, we propose that shear stress mediates endothelial permeability via modulation of tight junctions.

Moreover, the majority of BBB models encompass the paracrine interactions between endothelial cells and astrocytes, but fail to address the haemodynamic forces exerted on the luminal aspect of the cerebral microvascular endothelium. We hypothesize that microvascular endothelial tight junction formation and barrier function is modulated by both basolateral factors (serum, astrocytes, pericytes) and luminal forces (shear stress).

Thus, the aim of this chapter is to examine the role of physiological levels of laminar shear stress on endothelial tight junction formation and barrier function, with particular emphasis on the expression, association and subcellular localization of occludin and ZO-1.

6.2 Results

6.2.1 Shear stress-dependent increase in occludin expression in BBMvECs

Following exposure of BBMvECs to shear stress (10 dynes/cm², 24 h), occludin protein expression increased by 1.8 ± 0.0 fold (Fig. 6.2.1 a). Messenger RNA levels were also significantly increased following shear by 2.7 ± 0.3 fold (Fig. 6.2.1 b).

6.2.2 Shear stress-dependent increase in ZO-1 expression in BBMvECs

Following exposure of BBMvECs to shear stress (10 dynes/cm², 24 h), ZO-1 protein expression increased by 1.3 ± 0.0 fold (Fig. 6.2.2 a). Messenger RNA levels were also significantly increased following shear by 1.3 ± 0.0 fold (Fig. 6.2.2 b).

6.2.3 Shear stress-dependent association of occludin/ZO-1 in BBMvECs

Following exposure of BBMvECs to shear stress (10 dynes/cm², 24 h), association of occludin with ZO-1 was monitored in total BBMvEC lysates by IP/Western blot. In response to shear, the level of occludin detected in anti-ZO-1 immunoprecipitates was seen to increase by 1.9 ± 0.1 fold (Fig. 6.2.3)

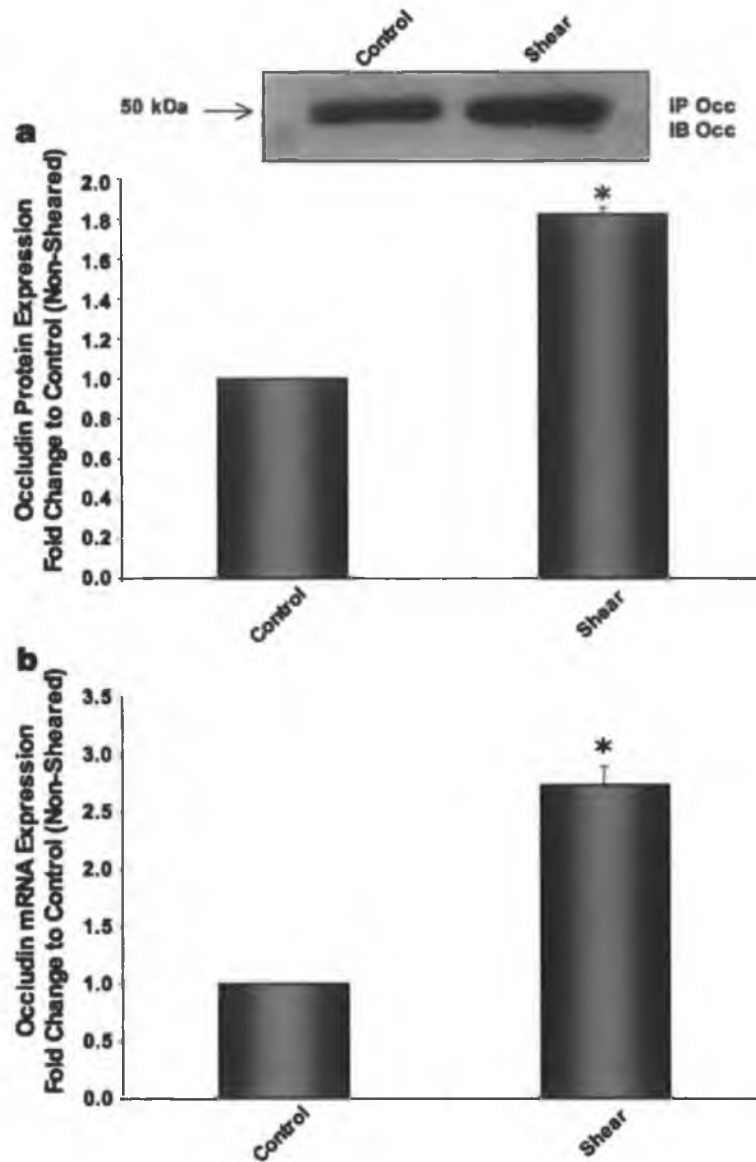


Fig. 6.2.1: Effect of shear stress on occludin expression in BBMvECs. Confluent BBMvEC were exposed to shear stress (10 dynes/cm², 24 h) and monitored for occludin protein expression (a) by immunoprecipitation/Western blot and for mRNA (b) by Real-Time PCR. Histograms represent fold change in product formation relative to unsheared control and are averaged from three independent experiments \pm SEM. * $P \leq 0.05$ relative to unsheared control. Gel shown is representative.

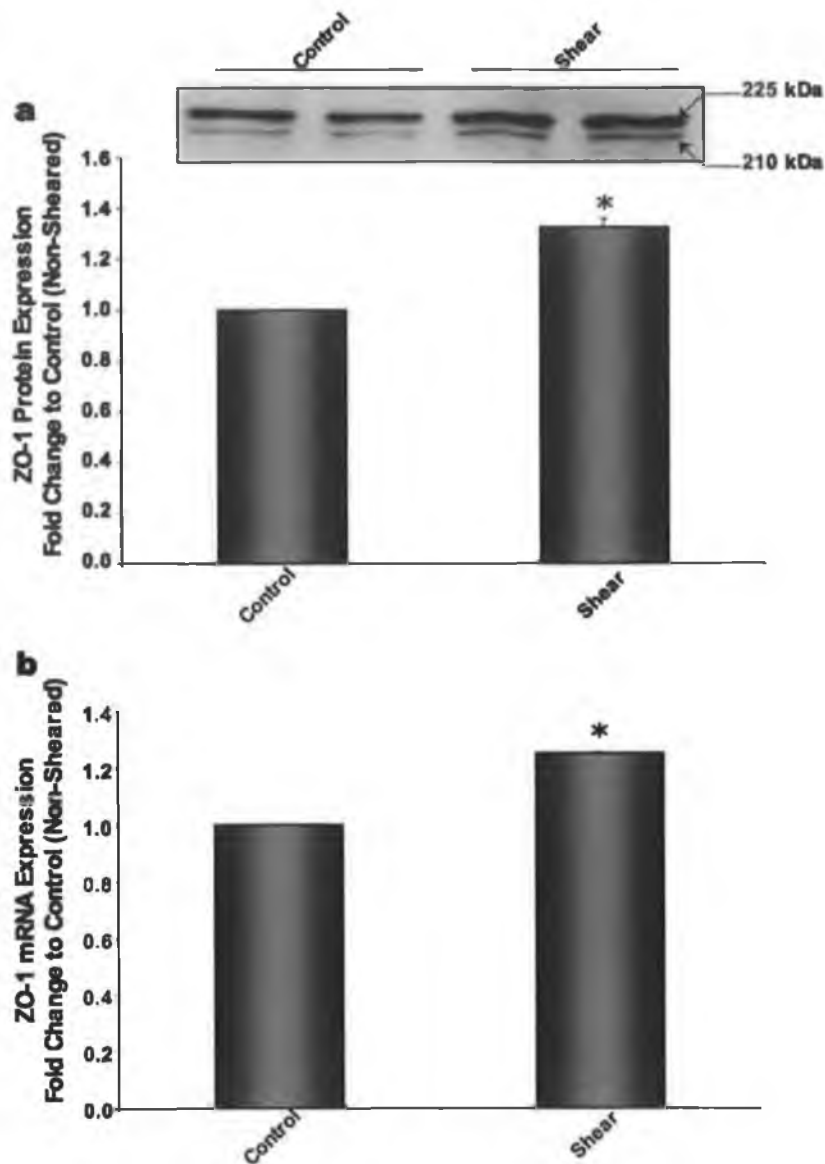


Fig. 6.2.2: Effect of shear stress on ZO-1 expression in BBMvECs. Confluent BBMvEC were exposed to shear stress (10 dynes/cm², 24 h) and monitored for ZO-1 protein expression (a) by Western blot and for mRNA (b) by Real-Time PCR. Histograms represent fold change in product formation relative to unsheared control and are averaged from three independent experiments \pm SEM. * $P < 0.05$ relative to unsheared control. Gel shown is representative.

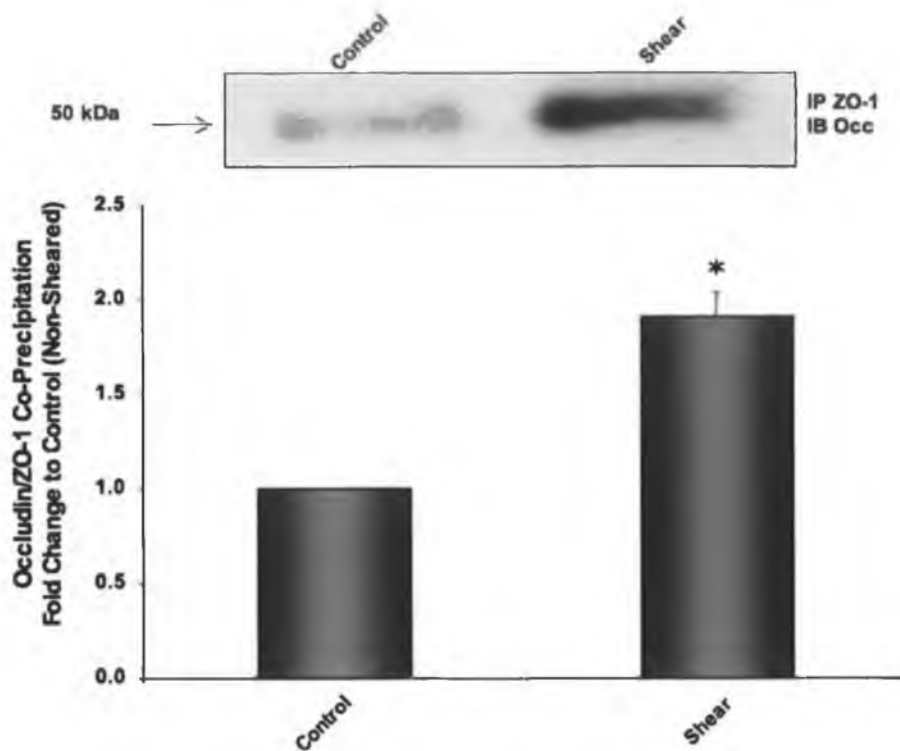


Fig. 6.2.3: Effect of shear stress on occludin/ZO-1 association in BBMvECs. Confluent BBMvEC were exposed to shear stress (10 dynes/cm², 24 h) and monitored for co-association of occludin and ZO-1 by immunoprecipitation and Western blotting. Histogram represents fold change in band intensity relative to unsheared control and is averaged from three independent experiments \pm SEM. * $P < 0.05$ relative to unsheared control. Gel shown is representative.

6.2.4 Shear stress-dependent cell realignment and occludin and ZO-1 subcellular localization

Following exposure of BBMvECs to shear stress (10 dynes/cm², 24 h), cellular realignment was monitored by phase contrast microscopy and F-actin staining as described in section 2.2.11. Subcellular localization of occludin and ZO-1 within BBMvEC monolayers was also monitored by immunocytochemistry as described in section 2.2.11. In the unsheared control cells (Fig. 6.2.4 a) cell alignment was random and multi-directional, however, following shear cells realigned in the direction of flow (Fig. 6.2.4 b). In parallel, F-actin staining with rhodamine phalloidin revealed significant redistribution of actin bundles following shear (Fig. 6.2.4 d) when compared to the unsheared control (Fig. 6.2.4 c). Moreover, in the unsheared control occludin was found solely in the cytoplasm (Fig. 6.2.4 e), but became significantly more concentrated at the cell membrane in response to shear (Fig. 6.2.4 f). Also, in unsheared cells ZO-1 immunoreactivity was discontinuous, with jagged finger-like projections at cell-cell contacts (Fig. 6.2.4 g). However, following 24 h shear, ZO-1 immunoreactivity became significantly more continuous along the membrane periphery (Fig. 6.2.4 h).

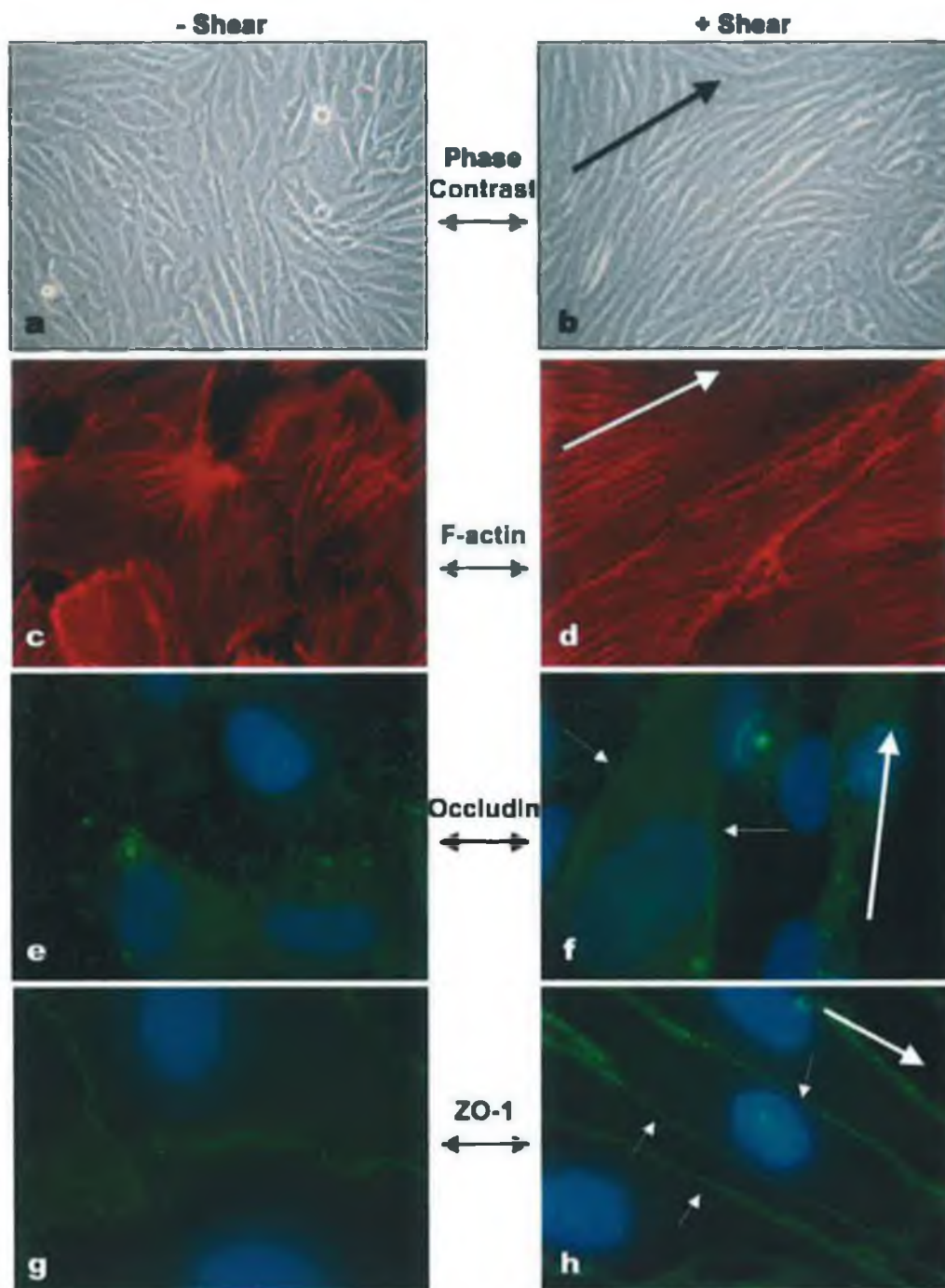


Fig. 6.2.4: Effect of shear stress on cell realignment and occludin and ZO-1 subcellular localization in BBMvECs. Following exposure of BBMvECs to shear stress (10 dynes/cm², 24 h) cellular realignment was monitored by phase contrast microscopy (a and b) (400x) and F-actin staining (c and d) using standard fluorescent microscopy (1000x). Subcellular localization of Occludin and ZO-1 was monitored by immunocytochemistry. Occludin protein (green e and f), ZO-1 protein (g and h) and nuclear DAPI staining (blue e-h) were monitored using standard fluorescent microscopy (1000x). White arrows indicate cell-cell border localization. Large arrows indicate direction of flow. Images are representative of at least three individual sets of experiments.

6.2.5 Shear stress decreases BBMvEC transendothelial permeability to FITC dextran

As transendothelial permeability cannot be directly monitored directly in 6-well plates post-shear, both control and “shear-conditioned” BBMvECs were trypsinized and re-plated into Transwell®-Clear plates at a density sufficient to reach confluency within 24 h. BBMvEC monolayer permeability to 40 kDa FITC-dextran was subsequently monitored as described in section 2.2.13. Results indicate that shear stress significantly reduces BBMvEC permeability to FITC-dextran, with unsheared cells showing a 2.7 ± 0.1 fold higher level of FITC-dextran in the subluminal chamber after 120 min relative to sheared cells (Fig. 6.2.5 i). Moreover, although this experimental paradigm necessitates testing transendothelial permeability 24 h after cessation of shear, we have monitored a number of strain-induced changes in occludin/ZO-1 properties (e.g. subcellular localization) and confirmed that they fully persist 24 h *after* passage from shear plates into Transwell®-Clear plates (Fig. 6.2.5 ii a - d).

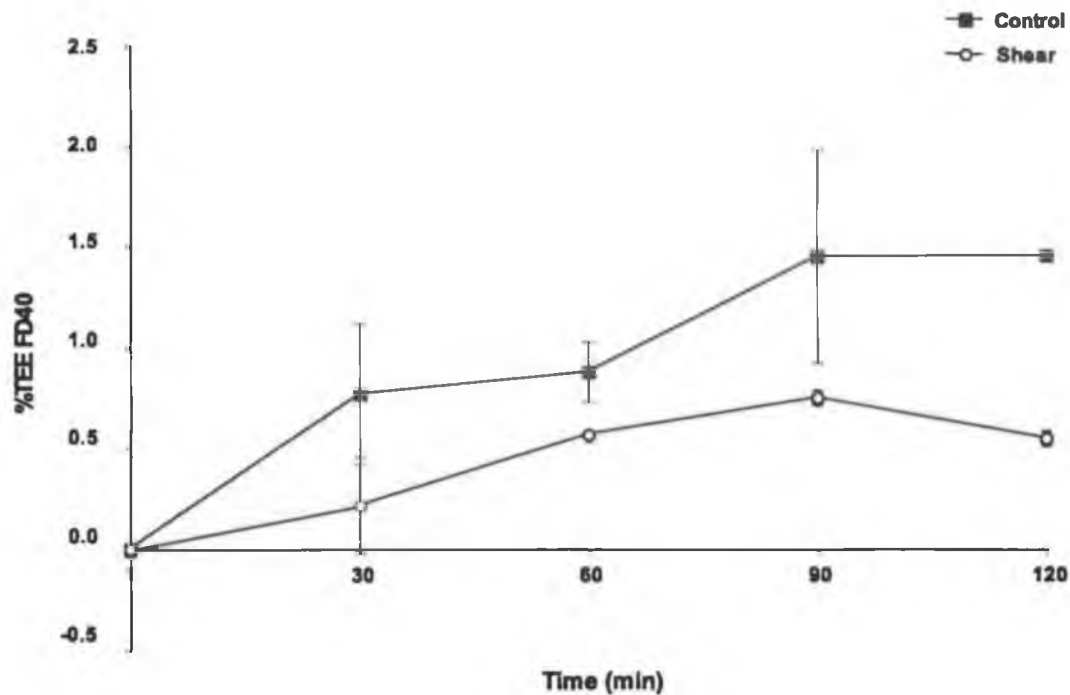


Fig. 6.2.5 i: Effect of shear stress on BBMvEC transendothelial permeability. Following exposure of BBMvECs to shear stress (10 dynes/cm², 24 h), control and “shear-conditioned” BBMvECs were trypsinized and re-plated into Transwell®-Clear plates and monitored for permeability to 40kDa FITC-dextran. Data points are shown as total subluminal fluorescence at a given time point (from 0-120 min) expressed as a percentage of total abluminal fluorescence at t=0 min (i.e. %TEE of FD40 or % Trans Endothelial Exchange of FITC-dextran 40 kDa). Results are averaged from two independent experiments ±SEM; $P \leq 0.005$ (Two-Way ANOVA, unsheared versus sheared BBMvECs).

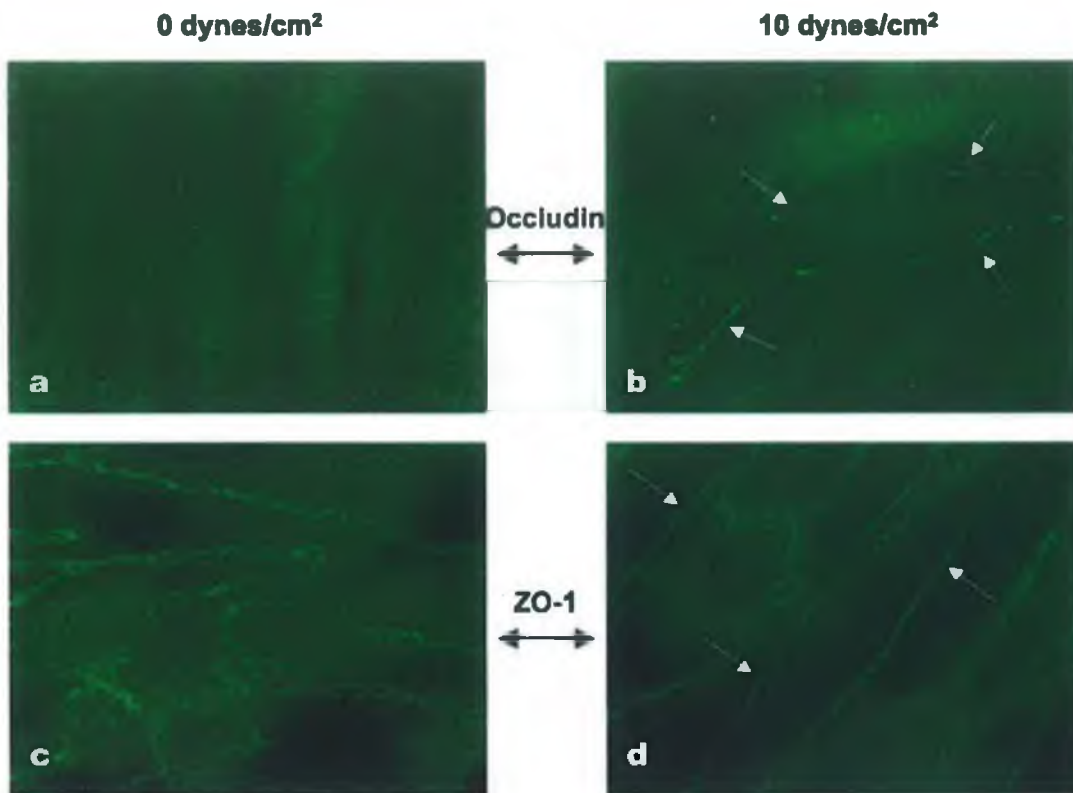


Fig. 6.2.5 ii: BBMvECs retain “sheared” characteristics following trypsinization. Following exposure of BBMvECs to shear stress (10 dynes/cm², 24 h), both control and “strain-conditioned” BBMvECs were trypsinized, re-plated and immunocytochemically monitored for localization of occludin and ZO-1 *after 24 h*. Membrane localization of occludin in (a) unsheared and (b) sheared BBMvECs and of ZO-1 in (c) unsheared and (d) sheared BBMvECs is shown 24 h after re-plating. Both proteins were monitored using standard fluorescence microscopy (1000x). White arrows indicate cell-cell border localization. Images are representative of at least three individual sets of experiments.

6.2.6 Shear stress-dependent association of occludin/ZO-1 in BBMvECs is partially attenuated by cycloheximide

Following exposure of BBMvECs, in the presence or absence of cycloheximide, to laminar shear stress (10 dynes/cm², 24 h), occludin expression (a), ZO-1 expression (b) and association of occludin with ZO-1 (c) was monitored in total BBMvEC lysates by IP/Western blot. Immunoblot images (a) occludin and (b) ZO-1 demonstrate the ability of cycloheximide to inhibit shear-dependent protein synthesis. In response to shear, the level of occludin detected in anti-ZO-1 immunoprecipitates was seen to increase by 2.4 ± 0.1 fold in the absence of cycloheximide and 1.9 ± 0.0 fold in the presence of cycloheximide. However, a non-specific effect of cycloheximide, led to a 1.5 ± 0.0 fold increase in occludin/ZO-1 association (i.e. under non-shear conditions) (Fig. 6.2.6).

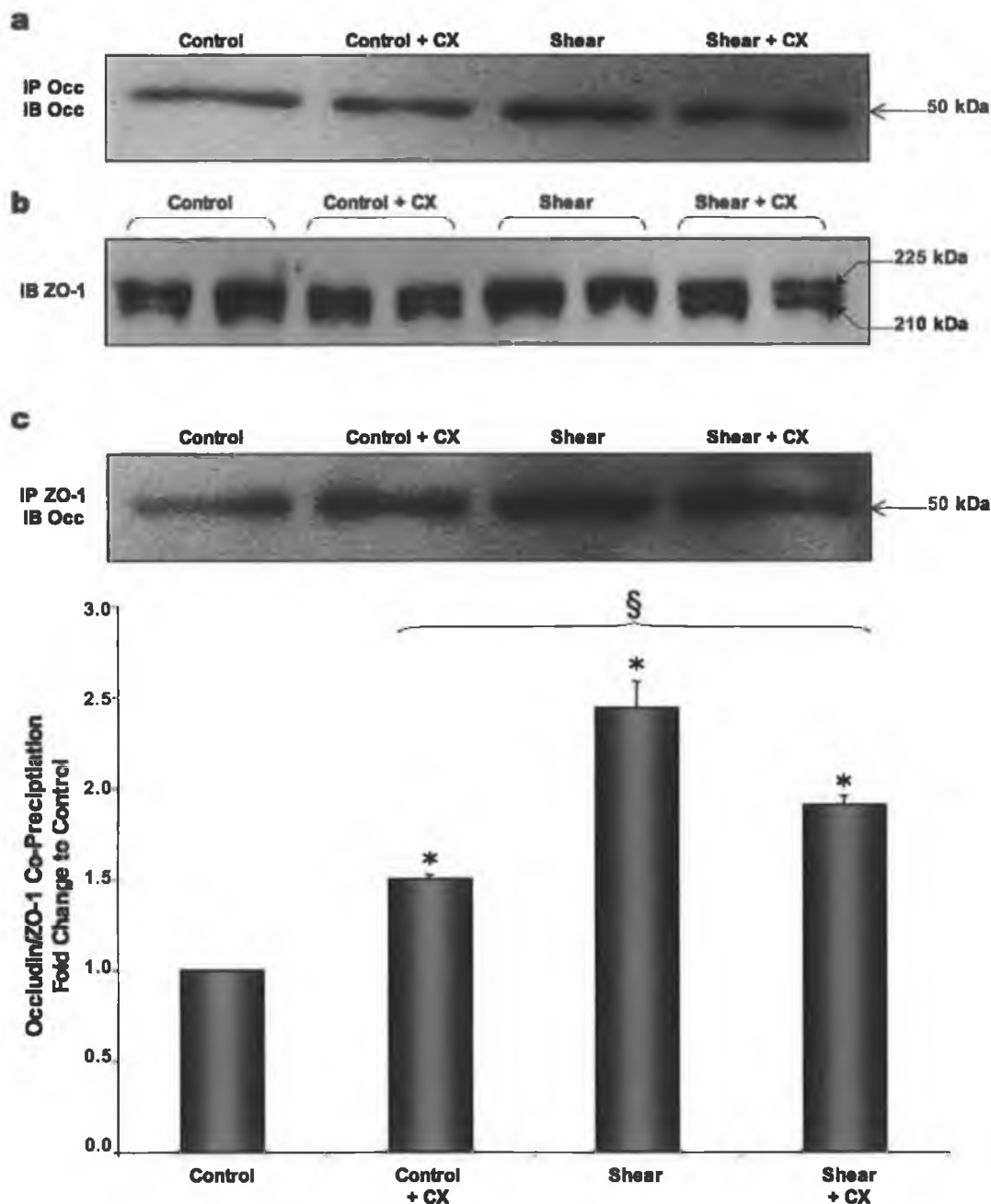


Fig. 6.2.6: Effect of cycloheximide on shear stress induced occludin/ZO-1 association in BBMvECs. Confluent BBMvEC were exposed to shear stress (10 dynes/cm², 24 h) in the presence and absence of cycloheximide and monitored for co-association of occludin and ZO-1 by immunoprecipitation and Western blotting (histogram and blot c). Histogram represents fold change in band intensity relative to unsheared control and is averaged from three independent experiments \pm SEM. * $P \leq 0.05$ relative to unsheared control, § $P \leq 0.05$ relative to unsheared with cycloheximide. Representative blots demonstrate the ability of cycloheximide to inhibit occludin (a) and ZO-1 (b) protein synthesis.

6.2.7 Shear stress-dependent occludin subcellular localization is partially attenuated by cycloheximide

Following exposure of BBMvECs, in the presence or absence of cycloheximide, to shear stress (10 dynes/cm², 24 h), subcellular localization of occludin and ZO-1 within BBMvEC monolayers was monitored by immunocytochemistry as described in section 2.2.11. In the unsheared cells, with and without cycloheximide (Fig. 6.2.7 a and b, respectively) occludin was found solely in the cytoplasm, but became significantly more concentrated at the cell membrane in response to shear in both the absence and presence of cycloheximide (Fig. 6.2.7 c and d, respectively).

6.2.8 Shear stress-dependent ZO-1 subcellular localization is partially attenuated by cycloheximide

Following exposure of BBMvECs, in the presence or absence of cycloheximide, to shear stress (10 dynes/cm², 24 h), subcellular localization of ZO-1 within BBMvEC monolayers was monitored by immunocytochemistry as described in section 2.2.11. In the unsheared cells, with and without cycloheximide (Fig. 6.2.8 a and b, respectively) ZO-1 staining was discontinuous with long finger like projections. However, in response to shear, ZO-1 staining became significantly more continuous at the cell periphery in both the presence and absence of cycloheximide (Fig. 6.2.8 c and d, respectively).

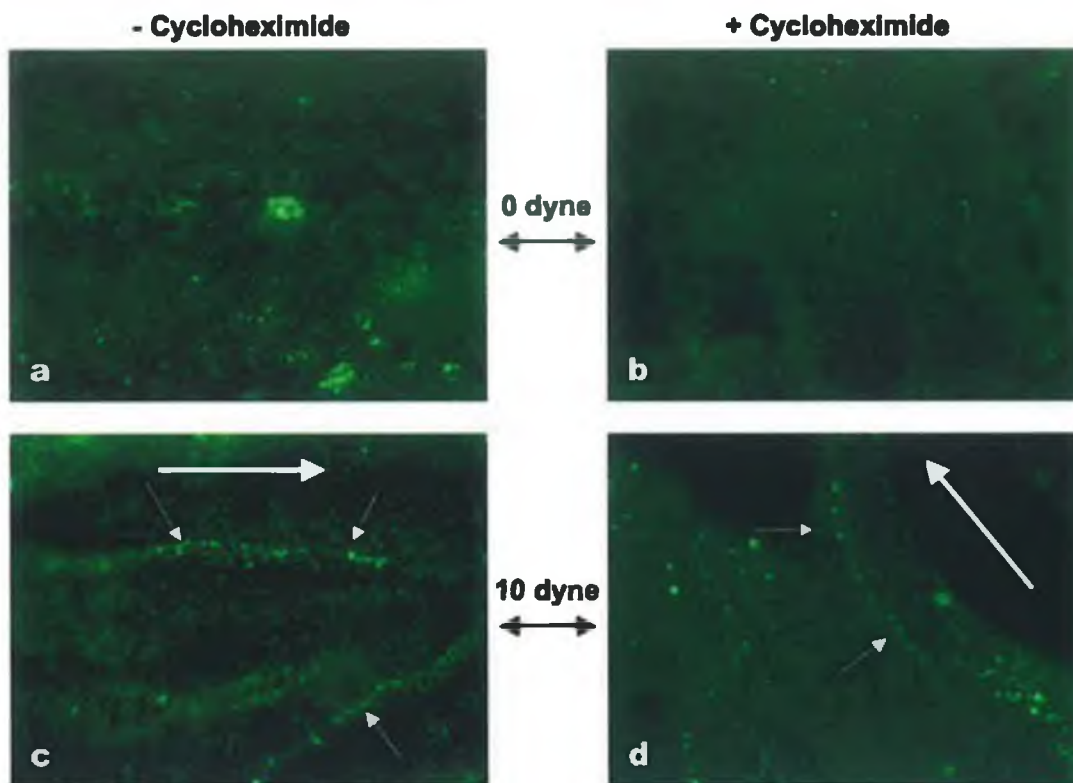


Fig. 6.2.7: Effect of shear stress and cycloheximide on occludin subcellular localization in BBMvECs. Following exposure of BBMvECs to shear stress (10 dynes/cm², 24 h) in the presence and absence of cycloheximide, subcellular localization of Occludin was monitored by immunocytochemistry. Occludin protein (green a and was monitored using standard fluorescent microscopy (1000x). White arrows indicate cell-cell border localization. Large arrows indicate direction of flow. Images are representative of at least three individual sets of experiments.

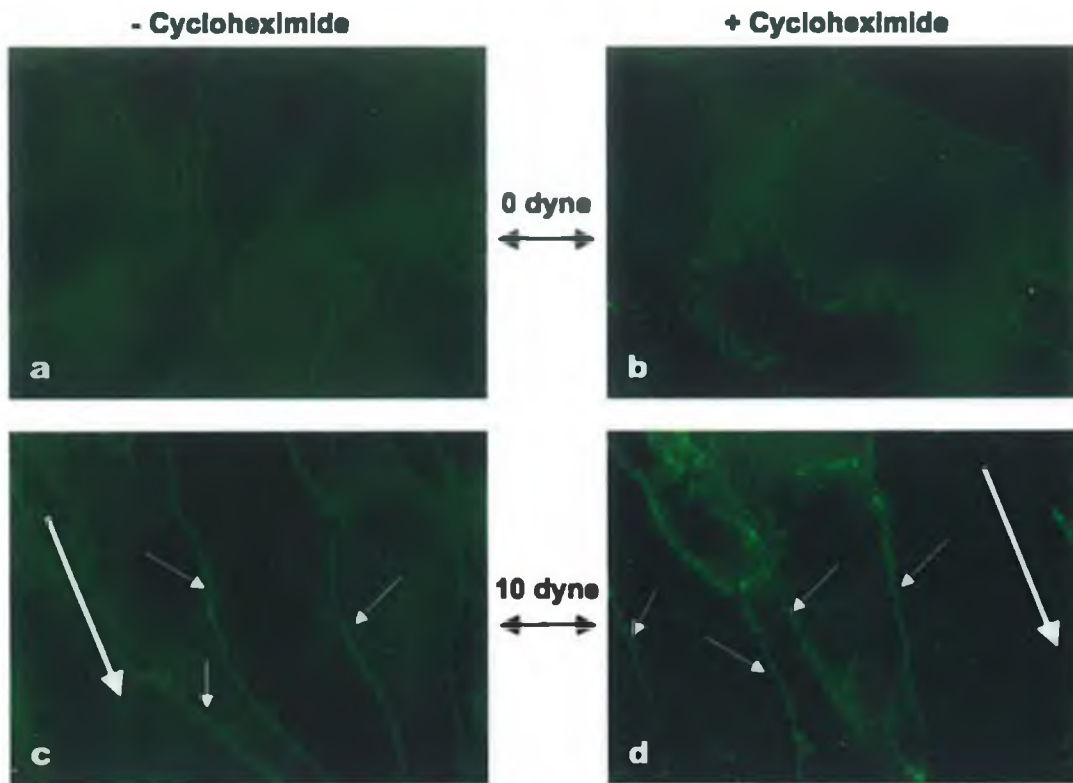


Fig. 6.2.8: Effect of shear stress and cycloheximide on ZO-1 subcellular localization in BBMvECs. Following exposure of BBMvECs to shear stress (10 dynes/cm², 24 h) in the presence and absence of cycloheximide, subcellular localization of ZO-1 was monitored by immunocytochemistry. ZO-1 protein (green a – d) was monitored using standard fluorescent microscopy (1000x). White arrows indicate cell-cell border localization. Large arrows indicate direction of flow. Images are representative of at least three individual sets of experiments.

6.2.9 Shear stress-dependent decrease in BBMvEC transendothelial permeability to FITC dextran is partially attenuated by cycloheximide

As transendothelial permeability cannot be directly monitored in 6-well plates post shear, both control and “shear-conditioned” BBMvECs were trypsinized and re-plated into Transwell®-Clear plates at a density sufficient to reach confluency within 24 h. BBMvEC monolayer permeability to 40 kDa FITC-dextran was subsequently monitored as described in section 2.2.13. Results indicate that inhibition of protein synthesis for 24 h by cycloheximide increases BBMvEC permeability to FITC-dextran by 1.7 ± 0.3 fold higher level of FITC-dextran in the basolateral compartment compared to unsheared control. Moreover, shear stress significantly reduced BBMvEC permeability to FITC-dextran, with sheared cells showing 0.4 ± 0.1 fold lower level of FITC-dextran in the subluminal chamber after 120 min relative to unsheared cells. Furthermore, cells sheared in the presence of cycloheximide showed 0.9 ± 0.0 fold lower level of FITC-dextran in the subluminal chamber after 120 min relative to unsheared cells, thus indicating that the shear-induced decrease in BBMvEC permeability was partly due to new protein synthesis and partly due to posttranslational modification of the existing proteins (Fig. 6.2.9 i). Moreover, although this experimental paradigm necessitates testing transendothelial permeability 24 h after cessation of shear, we have monitored a number of shear- and cycloheximide-induced changes in occludin/ZO-1 properties (e.g. subcellular localization) and confirmed that they fully persist 24 h *after* passage from shear plates into Transwell®-Clear plates (Fig. 6.2.9 ii).

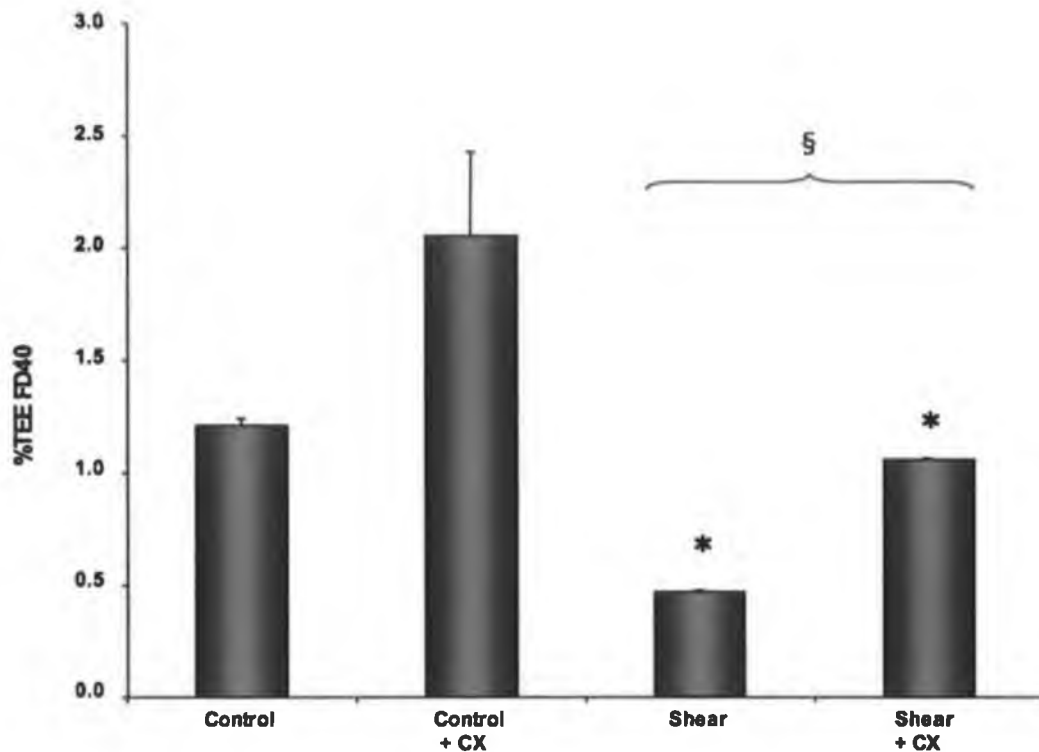


Fig. 6.2.9 i: Effect of shear stress and cycloheximide on BBMvEC transendothelial permeability. Following exposure of BBMvECs to shear stress (10 dynes/cm², 24 h), in the presence and absence of cycloheximide, control, “shear-conditioned” and “cycloheximide conditioned” BBMvECs were trypsinized and re-plated into Transwell®-Clear plates and monitored for permeability to 40kDa FITC-dextran. Data points are shown as total subluminal fluorescence at t=120 min expressed as a percentage of total abluminal fluorescence at t=0 min (i.e. %TEE of FD40 or % Trans Endothelial Exchange of FITC-dextran 40 kDa). Results are averaged from two independent experiments ±SEM; * $P \leq 0.05$ versus control BBMvECs, § $P \leq 0.05$ versus sheared BBMvECs.

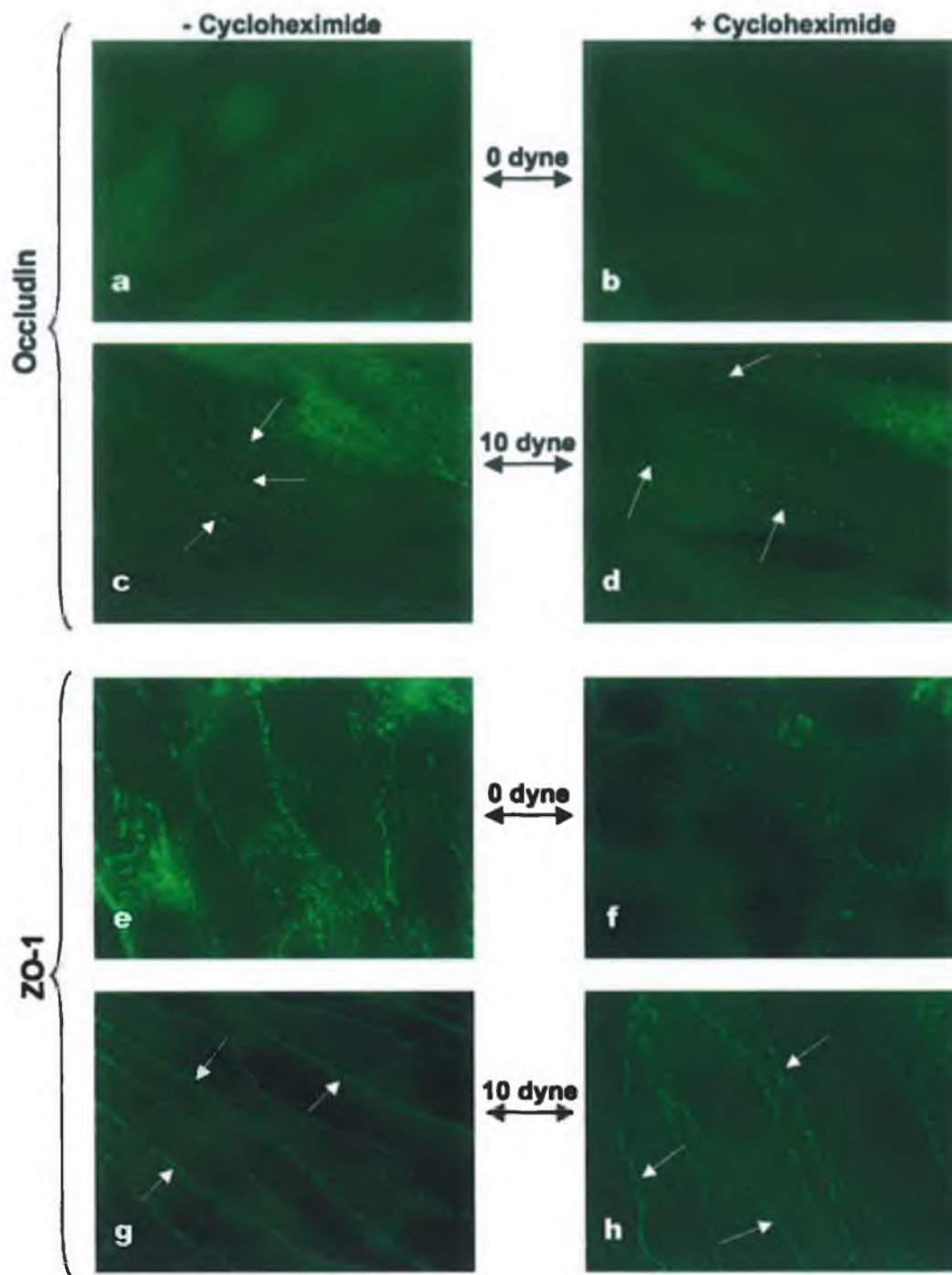


Fig. 6.2.9 ii: BBMvECs retain cycloheximide and “sheared” characteristics following trypsinization. Following exposure of BBMvECs to shear stress (10 dynes/cm², 24 h), in the absence and presence of cycloheximide, control and “strain-conditioned” BBMvECs were trypsinized, re-plated and immunocytochemically monitored for localization of occludin and ZO-1 after 24 h. Membrane localization of occludin (a – d) and of ZO-1 (e– h) in BBMvECs is shown 24 h after re-plating. Both proteins were monitored using standard fluorescence microscopy (1000x). White arrows indicate cell-cell border localization. Images are representative of at least three individual sets of experiments.

6.2.10 Pulsatile laminar shear stress-dependent increase in occludin and ZO-1 protein expression in BBMvECs

Following exposure of BBMvECs to pulsatile laminar shear stress (low 0.2 dynes/cm², high 14 dynes/cm², 24 h), occludin protein expression increased by 2.2 ± 0.0 fold (Fig. 6.10 b) under high shear conditions compared to low flow. A representative immunoblot (a) indicates an increase in ZO-1 protein expression under high shear conditions.

6.2.11 Pulsatile laminar shear stress-dependent association of occludin/ZO-1 in BBMvECs

Following exposure of BBMvECs to pulsatile laminar shear stress (low 0.2 dynes/cm², high 14 dynes/cm², 24 h), association of occludin with ZO-1 was monitored in total BBMvEC lysates by IP/Western blot. In response to high shear, the level of occludin detected in anti-ZO-1 immunoprecipitates was seen to increase by 3.2 ± 0.1 fold compared to low shear (Fig. 6.11).

6.2.12 Pulsatile laminar shear stress-dependent transendothelial permeability of BBMvECs to ¹⁴C-sucrose

Following exposure of BBMvECs to pulsatile laminar shear stress (low 0.2 dynes/cm², high 14 dynes/cm², 24 h) transendothelial permeability of ¹⁴C-sucrose was assessed. At t=30, 45 and 60, high shear stress led to a significant decrease in BBMvEC transendothelial permeability to ¹⁴C sucrose. At t=60 BBMvEC permeability under high shear conditions was approximately 20% less than that of the low shear conditions (Fig. 6.12).

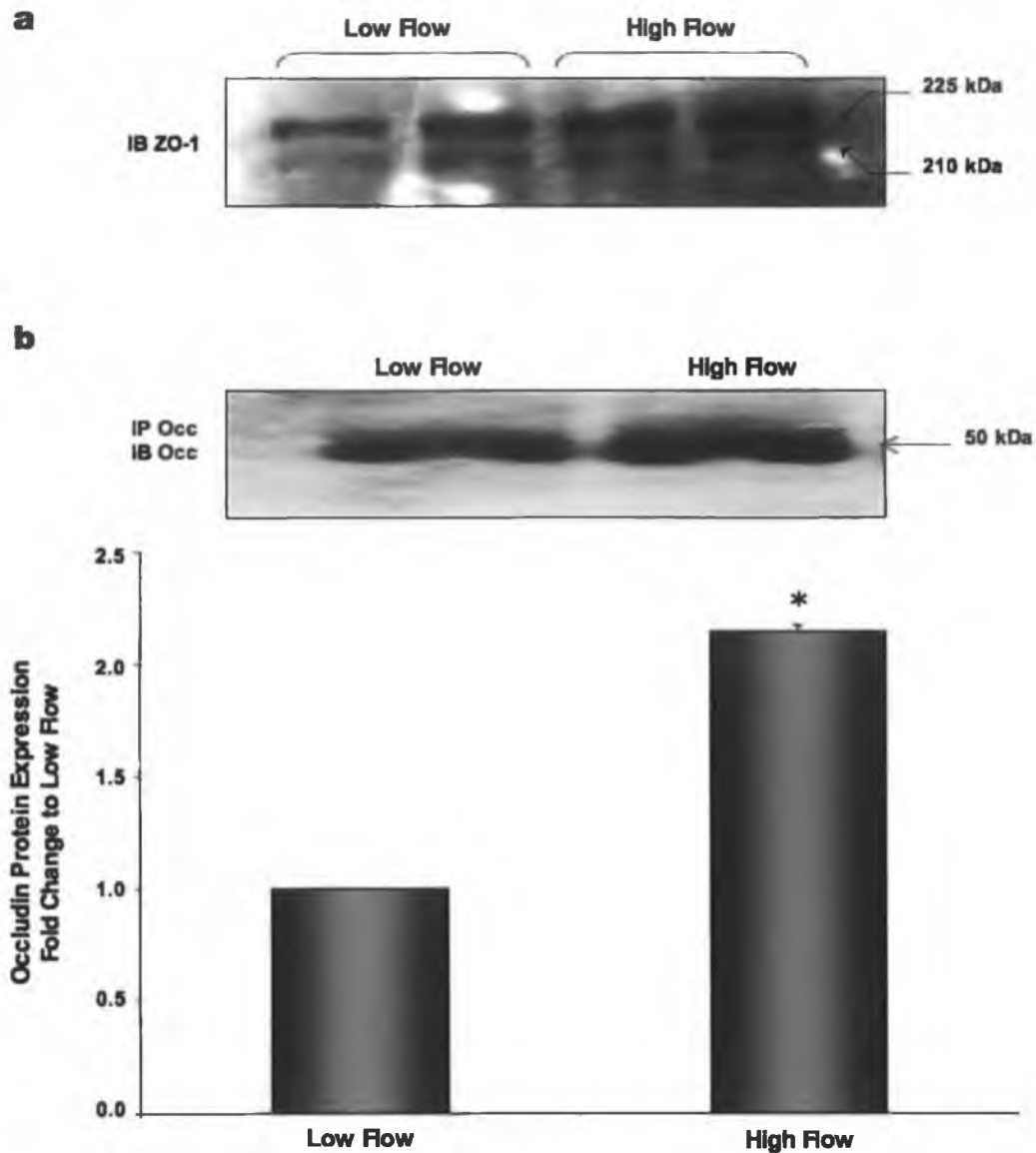


Fig. 6.2.10: Effect of pulsatile laminar shear stress on occludin and ZO-1 protein expression in BBMvECs. BBMvEC were exposed to pulsatile laminar shear stress (low – 0.2 dynes/cm²; high – 14 dynes/cm², 24 h) and monitored for ZO-1 protein expression (insert a) and occludin protein expression (b) by immunoprecipitation/Western blot. Representative blot (a) indicates the effect of pulsatile shear stress on ZO-1 protein expression. Histogram (b) represents fold change in occludin protein formation relative to low flow control and is averaged from three independent experiments \pm SEM. * $P \leq 0.0005$ relative to low flow.

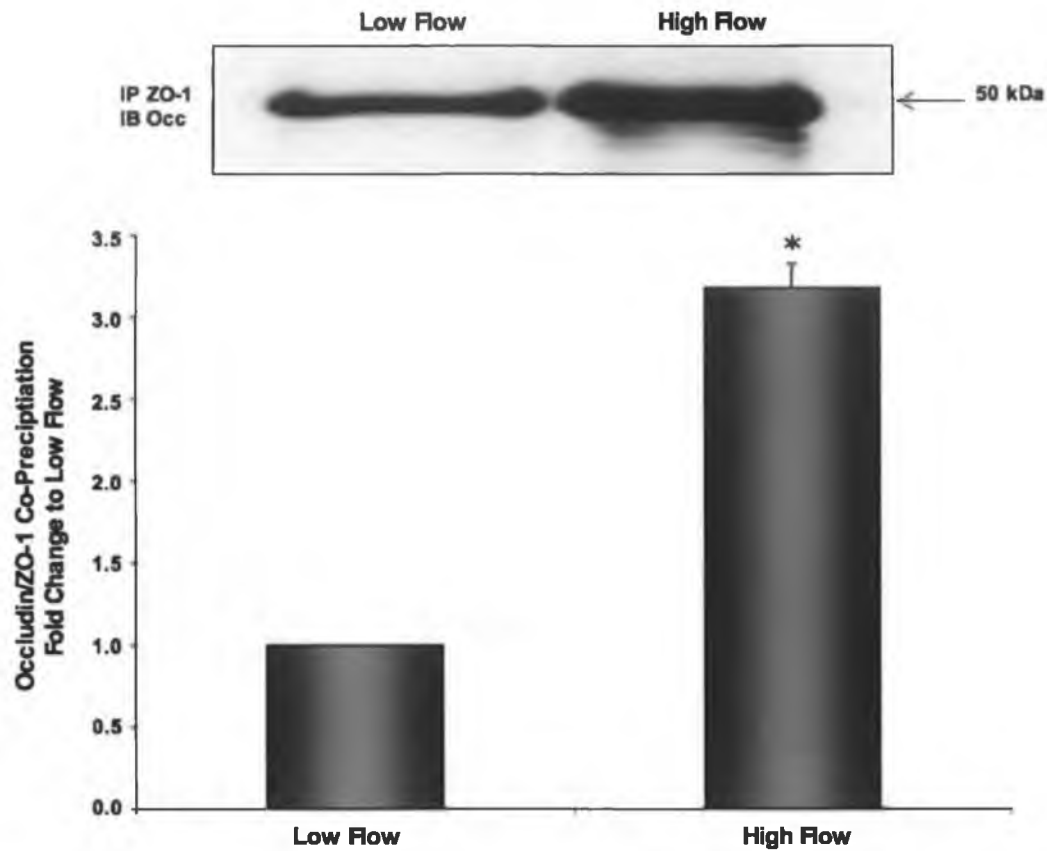


Fig. 6.2.11: Effect of pulsatile laminar shear stress on occludin/ZO-1 association in BBMvECs. BBMvEC were exposed to pulsatile laminar shear stress (low – 0.2 dynes/cm²; high – 14 dynes/cm², 24 h) and monitored for co-association of occludin and ZO-1 by immunoprecipitation and Western blotting. Histogram represents fold change in band intensity relative to low flow and is averaged from three independent experiments \pm SEM. * $P \leq 0.001$ relative to low flow. Gel shown is representative.

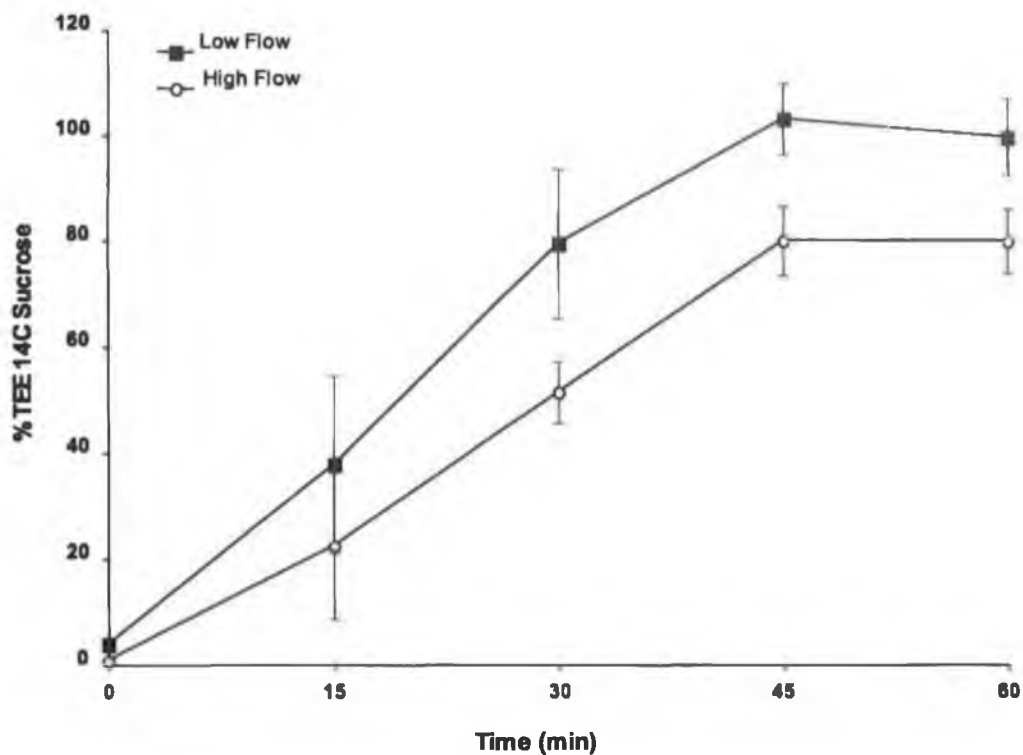


Fig. 6.2.12: Effect of pulsatile laminar shear stress on BBMvEC transendothelial permeability. Following 24 h pulsatile laminar shear stress (low flow – 0.2 dynes/cm²; high flow – 14 dynes/cm²), BBMvECs were monitored for permeability to ¹⁴C-sucrose. Data points shown are expressed as a percentage of the concentration of ¹⁴C-sucrose in the luminal space at t=180. Histogram represents percentage change in ECS ¹⁴C-sucrose concentration and is averaged from three independent experiments ±SEM. $P \leq 0.005$ (Two-Way ANOVA, low flow versus high flow).

6.3 Discussion

In vivo, the endothelial cells forming the BBB are basolaterally bathed in ISF (devoid of serum proteins) and encircled by astrocyte endfeet, whilst the luminal endothelial surface is exposed to laminar shear stress as a result of local haemodynamic forces. Chapter 3 and 4 clearly demonstrate the role serum and astrocytes, respectively on tight junction formation and microvascular barrier function. However, we believe that tight junction formation is a result of both basolateral and apical stimuli. Thus, in this chapter, the role of apically acting shear stress in modulating endothelial barrier function is examined.

Initial investigations clearly demonstrate that exposure of BBMvECs to chronic physiological non-pulsatile laminar shear stress (10 dynes/cm², 24 h) significantly increased occludin and ZO-1 protein expression in parallel with increased mRNA expression. Previous studies by DeMaio *et al.* demonstrated that exposure of bovine aortic endothelial cells (BAEC) to shear stress reduced occludin expression, without change in ZO-1 expression (DeMaio *et al.* 2001). Initially it would seem that these are two conflicting phenomena, however, the experimental paradigm used by DeMaio *et al.* involved exposure of BAECs to shear stress for 3 h as opposed to our paradigm of 24 h shear. Furthermore, studies by Galbraith *et al.* have shown that the shear stress-induced spatial reorganization of the actin cytoskeleton requires 12 –24 h shear for realignment of endothelial cells (Galbraith *et al.* 1998). Therefore, we postulate that the shear stress-dependent regulation of tight junction formation is not monotonic, but rather that there are several distinct phases. That is, disruption of previously formed tight junctions may be necessary to facilitate the shear-induced actin cytoskeleton reorganization, which is then followed by a subsequent increase in tight junction formation. Further studies employing time-lapse fluorescent microscopy to monitor actin, occludin and ZO-1 localization under shearing conditions from 0 – 24 h would address this hypothesis.

Exposure of BBMvECs to shear also resulted in significant increase in the co-association of occludin and ZO-1. Moreover, occludin, normally observed in the cytoplasm of unsheared cells exhibited increased localization at the cell membrane following shear, whilst ZO-1 immunoreactivity, which is discontinuous with long finger-like projections in unsheared conditions, became more continuous and linearly distributed at cell-cell contacts following shear. Phase contrast microscopy also revealed that following 24 h shear there was dramatic reorientation of BBMvECs in the direction of shear concomitant with profound α -actin reorganization. In parallel with these observations, shear stress significantly reduced BBMvEC permeability to FITC dextran, that is, the biochemical regulation of occludin and ZO-1 by shear is accompanied by increased BBMvEC barrier functionality.

In order to address if the shear-dependent modulation of tight junction formation and endothelial barrier function was a result of new protein synthesis or post-translational modification of existing protein, cells were sheared in the presence and absence of cycloheximide. Western blot analysis revealed that, as expected, incubation of BBMvECs with cycloheximide, in both sheared and unsheared cells, reduced the protein expression of both occludin and ZO-1. However, incubation of unsheared BBMvECs with cycloheximide caused a non-specific increase in association of occludin/ZO-1. Moreover, sheared BBMvECs, in both the presence and absence of cycloheximide, exhibited significantly increased levels of occludin/ZO-1 association compared to their unsheared counterparts. These data indicate that approximately 50% of the shear-induced increase in occludin/ZO-1 association is due to *de novo* protein synthesis and 50% due to post-translational modification of the existing protein pool. Furthermore, cycloheximide only partially attenuated the shear-dependent increased localization of occludin and ZO-1 to the cell membrane, whilst permeability tracer studies revealed that shear induces the increased formation of a functional barrier in both *de novo* protein-dependent and independent manners. In concert, these data suggest that the shear-dependent increase in BBMvEC tight junction formation and barrier function is modulated via

both *de novo* protein synthesis and modification of an existing protein pool. Previous studies by Collins *et al.* have revealed a similar response of endothelial cells to mechanical stimuli. In these studies, Collins *et al.* exposed BAECs to 5% cyclic strain, and similar to the findings discussed above, found that increased tight junction formation and associated barrier function was a result of both new protein synthesis and modification of existing proteins (Collins *et al.* 2006). Thus, it would seem that haemodynamic forces regulate endothelial barrier function via two separate pathways; firstly by the expression of new proteins and secondly by the modification of existing tight junction proteins.

Exposure of BBMvECs to pulsatile shear stress, which mimics the pressure changes exerted on cerebral capillaries caused by the opening and closing of arteriole sphincters and dilation/contraction of the capillaries, led to a significant increase in occludin protein expression, without significant change in ZO-1 expression. Furthermore, chronic pulsatile shear stress (14 dynes/cm²/24 h) led to a dramatic increase in association of occludin/ZO-1, which correlated with a significant decrease in permeability to ¹⁴C sucrose. Previous studies by Cucullo *et al.* demonstrated that BAECs grown in both the absence and presence of C6 glioma exhibited increased TEER following exposure to chronic shear stress in a perfused capillary system (Cucullo *et al.* 2002). However, in these studies by Cucullo *et al.*, the biochemical tight junction modifications, which potentially modulate the functional increase in electrical resistance are not investigated. Many recent studies have employed similar models to investigate BBB-specific markers, such as adenosine permeation or glucose transport (Stanness *et al.* 1996; Stanness *et al.* 1997; Pekny *et al.* 1998; Stanness *et al.* 1999; McAllister *et al.* 2001; Sinclair *et al.* 2001). However, to our knowledge this body of work is the first to address the role of shear stress, in a perfused capillary system, in modulating tight junction formation at the molecular level.

Pulsatile laminar shear stress led to a significant increase in occludin/ZO-1 association compared to the non-pulsatile shear stress. However, as the pulsatile

shear was carried out at 14 dynes/cm² and the non-pulsatile shear at 10 dynes/cm², no direct comparison between the two can be made. Further studies are required to elucidate if the differences between the two paradigms are due to a force-dependent or pulse-dependent increased association of occludin/ZO-1. Furthermore, as permeability cannot be assessed directly in the non-pulsatile laminar shear apparatus, no comparison can be made between the pulsatile and non-pulsatile laminar shear-dependent decrease in permeability. Further studies using a cone and plate viscometer to shear in a transwell plate would allow for direct permeability studies under non-pulsatile laminar shear stress without the need for replating.

Previous studies have shown that haemodynamic forces modulate the phosphorylation state of tight junction proteins (Conklin *et al.* 2002; Collins *et al.* 2006). Moreover, as discussed in chapter 1, both occludin and ZO-1 function is modulated via their phosphorylation states (Sakakibara *et al.* 1997; Balda and Matter 1998; Rao *et al.* 2002; Kale *et al.* 2003; Sheth *et al.* 2003). Thus, it would seem logical that further studies into shear-mediated tight junction formation should focus on the phosphorylation and de-phosphorylation of both occludin and ZO-1.

In conclusion, this chapter describes in part, the role of shear stress in microvascular tight junction regulation. These findings clearly indicate that shear stress modulates the expression, localization and association of occludin and ZO-1, two pivotal tight junction proteins. Furthermore, these findings correlate with decreased endothelial permeability, suggesting a putative relationship between occludin/ZO-1 modulation and tight junction barrier function. Further studies are required to fully elucidate the exact mechanisms by which these events occur, however this information enhances our overall understanding of how haemodynamic forces regulate microvascular endothelial function and behaviour.

Chapter 7

Final Summary

7.1 Final Summary

Homeostatic maintenance of the brain microenvironment is essential for normal brain function and neuronal activity and is facilitated by the BBB, a continuum of intercellular tight junctions between adjacent microvascular endothelial cells, which form an effective seal to prevent paracellular solute diffusion. *In vivo* this barrier exhibits high TEER and is impermeable to charged particles, proteins, ions, hydrophilic molecules and hormones that could act as neurotransmitters, thus protecting the CNS from changes in blood composition (Tanobe *et al.* 2003). Although this highly effective barrier functions to protect the CNS, it presents a major obstacle to CNS drug delivery, the major rate-limiting step preventing translation of drug development into effective neurotherapeutics (Pardridge 2002, 2003, 2005a, b). Conversely, disruption of the BBB is associated with a number of pathophysiological conditions including multiple sclerosis (Williams *et al.* 1994), meningitis/encephalitis (Tunkel and Scheld 1993), neurodegenerative diseases such as Parkinson's and Alzheimer's disease (Mattila *et al.* 1994) and progressive multifocal leukoencephalopathy (Poland *et al.* 1995). Thus, development of novel strategies to modulate barrier function within the brain microvasculature necessitates elucidating the etiology of intercellular tight junction formation and the pathophysiological factors effecting BBB permeability. This study attempts to extend our knowledge in this clinically significant field by investigating how both apical and basolateral conditions impact on endothelial tight junction assembly at both the molecular and functional level in an *in vitro* BBMvEC model. In this regard, the BBB endothelium *in vivo* is basolaterally encompassed by astrocyte end feet and bathed in serum-free ISF and apically exposed to shear stress caused by the drag force of blood flowing through cerebral capillaries. Thus, we hypothesized that basolaterally applied serum and/or astrocytes (C6 glioma), as well as apical shear stress, impacts on BBB function by directly modulating the expression and biochemical properties of two pivotal endothelial tight junction proteins, occludin and ZO-1. This knowledge may allow for the appropriate clinical

modulation of tight junction “open” and “closed” states, thus having a profound impact on several neurological disorders.

As the clinical significance of BBB function and dysfunction is now being recognized and the ensuing work is at the forefront of biomedical research, the aim of this study was to investigate the effect of physiologically relevant paradigms on brain microvascular endothelial tight junction formation and barrier function. Three potential mediators of tight junction formation were addressed, namely; the removal of basolateral serum, co-culture of BBMvECs with C6 glioma basolaterally and finally, the effect of shear stress apically. Due to the variety of potential stimuli being investigated, several experimental paradigms must be employed. For both serum and co-culture studies, transwell plates were used, which facilitated the *in situ* monitoring of BBMvEC TEER and permeability. However, as shearing of BBMvECs was not possible in transwell plates, cells were exposed to shear in either 6-well plates, which were rotated on an orbital shaker, or in a perfused capillary system. For all the experimental paradigms, focus was placed on the biochemical modulation of the tight junction proteins occludin and ZO-1, and the accompanying functional changes in electrical resistance and/or permeability, which occurred.

The initial focus of this study was to investigate if the removal of basolateral serum, thus mimicking the *in vivo* brain ISF, altered the state of BBMvEC tight junctions or the accompanying barrier functionality. Western blot analysis revealed that removal of basolateral serum resulted in a significant increase in occludin and ZO-1 protein expression, which was paralleled by a similar increase in mRNA. Furthermore, the association of occludin/ZO-1, and their subcellular localization to the cell membrane increased following serum removal. In addition, similar to findings by Nitz *et al.*, the application of serum-free media resulted in a significant increase in monolayer electrical resistance in a highly polar-specific manner (Nitz *et al.* 2003), which was associated with a decrease in paracellular permeability to a radiolabelled sucrose tracer. The serum-derived factors responsible for the reduction in tight junction formation and barrier function are yet to be elucidated, however, VEGF and LPA

have been implicated in reduction of endothelial barrier function via disruption of tight junctions.

In vivo, astrocyte foot processes encircle the endothelial basal laminae and have been shown to induce endothelial barrier function (Saunders *et al.* 1991), therefore, the role of astrocyte:endothelial interaction on tight junction formation was examined by co-culturing BBMvECs and C6 glioma (with the latter cells in the basolateral aspect). Under non-contact co-culture conditions, there was significant increase in both occludin and ZO-1 protein expression in BBMvECs without change in mRNA. This indicates that the apparent increase in protein may be due to decreased protein turnover rather than *de novo* protein synthesis. However, it is also possible that an increase in mRNA occurs, and is translated into protein prior to the 24 h time-point used in this paradigm. Furthermore, co-culture led to increased occludin/ZO-1 association and redistribution of the two to the cell periphery, which was correlated with decreased permeability and increased electrical resistance.

In view of these findings, we further sought to investigate if a combination of these conditions, i.e. co-culture of BBMvEC and C6 glioma in the absence of basolateral serum, would have an additive effect in relation to barrier formation and function. Under these conditions, occludin expression and occludin/ZO-1 association were increased significantly with respect to both the serum-free monoculture and serum-containing co-culture models. However, the increase observed was less than the predicted additive effect, indicating that there is only a *partial additive effect* of co-culture in the absence of basolateral serum. Furthermore, removal of basolateral serum from the co-culture resulted in the most continuous localization of both proteins at cell-cell contacts. Analysis of barrier function by TEER and ¹⁴C sucrose tracer studies reflected a similar trend.

Thus, it seems that the removal of basolateral serum and co-culturing with C6 glioma may cause increased BBMvEC tight junction formation and associated barrier function via two separate pathways (see figure 7.1). That is, removal of

basolateral serum causes increase in occludin and ZO-1 protein by elevated mRNA production, whilst co-culture leads to increased protein accumulation by decreasing protein turnover.

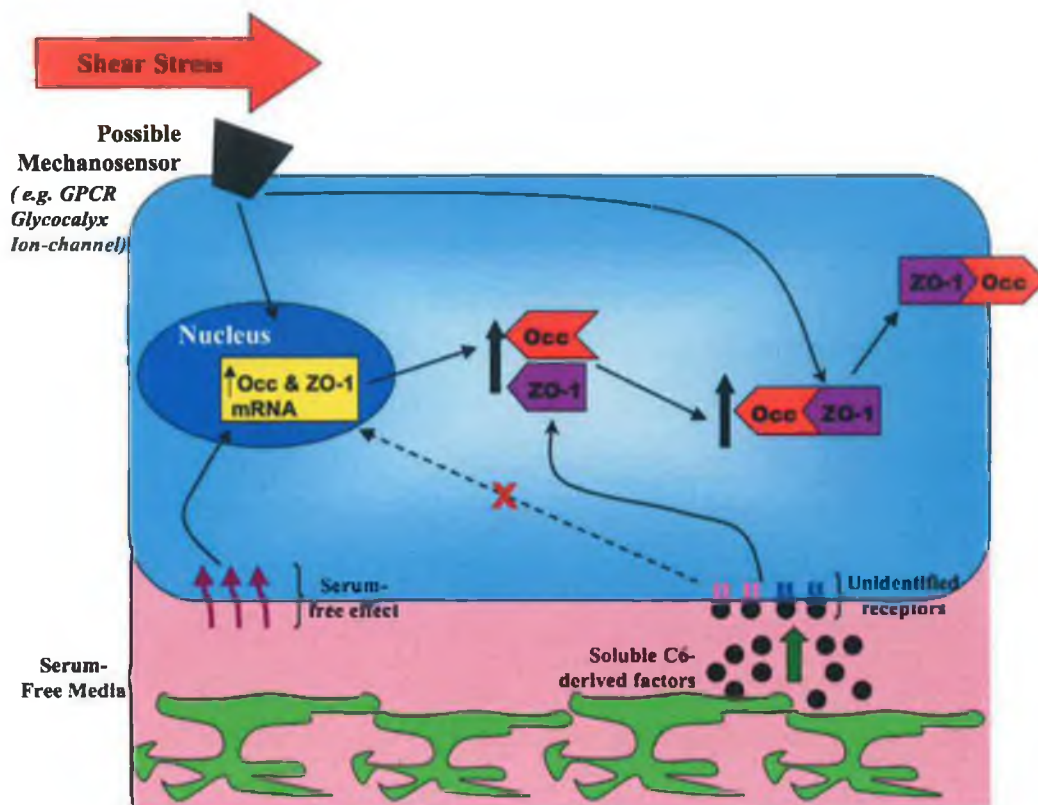


Figure 7.1: Schematic representation of thesis findings with respect to serum, co-culture and shear-induced modulation of occludin and ZO-1.

Brain microvascular endothelial cells, which form the BBB are exposed to shear stress on their apical surface caused by the flow of blood through cerebral capillaries. Haemodynamic forces have been shown to modulate a variety of endothelial responses, including cell morphology (Galbraith *et al.* 1998; Noria *et al.* 1999), gene expression (Patrick and McIntire 1995; Chien *et al.* 1998; Traub and Berk 1998) and function (Ballermann and Ott 1995; Ngai and Winn 1995; Ott and Ballermann 1995). Furthermore, recent studies have indicated a role for haemodynamic forces in regulating endothelial tight junction formation and barrier function (DeMaio *et al.* 2001; Conklin *et al.* 2002; Collins *et al.* 2006). Therefore,

we sought to investigate the effect of shear stress on BBMvEC occludin and ZO-1 regulation and to elucidate if these changes correlated with modification of barrier function. Exposure of BBMvECs to chronic non-pulsatile shear stress (10 dynes/cm², 24 h) resulted in increased occludin and ZO-1 expression, in parallel with increased association of the two. Furthermore, sheared cells exhibited increased occludin and ZO-1 localization at the cell periphery, which was associated with a decrease in paracellular permeability to FITC dextran. Furthermore, inhibition of new protein synthesis with cycloheximide revealed that the shear-induced increase in tight junction formation and barrier function was modulated via both *de novo* protein synthesis and post-translational modification of existing proteins. In addition, pulsatile shear stress (14 dynes/cm², 24 h) led to a significant increase in occludin expression and occludin/ZO-1 association, which correlated with a decrease in paracellular permeability to ¹⁴C sucrose.

Although this data provides insight into the factors modulating endothelial occludin and ZO-1, further research is required to investigate the mechanisms and pathways by which this occurs. As detailed in chapter 1, occludin and ZO-1 function is mediated via modulation of their phosphorylation state, therefore, the future logical focus of this work is to examine the specific serine, threonine and tyrosine phosphorylation states of both proteins in their active and inactive forms. Furthermore, delineation of the signaling pathways responsible for serum, astrocyte and shear-induced tight junction modulation will allow for the identification of possible targets for clinical intervention. Identification of the serum and astrocyte-derived factors, and their associated endothelial receptors, involved in tight junction assembly and function, may allow for manipulation of the “open” and “closed” state of the blood-brain barrier, and thus have a profound impact on both drug delivery to the brain and amelioration of neurological disorders associated with increased BBB permeability. Furthermore, elucidation of the mechanotransduction pathway responsible for the shear-induced increase in tight junction formation would greatly increase our knowledge as to how endothelial function is modulated via haemodynamic forces. Inhibition of possible mechanosensors, such as the

glycocalyx by neuraminidase, GPCR using pertussis toxin, or integrins by cyclic or linear RGD peptides etc., will allow for the identification of the specific mechanosensor responsible for translation of the physical force of shear stress into a cellular response. In addition, studies by Collins *et al.* have shown that tight junction assembly in response to cyclic strain occurs via both tyrosine phosphatase- and PKC-dependent pathways (Collins *et al.* 2006). The potential role of these pathways in shear stress-dependent modulation of tight junctions could be examined using specific tyrosine phosphatase and PKC inhibitors (dephostatin and rottlerin, respectively). Furthermore, recent studies have identified two Rho family GTPases, Rho and Rac, and p38 MAPK as key regulators of endothelial tight junction assembly and barrier function (Wojciak-Stothard and Ridley 2002, Collins *et al.* [unpublished]), and as such, their role in mediating the shear stress-dependent tight junction formation and barrier function must be investigated.

In vivo, sucrose permeability in the rat BBB is in the region of $0.18 - 0.6 \times 10^{-5}$ cm/min. However, in the experimental paradigms outlined in this thesis, both the transwell models and the perfused capillary system have sucrose permeability coefficients in the region of $0.5 - 1.0 \times 10^{-3}$ cm/min. Moreover, *in vivo* TEER in the BBB is estimated to be greater than $1000 \Omega \cdot \text{cm}^2$, whilst the maximum electrical resistance achieved in the transwell plates was approximately $80 \Omega \cdot \text{cm}^2$. Therefore, although we have clearly demonstrated the effect of serum, astrocytes and shear stress in modulating endothelial barrier function, these models do not reflect the electrical resistance or sucrose permeability properties expressed in the BBB *in vivo*. Therefore, a more physiologically relevant combination of the three factors investigated (i.e. basolateral serum-free media, co-culture with C6 and shear stress) would more closely resemble the *in vivo* situation, allow for a greater understanding of how these pathways interact and elucidate any synergistic relationships between the stimuli.

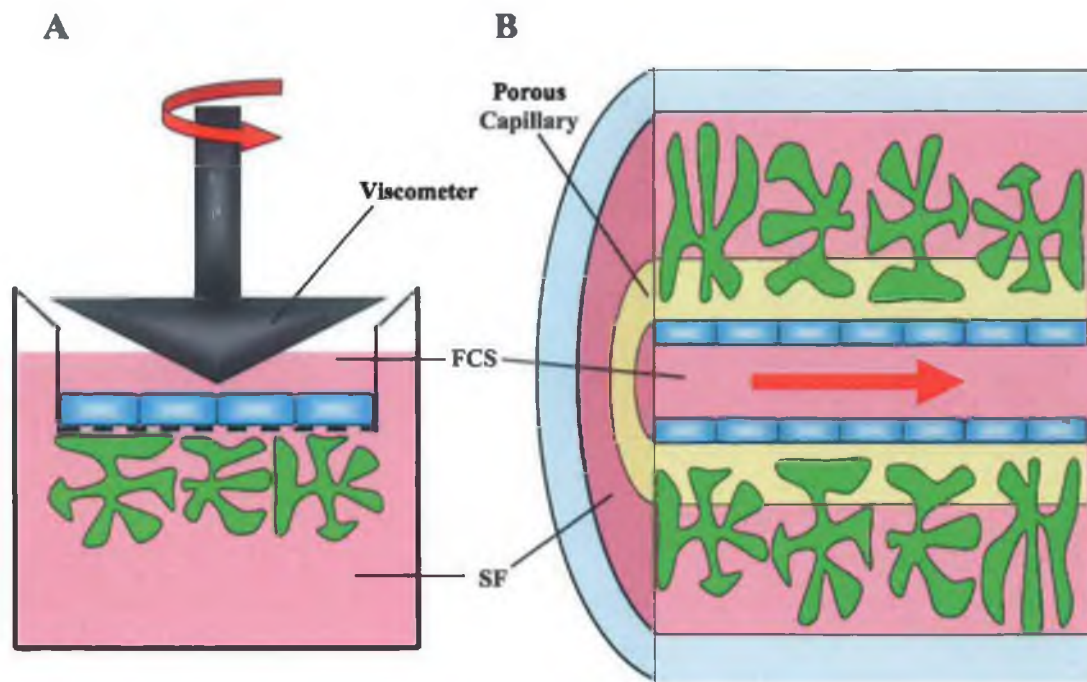


Figure 7.2: Schematic diagrams of the apparatus for proposed future work enabling co-culture of BBMvECs with C6 glioma, in basolaterally serum free (SF) media, whilst being exposed to shear stress caused by the movement of serum-containing media (FCS) on the endothelial apical surface. Shear stress is induced by either a cone and plate viscometer in a transwell plate (A) or in the perfused capillary system (B).

In chapter 5 we proposed that a synergistic contact-dependent relationship may exist between astrocytes and endothelial cells that allows for the continued viability of astrocytes in serum free conditions, and two-way cross-talk between the cells. As depicted in figure 7.2, growing astrocytes and endothelial cells on opposite sides of a porous membrane (A) or capillary (B), will allow for the infiltration of astrocyte end feet into the pores and contact with the basal surface of the BBMvECs without mixing of the two cell populations, as previously shown by Garcia *et al.* (Garcia *et al.* 2004). Furthermore, induction of haemodynamic forces using either a cone and plate viscometer in conjunction with a transwell plate or the perfused capillary system would facilitate examination of both the basolateral effects of C6 co-culture in a serum free environment in tandem with apically acting shear stress. In this way

the combination of modulatory effects on occludin and ZO-1 as well as barrier function may be examined. Thus, by mimicking *in vitro* the factors responsible for modulating the BBB *in vivo*, we may be able to develop a reproducible *in vitro* model of the BBB, which would express the high electrical resistance and low permeability characteristics of the BBB *in vivo*. This system would then allow for the high throughput screening required in drug development, thus reducing the need for clinical testing on animals. Moreover, the findings of this thesis coupled with a physiologically relevant model of the BBB could identify potential targets for clinical manipulation of tight junction integrity and thus drastically reduce the time-scale associated with the identification and testing of effective clinical neurotherapeutic agents.

Overall, the findings of this thesis indicate that tight junction formation and barrier function in brain microvascular endothelial cells is a result of both basolateral and apical stimuli. Moreover, these data suggest a putative link between occludin/ZO-1 regulation and endothelial barrier function. The potential value of these findings, with respect to clinical manipulation of BBB tight junctions, has been discussed at length throughout this thesis however, this data may also impact on several non-neurological diseases in the peripheral vasculature. As discussed in chapter 1, loss of occludin and/or ZO-1 is associated with pathogen-induced diarrhoea, allergies and cancer. Furthermore, increased arterial permeability, at areas of reduced haemodynamic loading, correlates with elevated atherosclerotic plaque formation. Therefore, elucidating the factors that modulate intercellular tight junction formation may allow for the development of novel strategies to modulate endothelial barrier function and thus have a profound impact on both neurological and peripheral diseases.

Chapter 8

Bibliography

Abbott N. J., Ronnback L. and Hansson E. (2006) Astrocyte-endothelial interactions at the blood-brain barrier. *Nat Rev Neurosci* **7**, 41-53.

Abbruscato T. J. and Davis T. P. (1999) Protein expression of brain endothelial cell E-cadherin after hypoxia/aglycemia: influence of astrocyte contact. *Brain Res* **842**, 277-286.

Akimoto S., Mitsumata M., Sasaguri T. and Yoshida Y. (2000) Laminar shear stress inhibits vascular endothelial cell proliferation by inducing cyclin-dependent kinase inhibitor p21(Sdi1/Cip1/Waf1). *Circ Res* **86**, 185-190.

Alevriadou B. R., Eskin S. G., McIntire L. V. and Schilling W. P. (1993) Effect of shear stress on 86Rb⁺ efflux from calf pulmonary artery endothelial cells. *Ann Biomed Eng* **21**, 1-7.

Amieva M. R., Vogelmann R., Covacci A., Tompkins L. S., Nelson W. J. and Falkow S. (2003) Disruption of the epithelial apical-junctional complex by *Helicobacter pylori* CagA. *Science* **300**, 1430-1434.

Anderson J. M. and Van Itallie C. M. (1995) Tight junctions and the molecular basis for regulation of paracellular permeability. *Am J Physiol* **269**, G467-475.

Anderson J. M., Stevenson B. R., Jesaitis L. A., Goodenough D. A. and Mooseker M. S. (1988) Characterization of ZO-1, a protein component of the tight junction from mouse liver and Madin-Darby canine kidney cells. *J Cell Biol* **106**, 1141-1149.

Ando-Akatsuka Y., Saitou M., Hirase T., Kishi M., Sakakibara A., Itoh M., Yonemura S., Furuse M. and Tsukita S. (1996) Interspecies diversity of the occludin sequence: cDNA cloning of human, mouse, dog, and rat-kangaroo homologues. *J Cell Biol* **133**, 43-47.

Antonetti D. A., Barber A. J., Hollinger L. A., Wolpert E. B. and Gardner T. W. (1999) Vascular endothelial growth factor induces rapid phosphorylation of tight junction proteins occludin and zonula occluden 1. A potential mechanism for vascular permeability in diabetic retinopathy and tumors. *J Biol Chem* **274**, 23463-23467.

Antonetti D. A., Barber A. J., Khin S., Lieth E., Tarbell J. M. and Gardner T. W. (1998) Vascular permeability in experimental diabetes is associated with reduced endothelial occludin content: vascular endothelial growth factor decreases occludin in retinal endothelial cells. Penn State Retina Research Group. *Diabetes* **47**, 1953-1959.

Aschner M. (1998) Immune and inflammatory responses in the CNS: modulation by astrocytes. *Toxicol Lett* **102-103**, 283-287.

- Audus K. L. and Borchardt R. T. (1987) Bovine brain microvessel endothelial cell monolayers as a model system for the blood-brain barrier. *Ann N Y Acad Sci* **507**, 9-18.
- Bai N., Moien-Afshari F., Washio H., Min A. and Laher I. (2004) Pharmacology of the mouse-isolated cerebral artery. *Vascul Pharmacol* **41**, 97-106.
- Balabanov R. and Dore-Duffy P. (1998) Role of the CNS microvascular pericyte in the blood-brain barrier. *J Neurosci Res* **53**, 637-644.
- Balda M. S. and Anderson J. M. (1993) Two classes of tight junctions are revealed by ZO-1 isoforms. *Am J Physiol* **264**, C918-924.
- Balda M. S. and Matter K. (1998) Tight junctions. *J Cell Sci* **111 (Pt 5)**, 541-547.
- Balda M. S. and Matter K. (2000) The tight junction protein ZO-1 and an interacting transcription factor regulate ErbB-2 expression. *Embo J* **19**, 2024-2033.
- Balda M. S., Anderson J. M. and Matter K. (1996a) The SH3 domain of the tight junction protein ZO-1 binds to a serine protein kinase that phosphorylates a region C-terminal to this domain. *FEBS Lett* **399**, 326-332.
- Balda M. S., Flores-Maldonado C., Cereijido M. and Matter K. (2000) Multiple domains of occludin are involved in the regulation of paracellular permeability. *J Cell Biochem* **78**, 85-96.
- Balda M. S., Gonzalez-Mariscal L., Matter K., Cereijido M. and Anderson J. M. (1993) Assembly of the tight junction: the role of diacylglycerol. *J Cell Biol* **123**, 293-302.
- Balda M. S., Whitney J. A., Flores C., Gonzalez S., Cereijido M. and Matter K. (1996b) Functional dissociation of paracellular permeability and transepithelial electrical resistance and disruption of the apical-basolateral intramembrane diffusion barrier by expression of a mutant tight junction membrane protein. *J Cell Biol* **134**, 1031-1049.
- Ballermann B. J. and Ott M. J. (1995) Adhesion and differentiation of endothelial cells by exposure to chronic shear stress: a vascular graft model. *Blood Purif* **13**, 125-134.
- Bamforth S. D., Kniesel U., Wolburg H., Engelhardt B. and Risau W. (1999) A dominant mutant of occludin disrupts tight junction structure and function. *J Cell Sci* **112 (Pt 12)**, 1879-1888.
- Barber A. J. and Antonetti D. A. (2003) Mapping the blood vessels with paracellular permeability in the retinas of diabetic rats. *Invest Ophthalmol Vis Sci* **44**, 5410-5416.

- Bazzoni G., Martinez-Estrada O. M., Orsenigo F., Cordenonsi M., Citi S. and Dejana E. (2000) Interaction of junctional adhesion molecule with the tight junction components ZO-1, cingulin, and occludin. *J Biol Chem* **275**, 20520-20526.
- Beck D. W., Roberts R. L. and Olson J. J. (1986) Glial cells influence membrane-associated enzyme activity at the blood-brain barrier. *Brain Res* **381**, 131-137.
- Beck D. W., Vinters H. V., Hart M. N. and Cancilla P. A. (1984) Glial cells influence polarity of the blood-brain barrier. *J Neuropathol Exp Neurol* **43**, 219-224.
- Benda P., Lightbody J., Sato G., Levine L. and Sweet W. (1968) Differentiated rat glial cell strain in tissue culture. *Science* **161**, 370-371.
- Benyo Z., Lacza Z., Hortobagyi T., Gorlach C. and Wahl M. (2000) Functional importance of neuronal nitric oxide synthase in the endothelium of rat basilar arteries. *Brain Res* **877**, 79-84.
- Berezowski V., Landry C., Dehouck M. P., Cecchelli R. and Fenart L. (2004) Contribution of glial cells and pericytes to the mRNA profiles of P-glycoprotein and multidrug resistance-associated proteins in an *in vitro* model of the blood-brain barrier. *Brain Res* **1018**, 1-9.
- Berthiaume F. and Frangos J. A. (1992) Flow-induced prostacyclin production is mediated by a pertussis toxin-sensitive G protein. *FEBS Lett* **308**, 277-279.
- Bhullar I. S., Li Y. S., Miao H., Zandi E., Kim M., Shyy J. Y. and Chien S. (1998) Fluid shear stress activation of IkappaB kinase is integrin-dependent. *J Biol Chem* **273**, 30544-30549.
- Billings S. D., Walsh S. V., Fisher C., Nusrat A., Weiss S. W. and Folpe A. L. (2004) Aberrant expression of tight junction-related proteins ZO-1, claudin-1 and occludin in synovial sarcoma: an immunohistochemical study with ultrastructural correlation. *Mod Pathol* **17**, 141-149.
- Bolanos J. P. and Almeida A. (1999) Roles of nitric oxide in brain hypoxia-ischemia. *Biochim Biophys Acta* **1411**, 415-436.
- Brenman J. E., Chao D. S., Gee S. H., McGee A. W., Craven S. E., Santillano D. R., Wu Z., Huang F., Xia H., Peters M. F., Froehner S. C. and Brecht D. S. (1996) Interaction of nitric oxide synthase with the postsynaptic density protein PSD-95 and alpha1-syntrophin mediated by PDZ domains. *Cell* **84**, 757-767.
- Brightman M. W. and Palay S. L. (1963) The Fine Structure of Ependyma in the Brain of the Rat. *J Cell Biol* **19**, 415-439.
- Brightman M. W. and Reese T. S. (1969) Junctions between intimately apposed cell membranes in the vertebrate brain. *J Cell Biol* **40**, 648-677.

- Butt A. M. (1995) Effect of inflammatory agents on electrical resistance across the blood-brain barrier in pial microvessels of anaesthetized rats. *Brain Res* **696**, 145-150.
- Butt A. M., Jones H. C. and Abbott N. J. (1990) Electrical resistance across the blood-brain barrier in anaesthetized rats: a developmental study. *J Physiol* **429**, 47-62.
- Cancilla P. A., Baker R. N., Pollock P. S. and Frommes S. P. (1972) The reaction of pericytes of the central nervous system to exogenous protein. *Lab Invest* **26**, 376-383.
- Castejon O. J. (1984) Submicroscopic changes of cortical capillary pericytes in human perifocal brain edema. *J Submicrosc Cytol* **16**, 601-618.
- Cereijido M., Valdes J., Shoshani L. and Contreras R. G. (1998) Role of tight junctions in establishing and maintaining cell polarity. *Annu Rev Physiol* **60**, 161-177.
- Chang C., Wang X. and Caldwell R. B. (1997) Serum opens tight junctions and reduces ZO-1 protein in retinal epithelial cells. *J Neurochem* **69**, 859-867.
- Chen S. H., Stins M. F., Huang S. H., Chen Y. H., Kwon-Chung K. J., Chang Y., Kim K. S., Suzuki K. and Jong A. Y. (2003) *Cryptococcus neoformans* induces alterations in the cytoskeleton of human brain microvascular endothelial cells. *J Med Microbiol* **52**, 961-970.
- Chen Y., Merzdorf C., Paul D. L. and Goodenough D. A. (1997) COOH terminus of occludin is required for tight junction barrier function in early *Xenopus* embryos. *J Cell Biol* **138**, 891-899.
- Chien S., Li S. and Shyy Y. J. (1998) Effects of mechanical forces on signal transduction and gene expression in endothelial cells. *Hypertension* **31**, 162-169.
- Chomczynski P. and Sacchi N. (1987) Single-step method of RNA isolation by acid guanidinium thiocyanate-phenol-chloroform extraction. *Anal Biochem* **162**, 156-159.
- Citi S. (1993) The molecular organization of tight junctions. *J Cell Biol* **121**, 485-489.
- Citi S., Sabanay H., Kendrick-Jones J. and Geiger B. (1989) Cingulin: characterization and localization. *J Cell Sci* **93 (Pt 1)**, 107-122.
- Citi S., Sabanay H., Jakes R., Geiger B. and Kendrick-Jones J. (1988) Cingulin, a new peripheral component of tight junctions. *Nature* **333**, 272-276.
- Claude P. (1978) Morphological factors influencing transepithelial permeability: a model for the resistance of the zonula occludens. *J Membr Biol* **39**, 219-232.

Claude P. and Goodenough D. A. (1973) Fracture faces of zonulae occludentes from "tight" and "leaky" epithelia. *J Cell Biol* **58**, 390-400.

Collares-Buzato C. B., Jepson M. A., Simmons N. L. and Hirst B. H. (1998) Increased tyrosine phosphorylation causes redistribution of adherens junction and tight junction proteins and perturbs paracellular barrier function in MDCK epithelia. *Eur J Cell Biol* **76**, 85-92.

Collins N. T., Cummins P. M., Colgan O. C., Ferguson G., Birney Y. A., Murphy R. P., Meade G. and Cahill P. A. (2006) Cyclic strain-mediated regulation of vascular endothelial occludin and ZO-1: influence on intercellular tight junction assembly and function. *Arterioscler Thromb Vasc Biol* **26**, 62-68.

Conklin B. S., Zhong D. S., Zhao W., Lin P. H. and Chen C. (2002) Shear stress regulates occludin and VEGF expression in porcine arterial endothelial cells. *J Surg Res* **102**, 13-21.

Cordenonsi M., D'Atri F., Hammar E., Parry D. A., Kendrick-Jones J., Shore D. and Citi S. (1999) Cingulin contains globular and coiled-coil domains and interacts with ZO-1, ZO-2, ZO-3, and myosin. *J Cell Biol* **147**, 1569-1582.

Crone C. and Olesen S. P. (1982) Electrical resistance of brain microvascular endothelium. *Brain Research* **241**, 49-55.

Cucullo L., McAllister M. S., Kight K., Krizanac-Bengez L., Marroni M., Mayberg M. R., Stanness K. A. and Janigro D. (2002) A new dynamic *in vitro* model for the multidimensional study of astrocyte-endothelial cell interactions at the blood-brain barrier. *Brain Res* **951**, 243-254.

Davies D. C. (2002) Blood-brain barrier breakdown in septic encephalopathy and brain tumours. *J Anat* **200**, 639-646.

Davies P. F. (1995) Flow-mediated endothelial mechanotransduction. *Physiol Rev* **75**, 519-560.

del Zoppo G. J. and Hallenbeck J. M. (2000) Advances in the vascular pathophysiology of ischemic stroke. *Thromb Res* **98**, 73-81.

DeMaio L., Chang Y. S., Gardner T. W., Tarbell J. M. and Antonetti D. A. (2001) Shear stress regulates occludin content and phosphorylation. *Am J Physiol Heart Circ Physiol* **281**, H105-113.

Demeuse P., Kerkhofs A., Struys-Ponsar C., Knoop B., Remacle C. and van den Bosch de Aguilar P. (2002) Compartmentalized coculture of rat brain endothelial cells and astrocytes: a syngenic model to study the blood-brain barrier. *J Neurosci Methods* **121**, 21-31.

- Denekamp J. (1993) Review article: angiogenesis, neovascular proliferation and vascular pathophysiology as targets for cancer therapy. *Br J Radiol* **66**, 181-196.
- Denisenko N., Burighel P. and Citi S. (1994) Different effects of protein kinase inhibitors on the localization of junctional proteins at cell-cell contact sites. *J Cell Sci* **107 (Pt 4)**, 969-981.
- Desai S. Y., Marroni M., Cucullo L., Krizanac-Bengez L., Mayberg M. R., Hossain M. T., Grant G. G. and Janigro D. (2002) Mechanisms of endothelial survival under shear stress. *Endothelium* **9**, 89-102.
- Dong Y. and Benveniste E. N. (2001) Immune function of astrocytes. *Glia* **36**, 180-190.
- Dzau V. J., Braun-Dullaeus R. C. and Sedding D. G. (2002) Vascular proliferation and atherosclerosis: new perspectives and therapeutic strategies. *Nat Med* **8**, 1249-1256.
- Ebnet K., Schulz C. U., Meyer Zu Brickwedde M. K., Pendl G. G. and Vestweber D. (2000) Junctional adhesion molecule interacts with the PDZ domain-containing proteins AF-6 and ZO-1. *J Biol Chem* **275**, 27979-27988.
- Estrada C., Bready J. V., Berliner J. A., Pardridge W. M. and Cancilla P. A. (1990) Astrocyte growth stimulation by a soluble factor produced by cerebral endothelial cells *in vitro*. *J Neuropathol Exp Neurol* **49**, 539-549.
- Fanning A. S. and Anderson J. M. (1999) PDZ domains: fundamental building blocks in the organization of protein complexes at the plasma membrane. *J Clin Invest* **103**, 767-772.
- Fanning A. S., Jameson B. J., Jesaitis L. A. and Anderson J. M. (1998) The tight junction protein ZO-1 establishes a link between the transmembrane protein occludin and the actin cytoskeleton. *J Biol Chem* **273**, 29745-29753.
- Faraci F. M. (1991) Role of endothelium-derived relaxing factor in cerebral circulation: large arteries vs. microcirculation. *Am J Physiol* **261**, H1038-1042.
- Farquhar M. G. and Palade G. E. (1963) Junctional complexes in various epithelia. *J Cell Biol* **17**, 375-412.
- Farrell C. R., Stewart P. A., Farrell C. L. and Del Maestro R. F. (1987) Pericytes in human cerebral microvasculature. *Anat Rec* **218**, 466-469.
- Farshori P. and Kachar B. (1999) Redistribution and phosphorylation of occludin during opening and resealing of tight junctions in cultured epithelial cells. *J Membr Biol* **170**, 147-156.

Feldman G. J., Mullin J. M. and Ryan M. P. (2005) Occludin: structure, function and regulation. *Adv Drug Deliv Rev* **57**, 883-917.

Felts P. A. and Smith K. J. (1996) Blood-brain barrier permeability in astrocyte-free regions of the central nervous system remyelinated by Schwann cells. *Neuroscience* **75**, 643-655.

Ferguson G., Watterson K. R. and Palmer T. M. (2000) Subtype-specific kinetics of inhibitory adenosine receptor internalization are determined by sensitivity to phosphorylation by G-protein-coupled receptor kinases. *Molecular Pharmacology* **57**, 546-552.

Ferrara N., Houck K. A., Jakeman L. B., Winer J. and Leung D. W. (1991) The vascular endothelial growth factor family of polypeptides. *J Cell Biochem* **47**, 211-218.

Flaherty J. T., Pierce J. E., Ferrans V. J., Patel D. J., Tucker W. K. and Fry D. L. (1972) Endothelial nuclear patterns in the canine arterial tree with particular reference to hemodynamic events. *Circ Res* **30**, 23-33.

Fleming I. and Busse R. (1999) NO: the primary EDRF. *J Mol Cell Cardiol* **31**, 5-14.

Florian J. A., Kosky J. R., Ainslie K., Pang Z., Dull R. O. and Tarbell J. M. (2003) Heparan sulfate proteoglycan is a mechanosensor on endothelial cells. *Circ Res* **93**, e136-142.

Francis S. A., Kelly J. M., McCormack J., Rogers R. A., Lai J., Schneeberger E. E. and Lynch R. D. (1999) Rapid reduction of MDCK cell cholesterol by methyl-beta-cyclodextrin alters steady state transepithelial electrical resistance. *Eur J Cell Biol* **78**, 473-484.

Frank R. N., Dutta S. and Mancini M. A. (1987) Pericyte coverage is greater in the retinal than in the cerebral capillaries of the rat. *Invest Ophthalmol Vis Sci* **28**, 1086-1091.

Fukushima H., Fujimoto M. and Ide M. (1990) Quantitative detection of blood-brain barrier-associated enzymes in cultured endothelial cells of porcine brain microvessels. *In Vitro Cell Dev Biol* **26**, 612-620.

Furuse M., Sasaki H. and Tsukita S. (1999) Manner of interaction of heterogeneous claudin species within and between tight junction strands. *J Cell Biol* **147**, 891-903.

Furuse M., Fujita K., Hிரagi T., Fujimoto K. and Tsukita S. (1998) Claudin-1 and -2: novel integral membrane proteins localizing at tight junctions with no sequence similarity to occludin. *J Cell Biol* **141**, 1539-1550.

- Furuse M., Hirase T., Itoh M., Nagafuchi A., Yonemura S. and Tsukita S. (1993) Occludin: a novel integral membrane protein localizing at tight junctions. *J Cell Biol* **123**, 1777-1788.
- Furuse M., Itoh M., Hirase T., Nagafuchi A., Yonemura S. and Tsukita S. (1994) Direct association of occludin with ZO-1 and its possible involvement in the localization of occludin at tight junctions. *J Cell Biol* **127**, 1617-1626.
- Galbraith C. G., Skalak R. and Chien S. (1998) Shear stress induces spatial reorganization of the endothelial cell cytoskeleton. *Cell Motil Cytoskeleton* **40**, 317-330.
- Garcia C. M., Darland D. C., Massingham L. J. and D'Amore P. A. (2004) Endothelial cell-astrocyte interactions and TGF beta are required for induction of blood-neural barrier properties. *Brain Res Dev Brain Res* **152**, 25-38.
- Gee J. R. and Keller J. N. (2005) Astrocytes: regulation of brain homeostasis via apolipoprotein E. *Int J Biochem Cell Biol* **37**, 1145-1150.
- Giancotti F. G. and Ruoslahti E. (1999) Integrin signaling. *Science* **285**, 1028-1032.
- Giepmans B. N. and Moolenaar W. H. (1998) The gap junction protein connexin43 interacts with the second PDZ domain of the zona occludens-1 protein. *Curr Biol* **8**, 931-934.
- Gillespie P. G. and Walker R. G. (2001) Molecular basis of mechanosensory transduction. *Nature* **413**, 194-202.
- Gloe T., Sohn H. Y., Meininger G. A. and Pohl U. (2002) Shear stress-induced release of basic fibroblast growth factor from endothelial cells is mediated by matrix interaction via integrin alpha(v)beta3. *J Biol Chem* **277**, 23453-23458.
- Gloor S. M., Weber A., Adachi N. and Frei K. (1997) Interleukin-1 modulates protein tyrosine phosphatase activity and permeability of brain endothelial cells. *Biochem Biophys Res Commun* **239**, 804-809.
- Goetzl E. J., Lee H., Azuma T., Stossel T. P., Turck C. W. and Karliner J. S. (2000) Gelsolin binding and cellular presentation of lysophosphatidic acid. *J Biol Chem* **275**, 14573-14578.
- Goldman J. E., Geier S. S. and Hirano M. (1986) Differentiation of astrocytes and oligodendrocytes from germinal matrix cells in primary culture. *J Neurosci* **6**, 52-60.
- Gopalakrishnan S., Raman N., Atkinson S. J. and Marrs J. A. (1998) Rho GTPase signaling regulates tight junction assembly and protects tight junctions during ATP depletion. *Am J Physiol* **275**, C798-809.

Gottardi C. J., Arpin M., Fanning A. S. and Louvard D. (1996) The junction-associated protein, zonula occludens-1, localizes to the nucleus before the maturation and during the remodeling of cell-cell contacts. *Proc Natl Acad Sci U S A* **93**, 10779-10784.

Grant T., Bennett-Wood V. and Robins-Browne R. M. (1999) Characterization of the interaction between *Yersinia enterocolitica* biotype 1A and phagocytes and epithelial cells in vitro. *Infect Immun* **67**, 4367-4375.

Groarke D. A., Drmota T., Bahia D. S., Evans N. A., Wilson S. and Milligan G. (2001) Analysis of the C-terminal tail of the rat thyrotropin-releasing hormone receptor-1 in interactions and cointernalization with beta-arrestin 1-green fluorescent protein. *Molecular Pharmacology* **59**, 375-385.

Gudi S., Nolan J. P. and Frangos J. A. (1998) Modulation of GTPase activity of G proteins by fluid shear stress and phospholipid composition. *Proc Natl Acad Sci U S A* **95**, 2515-2519.

Gudi S., Huvar I., White C. R., McKnight N. L., Dusserre N., Boss G. R. and Frangos J. A. (2003) Rapid activation of Ras by fluid flow is mediated by G-alpha(q) and G-beta-gamma subunits of heterotrimeric G-proteins in human endothelial cells. *Arterioscler Thromb Vasc Biol* **23**, 994-1000.

Gumbiner B. and Simons K. (1986) A functional assay for proteins involved in establishing an epithelial occluding barrier: identification of a uvomorulin-like polypeptide. *J Cell Biol* **102**, 457-468.

Hamazaki Y., Itoh M., Sasaki H., Furuse M. and Tsukita S. (2002) Multi-PDZ domain protein 1 (MUPP1) is concentrated at tight junctions through its possible interaction with claudin-1 and junctional adhesion molecule. *J Biol Chem* **277**, 455-461.

Haskins J., Gu L., Wittchen E. S., Hibbard J. and Stevenson B. R. (1998) ZO-3, a novel member of the MAGUK protein family found at the tight junction, interacts with ZO-1 and occludin. *J Cell Biol* **141**, 199-208.

Hawkins B. T. and Davis T. P. (2005) The blood-brain barrier/neurovascular unit in health and disease. *Pharmacol Rev* **57**, 173-185.

Haydon P. G. (2001) GLIA: listening and talking to the synapse. *Nat Rev Neurosci* **2**, 185-193.

Hendrickson R. J., Cahill P. A., Sitzmann J. V. and Redmond E. M. (1999) Ethanol enhances basal and flow-stimulated nitric oxide synthase activity *in vitro* by activating an inhibitory guanine nucleotide binding protein. *J Pharmacol Exp Ther* **289**, 1293-1300.

Henry C. B. and Duling B. R. (1999) Permeation of the luminal capillary glycocalyx is determined by hyaluronan. *Am J Physiol* **277**, H508-514.

Hirschi K. K. and D'Amore P. A. (1996) Pericytes in the microvasculature. *Cardiovasc Res* **32**, 687-698.

Hoheisel D., Nitz T., Franke H., Wegener J., Hakvoort A., Tilling T. and Galla H. J. (1998) Hydrocortisone reinforces the blood-brain barrier properties in a serum free cell culture system. *Biochem Biophys Res Commun* **244**, 312-316.

Hoover K. B., Liao S. Y. and Bryant P. J. (1998) Loss of the tight junction MAGUK ZO-1 in breast cancer: relationship to glandular differentiation and loss of heterozygosity. *Am J Pathol* **153**, 1767-1773.

Houck K. A., Leung D. W., Rowland A. M., Winer J. and Ferrara N. (1992) Dual regulation of vascular endothelial growth factor bioavailability by genetic and proteolytic mechanisms. *J Biol Chem* **267**, 26031-26037.

Howarth A. G. and Stevenson B. R. (1995) Molecular environment of ZO-1 in epithelial and non-epithelial cells. *Cell Motil Cytoskeleton* **31**, 323-332.

Huber D., Balda M. S. and Matter K. (2000) Occludin modulates transepithelial migration of neutrophils. *J Biol Chem* **275**, 5773-5778.

Huber J. D., Egleton R. D. and Davis T. P. (2001) Molecular physiology and pathophysiology of tight junctions in the blood-brain barrier. *Trends Neurosci* **24**, 719-725.

Hurter T. (1984) Experimental brain tumors and edema in rats. III. Peritumorous edema. *Exp Pathol* **26**, 227-234.

Hutcheson I. R. and Griffith T. M. (1994) Heterogeneous populations of K⁺ channels mediate EDRF release to flow but not agonists in rabbit aorta. *Am J Physiol* **266**, H590-596.

Iadecola C. (2004) Neurovascular regulation in the normal brain and in Alzheimer's disease. *Nat Rev Neurosci* **5**, 347-360.

Ihrcke N. S., Wrenshall L. E., Lindman B. J. and Platt J. L. (1993) Role of heparan sulfate in immune system-blood vessel interactions. *Immunol Today* **14**, 500-505.

Ishida T., Peterson T. E., Kovach N. L. and Berk B. C. (1996) MAP kinase activation by flow in endothelial cells. Role of beta 1 integrins and tyrosine kinases. *Circ Res* **79**, 310-316.

Itoh M., Furuse M., Morita K., Kubota K., Saitou M. and Tsukita S. (1999) Direct binding of three tight junction-associated MAGUKs, ZO-1, ZO-2, and ZO-3, with the COOH termini of claudins. *J Cell Biol* **147**, 1351-1363.

Jaeger C. B. and Blight A. R. (1997) Spinal cord compression injury in guinea pigs: structural changes of endothelium and its perivascular cell associations after blood-brain barrier breakdown and repair. *Exp Neurol* **144**, 381-399.

Jalali S., del Pozo M. A., Chen K., Miao H., Li Y., Schwartz M. A., Shyy J. Y. and Chien S. (2001) Integrin-mediated mechanotransduction requires its dynamic interaction with specific extracellular matrix (ECM) ligands. *Proc Natl Acad Sci U S A* **98**, 1042-1046.

Jeliazkova-Mecheva V. V. and Bobilya D. J. (2003) A porcine astrocyte/endothelial cell co-culture model of the blood-brain barrier. *Brain Res Brain Res Protoc* **12**, 91-98.

Jesaitis L. A. and Goodenough D. A. (1994) Molecular characterization and tissue distribution of ZO-2, a tight junction protein homologous to ZO-1 and the Drosophila discs-large tumor suppressor protein. *J Cell Biol* **124**, 949-961.

Jiang W. G., Martin T. A., Matsumoto K., Nakamura T. and Mansel R. E. (1999) Hepatocyte growth factor/scatter factor decreases the expression of occludin and transendothelial resistance (TER) and increases paracellular permeability in human vascular endothelial cells. *J Cell Physiol* **181**, 319-329.

Jo H., Sipos K., Go Y. M., Law R., Rong J. and McDonald J. M. (1997) Differential effect of shear stress on extracellular signal-regulated kinase and N-terminal Jun kinase in endothelial cells. Gi2- and Gbeta/gamma-dependent signaling pathways. *J Biol Chem* **272**, 1395-1401.

Jones H. C., Keep R. F. and Butt A. M. (1992) The development of ion regulation at the blood-brain barrier. *Progress in Brain Research* **91**, 123-131.

Jou T. S., Schneeberger E. E. and Nelson W. J. (1998) Structural and functional regulation of tight junctions by RhoA and Rac1 small GTPases. *J Cell Biol* **142**, 101-115.

Juurlink B. H., Fedoroff S., Hall C. and Nathaniel E. J. (1981) Astrocyte cell lineage. I. Astrocyte progenitor cells in mouse neopallium. *J Comp Neurol* **200**, 375-391.

Kacem K., Lacombe P., Seylaz J. and Bonvento G. (1998) Structural organization of the perivascular astrocyte endfeet and their relationship with the endothelial glucose transporter: a confocal microscopy study. *Glia* **23**, 1-10.

Kale G., Naren A. P., Sheth P. and Rao R. K. (2003) Tyrosine phosphorylation of occludin attenuates its interactions with ZO-1, ZO-2, and ZO-3. *Biochem Biophys Res Commun* **302**, 324-329.

Katsube T., Takahisa M., Ueda R., Hashimoto N., Kobayashi M. and Togashi S. (1998) Cortactin associates with the cell-cell junction protein ZO-1 in both Drosophila and mouse. *J Biol Chem* **273**, 29672-29677.

- Kim J. A., Tran N. D., Li Z., Yang F., Zhou W. and Fisher M. J. (2006) Brain endothelial hemostasis regulation by pericytes. *J Cereb Blood Flow Metab* **26**, 209-217.
- Kiuchi-Saishin Y., Gotoh S., Furuse M., Takasuga A., Tano Y. and Tsukita S. (2002) Differential expression patterns of claudins, tight junction membrane proteins, in mouse nephron segments. *J Am Soc Nephrol* **13**, 875-886.
- Kniesel U. and Wolburg H. (2000) Tight junctions of the blood-brain barrier. *Cell Mol Neurobiol* **20**, 57-76.
- Krizanac-Bengez L., Mayberg M. R. and Janigro D. (2004) The cerebral vasculature as a therapeutic target for neurological disorders and the role of shear stress in vascular homeostatis and pathophysiology. *Neurol Res* **26**, 846-853.
- Krizanac-Bengez L., Kapural M., Parkinson F., Cucullo L., Hossain M., Mayberg M. R. and Janigro D. (2003) Effects of transient loss of shear stress on blood-brain barrier endothelium: role of nitric oxide and IL-6. *Brain Res* **977**, 239-246.
- Lacaz-Vieira F., Jaeger M. M., Farshori P. and Kachar B. (1999) Small synthetic peptides homologous to segments of the first external loop of occludin impair tight junction resealing. *J Membr Biol* **168**, 289-297.
- Laemmli U. (1970) Cleavage of structural proteins during the assembly of the head of bacteriophage T4. *Nature* **227**, 680-685.
- Lafarga M. and Palacios G. (1975) Ultrastructural study of pericytes in the rat supraoptic nucleus. *J Anat* **120**, 433-438.
- Lee S. W., Kim W. J., Choi Y. K., Song H. S., Son M. J., Gelman I. H., Kim Y. J. and Kim K. W. (2003) SSeCKS regulates angiogenesis and tight junction formation in blood-brain barrier. *Nat Med* **9**, 900-906.
- Lehoux S. and Tedgui A. (2003) Cellular mechanics and gene expression in blood vessels. *J Biomech* **36**, 631-643.
- Lehoux S., Castier Y. and Tedgui A. (2006) Molecular mechanisms of the vascular responses to haemodynamic forces. *J Intern Med* **259**, 381-392.
- Li D. and Mrsny R. J. (2000) Oncogenic Raf-1 disrupts epithelial tight junctions via downregulation of occludin. *J Cell Biol* **148**, 791-800.
- Li S., Kim M., Hu Y. L., Jalali S., Schlaepfer D. D., Hunter T., Chien S. and Shyy J. Y. (1997) Fluid shear stress activation of focal adhesion kinase. Linking to mitogen-activated protein kinases. *J Biol Chem* **272**, 30455-30462.

- Lin K., Hsu P. P., Chen B. P., Yuan S., Usami S., Shyy J. Y., Li Y. S. and Chien S. (2000) Molecular mechanism of endothelial growth arrest by laminar shear stress. *Proc Natl Acad Sci U S A* **97**, 9385-9389.
- Lin L. F., Doherty D. H., Lile J. D., Bektesh S. and Collins F. (1993) GDNF: a glial cell line-derived neurotrophic factor for midbrain dopaminergic neurons. *Science* **260**, 1130-1132.
- Lin S. C. and Bergles D. E. (2004a) Synaptic signaling between GABAergic interneurons and oligodendrocyte precursor cells in the hippocampus. *Nat Neurosci* **7**, 24-32.
- Lin S. C. and Bergles D. E. (2004b) Synaptic signaling between neurons and glia. *Glia* **47**, 290-298.
- Liu D. Z., LeCluyse E. L. and Thakker D. R. (1999) Dodecylphosphocholine-mediated enhancement of paracellular permeability and cytotoxicity in Caco-2 cell monolayers. *J Pharm Sci* **88**, 1161-1168.
- Lohmann C., Krischke M., Wegener J. and Galla H. J. (2004) Tyrosine phosphatase inhibition induces loss of blood-brain barrier integrity by matrix metalloproteinase-dependent and -independent pathways. *Brain Res* **995**, 184-196.
- Lui W. Y., Lee W. M. and Cheng C. Y. (2001) Transforming growth factor-beta3 perturbs the inter-Sertoli tight junction permeability barrier *in vitro* possibly mediated via its effects on occludin, zonula occludens-1, and claudin-11. *Endocrinology* **142**, 1865-1877.
- Lui W. Y., Lee W. M. and Cheng C. Y. (2003) Transforming growth factor beta3 regulates the dynamics of Sertoli cell tight junctions via the p38 mitogen-activated protein kinase pathway. *Biol Reprod* **68**, 1597-1612.
- MacIntyre A., Hammond C. J., Little C. S., Appelt D. M. and Balin B. J. (2002) Chlamydia pneumoniae infection alters the junctional complex proteins of human brain microvascular endothelial cells. *FEMS Microbiol Lett* **217**, 167-172.
- MacRobbie E. A. (1998) Signal transduction and ion channels in guard cells. *Philos Trans R Soc Lond B Biol Sci* **353**, 1475-1488.
- Madara J. L. (1998) Regulation of the movement of solutes across tight junctions. *Annu Rev Physiol* **60**, 143-159.
- Mankertz J., Waller J. S., Hillenbrand B., Tavalali S., Florian P., Schoneberg T., Fromm M. and Schulzke J. D. (2002) Gene expression of the tight junction protein occludin includes differential splicing and alternative promoter usage. *Biochem Biophys Res Commun* **298**, 657-666.

Marmorstein A. D., Mortell K. H., Ratcliffe D. R. and Cramer E. B. (1992) Epithelial permeability factor: a serum protein that condenses actin and opens tight junctions. *Am J Physiol* **262**, C1403-1410.

Martin-Padura I., Lostaglio S., Schneemann M., Williams L., Romano M., Fruscella P., Panzeri C., Stoppacciaro A., Ruco L., Villa A., Simmons D. and Dejana E. (1998) Junctional adhesion molecule, a novel member of the immunoglobulin superfamily that distributes at intercellular junctions and modulates monocyte transmigration. *J Cell Biol* **142**, 117-127.

Matter K. and Balda M. S. (1998) Biogenesis of tight junctions: the C-terminal domain of occludin mediates basolateral targeting. *J Cell Sci* **111** (Pt 4), 511-519.

Mattila K. M., Pirttila T., Blennow K., Wallin A., Viitanen M. and Frey H. (1994) Altered blood-brain-barrier function in Alzheimer's disease? *Acta Neurol Scand* **89**, 192-198.

McAllister M. S., Krizanac-Bengez L., Macchia F., Naftalin R. J., Pedley K. C., Mayberg M. R., Marroni M., Leaman S., Stanness K. A. and Janigro D. (2001) Mechanisms of glucose transport at the blood-brain barrier: an *in vitro* study. *Brain Res* **904**, 20-30.

McCarthy K. M., Skare I. B., Stankewich M. C., Furuse M., Tsukita S., Rogers R. A., Lynch R. D. and Schneeberger E. E. (1996) Occludin is a functional component of the tight junction. *J Cell Sci* **109** (Pt 9), 2287-2298.

McNamara B. P., Koutsouris A., O'Connell C. B., Nougayrede J. P., Donnenberg M. S. and Hecht G. (2001) Translocated EspF protein from enteropathogenic *Escherichia coli* disrupts host intestinal barrier function. *J Clin Invest* **107**, 621-629.

Medina R., Rahner C., Mitic L. L., Anderson J. M. and Van Itallie C. M. (2000) Occludin localization at the tight junction requires the second extracellular loop. *J Membr Biol* **178**, 235-247.

Meresse S., Dehouck M. P., Delorme P., Bensaïd M., Tauber J. P., Delbart C., Fruchart J. C. and Cecchelli R. (1989) Bovine brain endothelial cells express tight junctions and monoamine oxidase activity in long-term culture. *J Neurochem* **53**, 1363-1371.

Meyer J., Mischeck U., Veyhl M., Henzel K. and Galla H. J. (1990) Blood-brain barrier characteristic enzymatic properties in cultured brain capillary endothelial cells. *Brain Res* **514**, 305-309.

Mi H., Haerberle H. and Barres B. A. (2001) Induction of astrocyte differentiation by endothelial cells. *J Neurosci* **21**, 1538-1547.

Millauer B., Wизigmann-Voos S., Schnurch H., Martinez R., Moller N. P., Risau W. and Ullrich A. (1993) High affinity VEGF binding and developmental expression

suggest Flk-1 as a major regulator of vasculogenesis and angiogenesis. *Cell* **72**, 835-846.

Mischeck U., Meyer J. and Galla H. J. (1989) Characterization of gamma-glutamyl transpeptidase activity of cultured endothelial cells from porcine brain capillaries. *Cell Tissue Res* **256**, 221-226.

Mizuguchi H., Utoguchi N. and Mayumi T. (1997) Preparation of glial extracellular matrix: a novel method to analyze glial-endothelial cell interaction. *Brain Res Brain Res Protoc* **1**, 339-343.

Mizuguchi H., Hashioka Y., Utoguchi N., Kubo K., Nakagawa S. and Mayumi T. (1994) A comparison of drug transport through cultured monolayers of bovine brain capillary and bovine aortic endothelial cells. *Biol Pharm Bull* **17**, 1385-1390.

Mollgard K. and Saunders N. R. (1986) The development of the human blood-brain and blood-CSF barriers. *Neuropathol Appl Neurobiol* **12**, 337-358.

Muir A. R. and Peters A. (1962) Quintuple-layered membrane junctions at terminal bars between endothelial cells. *J Cell Biol* **12**, 443-448.

Muller S. L., Portwich M., Schmidt A., Utepbergenov D. I., Huber O., Blasig I. E. and Krause G. (2005) The tight junction protein occludin and the adherens junction protein alpha-catenin share a common interaction mechanism with ZO-1. *J Biol Chem* **280**, 3747-3756.

Muresan Z., Paul D. L. and Goodenough D. A. (2000) Occludin 1B, a variant of the tight junction protein occludin. *Mol Biol Cell* **11**, 627-634.

Nabeshima S., Reese T. S., Landis D. M. and Brightman M. W. (1975) Junctions in the meninges and marginal glia. *J Comp Neurol* **164**, 127-169.

Nagel T., Resnick N., Dewey C. F., Jr. and Gimbrone M. A., Jr. (1999) Vascular endothelial cells respond to spatial gradients in fluid shear stress by enhanced activation of transcription factors. *Arterioscler Thromb Vasc Biol* **19**, 1825-1834.

Nehls V. and Drenckhahn D. (1991) Heterogeneity of microvascular pericytes for smooth muscle type alpha-actin. *J Cell Biol* **113**, 147-154.

Neufeld G., Cohen T., Gengrinovitch S. and Poltorak Z. (1999) Vascular endothelial growth factor (VEGF) and its receptors. *Faseb J* **13**, 9-22.

Ngai A. C. and Winn H. R. (1995) Modulation of cerebral arteriolar diameter by intraluminal flow and pressure. *Circ Res* **77**, 832-840.

Nitz T., Eisenblatter T., Psathaki K. and Galla H. J. (2003) Serum-derived factors weaken the barrier properties of cultured porcine brain capillary endothelial cells *in vitro*. *Brain Res* **981**, 30-40.

- Noria S., Cowan D. B., Gotlieb A. I. and Langille B. L. (1999) Transient and steady-state effects of shear stress on endothelial cell adherens junctions. *Circ Res* **85**, 504-514.
- Nybom P. and Magnusson K. E. (1996) Modulation of the junctional integrity by low or high concentrations of cytochalasin B and dihydrocytochalasin B is associated with distinct changes in F-actin and ZO-1. *Biosci Rep* **16**, 313-326.
- Odenbreit S., Puls J., Sedlmaier B., Gerland E., Fischer W. and Haas R. (2000) Translocation of *Helicobacter pylori* CagA into gastric epithelial cells by type IV secretion. *Science* **287**, 1497-1500.
- Olesen S. P., Clapham D. E. and Davies P. F. (1988) Haemodynamic shear stress activates a K⁺ current in vascular endothelial cells. *Nature* **331**, 168-170.
- Ott M. J. and Ballermann B. J. (1995) Shear stress-conditioned, endothelial cell-seeded vascular grafts: improved cell adherence in response to *in vitro* shear stress. *Surgery* **117**, 334-339.
- Pang Z., Antonetti D. A. and Tarbell J. M. (2005) Shear stress regulates HUVEC hydraulic conductivity by occludin phosphorylation. *Ann Biomed Eng* **33**, 1536-1545.
- Papadopoulos M. C., Saadoun S., Woodrow C. J., Davies D. C., Costa-Martins P., Moss R. F., Krishna S. and Bell B. A. (2001) Occludin expression in microvessels of neoplastic and non-neoplastic human brain. *Neuropathol Appl Neurobiol* **27**, 384-395.
- Pardridge W. M. (2002) Targeting Neurotherapeutic Agents Through the Blood-Brain Barrier. *Archives of Neurology* **59**, 35-40.
- Pardridge W. M. (2003) Blood-brain barrier drug targeting: the future of brain drug development. *Mol Interv* **3**, 90-105, 151.
- Pardridge W. M. (2005a) The blood-brain barrier: bottleneck in brain drug development. *NeuroRx* **2**, 3-14.
- Pardridge W. M. (2005b) The Blood-Brain Barrier and Neurotherapeutics. *NeuroRx* **2**, 1-2.
- Patel T. R., Galbraith S., Graham D. I., Hallak H., Doherty A. M. and McCulloch J. (1996) Endothelin receptor antagonist increases cerebral perfusion and reduces ischaemic damage in feline focal cerebral ischaemia. *J Cereb Blood Flow Metab* **16**, 950-958.
- Patrick C. W., Jr. and McIntire L. V. (1995) Shear stress and cyclic strain modulation of gene expression in vascular endothelial cells. *Blood Purif* **13**, 112-124.

- Pekny M., Stanness K. A., Eliasson C., Betsholtz C. and Janigro D. (1998) Impaired induction of blood-brain barrier properties in aortic endothelial cells by astrocytes from GFAP-deficient mice. *Glia* **22**, 390-400.
- Peters A. (1962) Plasma membrane contacts in the central nervous system. *J Anat* **96**, 237-248.
- Pierre L. N. and Davenport A. P. (1999) Blockade and reversal of endothelin-induced constriction in pial arteries from human brain. *Stroke* **30**, 638-643.
- Plateel M., Teissier E. and Cecchelli R. (1997) Hypoxia dramatically increases the nonspecific transport of blood-borne proteins to the brain. *J Neurochem* **68**, 874-877.
- Poland S. D., Rice G. P. and Dekaban G. A. (1995) HIV-1 infection of human brain-derived microvascular endothelial cells *in vitro*. *J Acquir Immune Defic Syndr Hum Retrovirol* **8**, 437-445.
- Prado R., Watson B. D., Kuluz J. and Dietrich W. D. (1992) Endothelium-derived nitric oxide synthase inhibition. Effects on cerebral blood flow, pial artery diameter, and vascular morphology in rats. *Stroke* **23**, 1118-1123; discussion 1124.
- Prasadarao N. V., Wass C. A., Huang S. H. and Kim K. S. (1999) Identification and characterization of a novel Ibe10 binding protein that contributes to *Escherichia coli* invasion of brain microvascular endothelial cells. *Infect Immun* **67**, 1131-1138.
- Qin Y. and Sato T. N. (1995) Mouse multidrug resistance 1a/3 gene is the earliest known endothelial cell differentiation marker during blood-brain barrier development. *Dev Dyn* **202**, 172-180.
- Rahner C., Mitic L. L. and Anderson J. M. (2001) Heterogeneity in expression and subcellular localization of claudins 2, 3, 4, and 5 in the rat liver, pancreas, and gut. *Gastroenterology* **120**, 411-422.
- Ramsauer M., Krause D. and Dermietzel R. (2002) Angiogenesis of the blood-brain barrier *in vitro* and the function of cerebral pericytes. *Faseb J* **16**, 1274-1276.
- Ransom C. B. and Sontheimer H. (1995) Biophysical and pharmacological characterization of inwardly rectifying K⁺ currents in rat spinal cord astrocytes. *J Neurophysiol* **73**, 333-346.
- Rao R. K., Basuroy S., Rao V. U., Karnaky Jr K. J. and Gupta A. (2002) Tyrosine phosphorylation and dissociation of occludin-ZO-1 and E-cadherin-beta-catenin complexes from the cytoskeleton by oxidative stress. *Biochem J* **368**, 471-481.
- Rascher G. and Wolburg H. (1997) The tight junctions of the leptomeningeal blood-cerebrospinal fluid barrier during development. *J Hirnforsch* **38**, 525-540.

Reese T. S. and Karnovsky M. J. (1967) Fine structural localization of a blood-brain barrier to exogenous peroxidase. *J Cell Biol* **34**, 207-217.

Robertson J. D. (1957) New observations on the ultrastructure of the membranes of frog peripheral nerve fibers. *J Biophys Biochem Cytol* **3**, 1043-1048.

Robinson C., Baker S. F. and Garrod D. R. (2001) Peptidase allergens, occludin and claudins. Do their interactions facilitate the development of hypersensitivity reactions at mucosal surfaces? *Clin Exp Allergy* **31**, 186-192.

Roux F., Durieu-Trautmann O., Chaverot N., Claire M., Maily P., Bourre J. M., Strosberg A. D. and Couraud P. O. (1994) Regulation of gamma-glutamyl transpeptidase and alkaline phosphatase activities in immortalized rat brain microvessel endothelial cells. *J Cell Physiol* **159**, 101-113.

Rubin L. L. and Staddon J. M. (1999) The cell biology of the blood-brain barrier. *Annu Rev Neurosci* **22**, 11-28.

Rubin L. L., Hall D. E., Porter S., Barbu K., Cannon C., Horner H. C., Janatpour M., Liaw C. W., Manning K., Morales J. (1991) A cell culture model of the blood-brain barrier. *J Cell Biol* **115**, 1725-1735.

Rupp P. A. and Little C. D. (2001) Integrins in vascular development. *Circ Res* **89**, 566-572.

Saitou M., Ando-Akatsuka Y., Itoh M., Furuse M., Inazawa J., Fujimoto K. and Tsukita S. (1997) Mammalian occludin in epithelial cells: its expression and subcellular distribution. *Eur J Cell Biol* **73**, 222-231.

Sakakibara A., Furuse M., Saitou M., Ando-Akatsuka Y. and Tsukita S. (1997) Possible involvement of phosphorylation of occludin in tight junction formation. *J Cell Biol* **137**, 1393-1401.

Satoh H., Zhong Y., Isomura H., Saitoh M., Enomoto K., Sawada N. and Mori M. (1996) Localization of 7H6 tight junction-associated antigen along the cell border of vascular endothelial cells correlates with paracellular barrier function against ions, large molecules, and cancer cells. *Exp Cell Res* **222**, 269-274.

Saunders N. R., Dziegielewska K. M. and Møllgård K. (1991) The importance of the blood-brain barrier in fetuses and embryos. *Trends Neurosci* **14**, 14-15.

Sawada N., Murata M., Kikuchi K., Osanai M., Tobioka H., Kojima T. and Chiba H. (2003) Tight junctions and human diseases. *Med Electron Microsc* **36**, 147-156.

Schinkel A. H. (1999) P-Glycoprotein, a gatekeeper in the blood-brain barrier. *Adv Drug Deliv Rev* **36**, 179-194.

Schinkel A. H., Wagenaar E., Mol C. A. and van Deemter L. (1996) P-glycoprotein in the blood-brain barrier of mice influences the brain penetration and pharmacological activity of many drugs. *J Clin Invest* **97**, 2517-2524.

Schinkel A. H., Smit J. J., van Tellingen O., Beijnen J. H., Wagenaar E., van Deemter L., Mol C. A., van der Valk M. A., Robanus-Maandag E. C., te Riele H. P. (1994) Disruption of the mouse *mdr1a* P-glycoprotein gene leads to a deficiency in the blood-brain barrier and to increased sensitivity to drugs. *Cell* **77**, 491-502.

Schneeberger E. E., Walters D. V. and Olver R. E. (1978) Development of intercellular junctions in the pulmonary epithelium of the foetal lamb. *J Cell Sci* **32**, 307-324.

Schoenwaelder S. M. and Burridge K. (1999) Bidirectional signaling between the cytoskeleton and integrins. *Curr Opin Cell Biol* **11**, 274-286.

Schulze C. and Firth J. A. (1993) Immunohistochemical localization of adherens junction components in blood-brain barrier microvessels of the rat. *J Cell Sci* **104** (Pt 3), 773-782.

Schulze C., Smales C., Rubin L. L. and Staddon J. M. (1997) Lysophosphatidic acid increases tight junction permeability in cultured brain endothelial cells. *J Neurochem* **68**, 991-1000.

Schwarz G., Droogmans G. and Nilius B. (1992a) Shear stress induced membrane currents and calcium transients in human vascular endothelial cells. *Pflugers Arch* **421**, 394-396.

Schwarz G., Callewaert G., Droogmans G. and Nilius B. (1992b) Shear stress-induced calcium transients in endothelial cells from human umbilical cord veins. *J Physiol* **458**, 527-538.

Seetharam L., Gotoh N., Maru Y., Neufeld G., Yamaguchi S. and Shibuya M. (1995) A unique signal transduction from FLT tyrosine kinase, a receptor for vascular endothelial growth factor VEGF. *Oncogene* **10**, 135-147.

Senger D. R., Galli S. J., Dvorak A. M., Perruzzi C. A., Harvey V. S. and Dvorak H. F. (1983) Tumor cells secrete a vascular permeability factor that promotes accumulation of ascites fluid. *Science* **219**, 983-985.

Sheth P., Basuroy S., Li C., Naren A. P. and Rao R. K. (2003) Role of phosphatidylinositol 3-kinase in oxidative stress-induced disruption of tight junctions. *J Biol Chem* **278**, 49239-49245.

Shibuya M., Ito N. and Claesson-Welsh L. (1999) Structure and function of vascular endothelial growth factor receptor-1 and -2. *Curr Top Microbiol Immunol* **237**, 59-83.

- Shyy J. Y. and Chien S. (1997) Role of integrins in cellular responses to mechanical stress and adhesion. *Curr Opin Cell Biol* **9**, 707-713.
- Shyy J. Y. and Chien S. (2002) Role of integrins in endothelial mechanosensing of shear stress. *Circ Res* **91**, 769-775.
- Simard M., Arcuino G., Takano T., Liu Q. S. and Nedergaard M. (2003) Signaling at the gliovascular interface. *J Neurosci* **23**, 9254-9262.
- Sinclair C. J., Krizanac-Bengez L., Stanness K. A., Janigro D. and Parkinson F. E. (2001) Adenosine permeation of a dynamic *in vitro* blood-brain barrier inhibited by dipyridamole. *Brain Res* **898**, 122-125.
- Singh U., Van Itallie C. M., Mitic L. L., Anderson J. M. and McClane B. A. (2000) CaCo-2 cells treated with *Clostridium perfringens* enterotoxin form multiple large complex species, one of which contains the tight junction protein occludin. *J Biol Chem* **275**, 18407-18417.
- Smith W. L., Garavito R. M. and DeWitt D. L. (1996) Prostaglandin endoperoxide H synthases (cyclooxygenases)-1 and -2. *J Biol Chem* **271**, 33157-33160.
- Sobue K., Yamamoto N., Yoneda K., Hodgson M. E., Yamashiro K., Tsuruoka N., Tsuda T., Katsuya H., Miura Y., Asai K. and Kato T. (1999) Induction of blood-brain barrier properties in immortalized bovine brain endothelial cells by astrocytic factors. *Neurosci Res* **35**, 155-164.
- Squire J. M., Chew M., Nneji G., Neal C., Barry J. and Michel C. (2001) Quasi-periodic substructure in the microvessel endothelial glycocalyx: a possible explanation for molecular filtering? *J Struct Biol* **136**, 239-255.
- Staddon J. M., Herrenknecht K., Smales C. and Rubin L. L. (1995) Evidence that tyrosine phosphorylation may increase tight junction permeability. *J Cell Sci* **108** (Pt 2), 609-619.
- Stamatovic S. M., Dimitrijevic O. B., Keep R. F. and Andjelkovic A. V. (2006) Inflammation and brain edema: new insights into the role of chemokines and their receptors. *Acta Neurochir Suppl* **96**, 444-450.
- Stanness K. A., Guatteo E. and Janigro D. (1996) A dynamic model of the blood-brain barrier "*in vitro*". *Neurotoxicology* **17**, 481-496.
- Stanness K. A., Neumaier J. F., Sexton T. J., Grant G. A., Emmi A., Maris D. O. and Janigro D. (1999) A new model of the blood--brain barrier: co-culture of neuronal, endothelial and glial cells under dynamic conditions. *Neuroreport* **10**, 3725-3731.
- Stanness K. A., Westrum L. E., Fornaciari E., Mascagni P., Nelson J. A., Stenglein S. G., Myers T. and Janigro D. (1997) Morphological and functional characterization of an *in vitro* blood-brain barrier model. *Brain Res* **771**, 329-342.

Stevenson B. R., Siliciano J. D., Mooseker M. S. and Goodenough D. A. (1986) Identification of ZO-1: a high molecular weight polypeptide associated with the tight junction (zonula occludens) in a variety of epithelia. *J Cell Biol* **103**, 755-766.

Tai Y. H., Flick J., Levine S. A., Madara J. L., Sharp G. W. and Donowitz M. (1996) Regulation of tight junction resistance in T84 monolayers by elevation in intracellular Ca²⁺: a protein kinase C effect. *J Membr Biol* **149**, 71-79.

Takahashi M. and Berk B. C. (1996) Mitogen-activated protein kinase (ERK1/2) activation by shear stress and adhesion in endothelial cells. Essential role for a herbimycin-sensitive kinase. *J Clin Invest* **98**, 2623-2631.

Takeda H. and Tsukita S. (1995) Effects of tyrosine phosphorylation on tight junctions in temperature-sensitive v-src-transfected MDCK cells. *Cell Struct Funct* **20**, 387-393.

Tanobe K., Nishikawa K., Hinohara H., Okamoto T., Saito S. and Goto F. (2003) Blood-brain barrier and general anesthetics. *Masui* **52**, 840-845.

Thi M. M., Tarbell J. M., Weinbaum S. and Spray D. C. (2004) The role of the glycocalyx in reorganization of the actin cytoskeleton under fluid shear stress: a "bumper-car" model. *Proc Natl Acad Sci U S A* **101**, 16483-16488.

Tigyi G. and Miledi R. (1992) Lysophosphatidates bound to serum albumin activate membrane currents in *Xenopus* oocytes and neurite retraction in PC12 pheochromocytoma cells. *J Biol Chem* **267**, 21360-21367.

Tobioka H., Tokunaga Y., Isomura H., Kokai Y., Yamaguchi J. and Sawada N. (2004a) Expression of occludin, a tight-junction-associated protein, in human lung carcinomas. *Virchows Arch* **445**, 472-476.

Tobioka H., Isomura H., Kokai Y., Tokunaga Y., Yamaguchi J. and Sawada N. (2004b) Occludin expression decreases with the progression of human endometrial carcinoma. *Hum Pathol* **35**, 159-164.

Tokunaga Y., Tobioka H., Isomura H., Kokai Y. and Sawada N. (2004) Expression of occludin in human rectal carcinoid tumours as a possible marker for glandular differentiation. *Histopathology* **44**, 247-250.

Torok M., Huwyler J., Gutmann H., Fricker G. and Drewe J. (2003) Modulation of transendothelial permeability and expression of ATP-binding cassette transporters in cultured brain capillary endothelial cells by astrocytic factors and cell-culture conditions. *Exp Brain Res* **153**, 356-365.

Tran N. D., Correale J., Schreiber S. S. and Fisher M. (1999) Transforming growth factor-beta mediates astrocyte-specific regulation of brain endothelial anticoagulant factors. *Stroke* **30**, 1671-1678.

Traub O. and Berk B. C. (1998) Laminar shear stress: mechanisms by which endothelial cells transduce an atheroprotective force. *Arterioscler Thromb Vasc Biol* **18**, 677-685.

Tunkel A. R. and Scheld W. M. (1993) Pathogenesis and pathophysiology of bacterial meningitis. *Annu Rev Med* **44**, 103-120.

Tzima E., del Pozo M. A., Shattil S. J., Chien S. and Schwartz M. A. (2001) Activation of integrins in endothelial cells by fluid shear stress mediates Rho-dependent cytoskeletal alignment. *Embo J* **20**, 4639-4647.

Urbich C., Walter D. H., Zeiher A. M. and Dimmeler S. (2000) Laminar shear stress upregulates integrin expression: role in endothelial cell adhesion and apoptosis. *Circ Res* **87**, 683-689.

van Deurs B. and Koehler J. K. (1979) Tight junctions in the choroid plexus epithelium. A freeze-fracture study including complementary replicas. *J Cell Biol* **80**, 662-673.

Wachtel M., Frei K., Ehler E., Fontana A., Winterhalter K. and Gloor S. M. (1999) Occludin proteolysis and increased permeability in endothelial cells through tyrosine phosphatase inhibition. *J Cell Sci* **112** (Pt 23), 4347-4356.

Wahl M. and Schilling L. (1993) Regulation of cerebral blood flow--a brief review. *Acta Neurochir Suppl (Wien)* **59**, 3-10.

Waltenberger J., Claesson-Welsh L., Siegbahn A., Shibuya M. and Heldin C. H. (1994) Different signal transduction properties of KDR and Flt1, two receptors for vascular endothelial growth factor. *J Biol Chem* **269**, 26988-26995.

Wan H., Winton H. L., Soeller C., Gruenert D. C., Thompson P. J., Cannell M. B., Stewart G. A., Garrod D. R. and Robinson C. (2000) Quantitative structural and biochemical analyses of tight junction dynamics following exposure of epithelial cells to house dust mite allergen Der p 1. *Clin Exp Allergy* **30**, 685-698.

Wan H., Winton H. L., Soeller C., Taylor G. W., Gruenert D. C., Thompson P. J., Cannell M. B., Stewart G. A., Garrod D. R. and Robinson C. (2001) The transmembrane protein occludin of epithelial tight junctions is a functional target for serine peptidases from faecal pellets of *Dermatophagoides pteronyssinus*. *Clin Exp Allergy* **31**, 279-294.

Wan H., Winton H. L., Soeller C., Tovey E. R., Gruenert D. C., Thompson P. J., Stewart G. A., Taylor G. W., Garrod D. R., Cannell M. B. and Robinson C. (1999) Der p 1 facilitates transepithelial allergen delivery by disruption of tight junctions. *J Clin Invest* **104**, 123-133.

- Wieland T. and Mittmann C. (2003) Regulators of G-protein signalling: multifunctional proteins with impact on signalling in the cardiovascular system. *Pharmacol Ther* **97**, 95-115.
- Williams K. C., Ulvestad E. and Hickey W. F. (1994) Immunology of multiple sclerosis. *Clin Neurosci* **2**, 229-245.
- Willott E., Balda M. S., Heintzelman M., Jameson B. and Anderson J. M. (1992) Localization and differential expression of two isoforms of the tight junction protein ZO-1. *Am J Physiol* **262**, C1119-1124.
- Willott E., Balda M. S., Fanning A. S., Jameson B., Van Itallie C. and Anderson J. M. (1993) The tight junction protein ZO-1 is homologous to the *Drosophila* discs-large tumor suppressor protein of septate junctions. *Proc Natl Acad Sci U S A* **90**, 7834-7838.
- Wittchen E. S., Haskins J. and Stevenson B. R. (1999) Protein interactions at the tight junction. Actin has multiple binding partners, and ZO-1 forms independent complexes with ZO-2 and ZO-3. *J Biol Chem* **274**, 35179-35185.
- Wojciak-Stothard B. and Ridley A. J. (2002) Rho GTPases and the regulation of endothelial permeability. *Vascul Pharmacol* **39**, 187-199.
- Wong V. (1997) Phosphorylation of occludin correlates with occludin localization and function at the tight junction. *Am J Physiol* **273**, C1859-1867.
- Wong V. and Gumbiner B. M. (1997) A synthetic peptide corresponding to the extracellular domain of occludin perturbs the tight junction permeability barrier. *J Cell Biol* **136**, 399-409.
- Wu Z., Nybom P. and Magnusson K. E. (2000) Distinct effects of *Vibrio cholerae* haemagglutinin/protease on the structure and localization of the tight junction-associated proteins occludin and ZO-1. *Cell Microbiol* **2**, 11-17.
- Yamada M., Lamping K. G., Duttaroy A., Zhang W., Cui Y., Bymaster F. P., McKinzie D. L., Felder C. C., Deng C. X., Faraci F. M. and Wess J. (2001) Cholinergic dilation of cerebral blood vessels is abolished in M(5) muscarinic acetylcholine receptor knockout mice. *Proc Natl Acad Sci U S A* **98**, 14096-14101.
- Yamamoto T., Harada N., Kano K., Taya S., Canaani E., Matsuura Y., Mizoguchi A., Ide C. and Kaibuchi K. (1997) The Ras target AF-6 interacts with ZO-1 and serves as a peripheral component of tight junctions in epithelial cells. *J Cell Biol* **139**, 785-795.
- You J., Johnson T. D., Childres W. F. and Bryan R. M., Jr. (1997) Endothelial-mediated dilations of rat middle cerebral arteries by ATP and ADP. *Am J Physiol* **273**, H1472-1477.

You J., Johnson T. D., Marrelli S. P., Mombouli J. V. and Bryan R. M., Jr. (1999) P2u receptor-mediated release of endothelium-derived relaxing factor/nitric oxide and endothelium-derived hyperpolarizing factor from cerebrovascular endothelium in rats. *Stroke* **30**, 1125-1133.

Yu A. S., McCarthy K. M., Francis S. A., McCormack J. M., Lai J., Rogers R. A., Lynch R. D. and Schneeberger E. E. (2005) Knockdown of occludin expression leads to diverse phenotypic alterations in epithelial cells. *Am J Physiol Cell Physiol* **288**, C1231-1241.

Zhang C. and Harder D. R. (2002) Cerebral capillary endothelial cell mitogenesis and morphogenesis induced by astrocytic epoxyeicosatrienoic Acid. *Stroke* **33**, 2957-2964.

Zhang J., Tan Z. and Tran N. D. (2000) Chemical hypoxia-ischemia induces apoptosis in cerebromicrovascular endothelial cells. *Brain Res* **877**, 134-140.

Zhong Y., Saitoh T., Minase T., Sawada N., Enomoto K. and Mori M. (1993) Monoclonal antibody 7H6 reacts with a novel tight junction-associated protein distinct from ZO-1, cingulin and ZO-2. *J Cell Biol* **120**, 477-483.

Zhong Y., Enomoto K., Tobioka H., Konishi Y., Satoh M. and Mori M. (1994) Sequential decrease in tight junctions as revealed by 7H6 tight junction-associated protein during rat hepatocarcinogenesis. *Jpn J Cancer Res* **85**, 351-356.

Zhou Y., Dirksen W. P., Zweier J. L. and Periasamy M. (2004) Endothelin-1-induced responses in isolated mouse vessels: the expression and function of receptor types. *Am J Physiol Heart Circ Physiol* **287**, H573-578.

Zimmermann K. W. (1923) Der feinere bau der blutkapillaren. *Z Anat Entwicklunghesch* **68**, 29-109.

Zysk G., Schneider-Wald B. K., Hwang J. H., Bejo L., Kim K. S., Mitchell T. J., Hakenbeck R. and Heinz H. P. (2001) Pneumolysin is the main inducer of cytotoxicity to brain microvascular endothelial cells caused by *Streptococcus pneumoniae*. *Infect Immun* **69**, 845-852.